MULTIPLE PRODUCTION AND PROCESSES AT ULTRA HIGH ENERGIES

Chairman	M. Danysh
Rapporteur	A. Wroblewski
Discussion leaders	S. Slavatinsky
	F. Muller
Secretaries	E. Kladnitskaya
	V. Maksimenko
	V. Kolybasov
	I. Saitov
	V. Akimov

MULTIPLE PRODUCTION AND PROCESSES AT ULTRA HIGH EHERGIES

A. Wróblewski

I am expected to cover energy region from threshold to superhigh energies. I am expected to report on papers submitted to this conference (about 90 papers with about 800 authors) but also to show progress since last conferences in Vienna and Lund. I am also expected to talk not only about interactions with nucleous but also with nuclei. It is obviously an impossible task for one hour so I have to make a choice of subjects.

I shall use a following definition: Many body process is one in which we have $\geqslant 3$ particles in the final state (resonances not included). Further it may appear that many body processes are found to be quasi-two-body ones as in the example:

$$\pi^+ p \to \underbrace{p\pi^+}_{\Delta^{++}} \underbrace{\pi^+\pi^-\pi^+\pi^-\pi^0}_{X^0}$$

so there will be some overlap between this report and that on quasi-two-body reaction of D. R. O. Morrison.

As an introduction let me show you a slide (Fig. 1), which shows qualitatively the amount of information which we have in different regions of energy.

The most basic information we have is the existence of strong interactions up to the energy of the order of 10^{10} *GeV*. Cross sections and multiplicity of charged particles are fairly well known, as I will show you, up to about 1000 *GeV*. Much less known are the distributions of angles and momenta of secondary particles and correlations both of resonant and nonresonant type (i. e. *GGLP* effect). These are well studied only in a limited energy range (< 30 *GeV*). Finally, still lower energy region is the only one in which we have data complete enough to attempt more detailed description of interactions in terms of exchange mechanism and models.

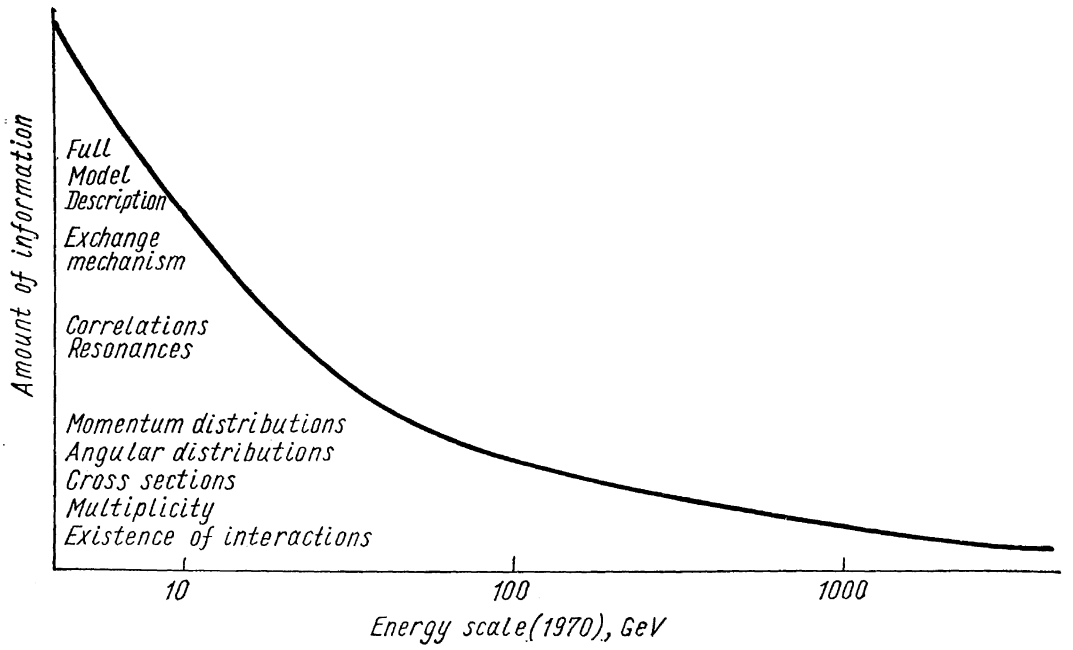

Fig. 1.

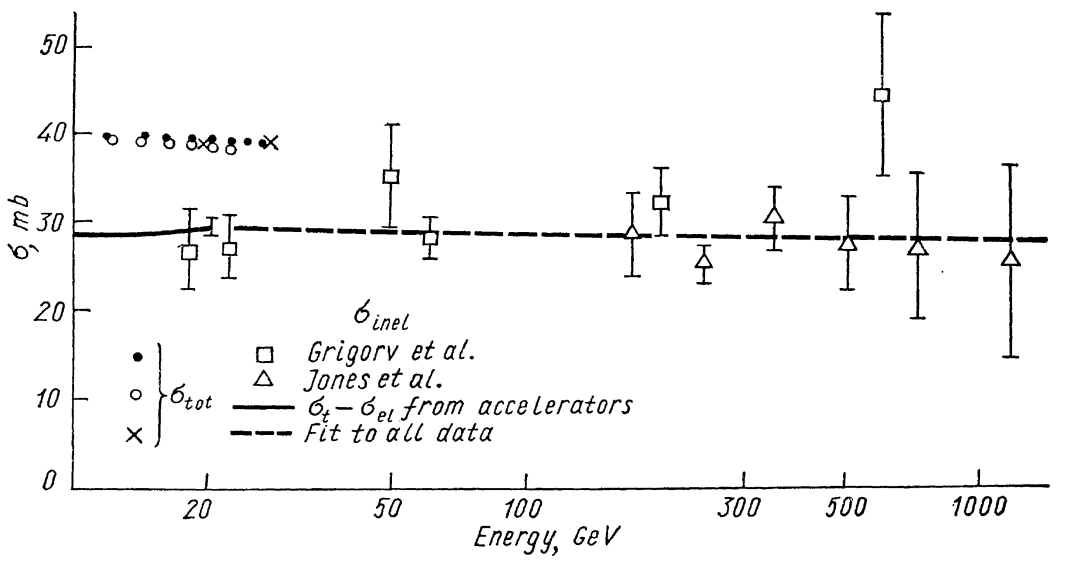

Fig. 2. Proton-proton cross sections.

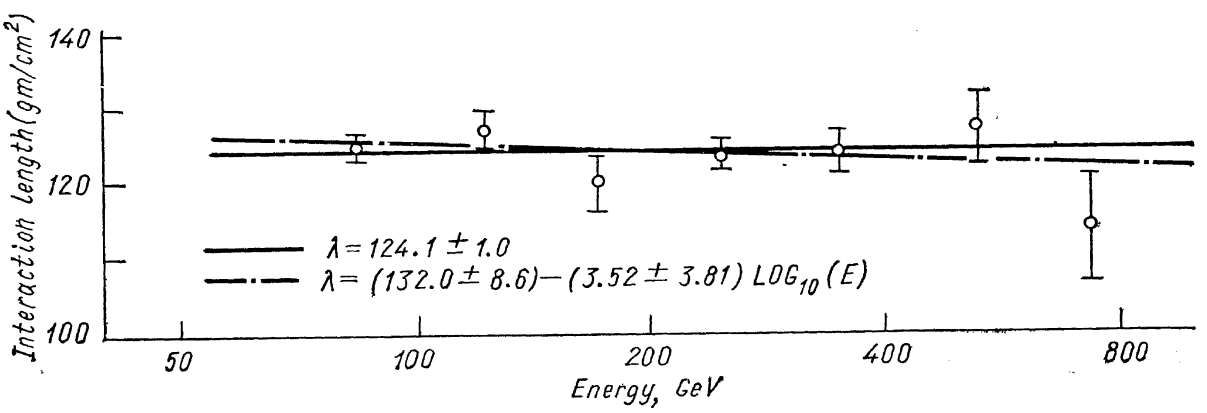

Fig. 3. Maximum likelihood fit to interaction length in iron.

In my talk I shall present problems roughly in the order in which they are placed along the vertical axis. I shall start with cross sections and multiplicities and then proceed through more detailed description of interactions to a recent experimental checks of various models. The last part of my talk will be devoted to interactions with nuclei.

1. Cross sections

1.1. TOTAL INELASTIC CROSS SECTIONS

The total inelastic proton-proton cross section was measured recently up to ∞ 1000 *GeV* in two experiments by N. L. Grigorov et al. [1] and by L. W. Jones, D. D. Reeder et al. [2, 3, 4]. Grigorov et al. used graphite and polyethylene targets installed in the «Proton» satellites.

The instrument used to determine cross sections was calibrated at an accelerator with $E = 5$ *GeV*. The *p-p* inelastic cross section was deduced from the comparison of results with the two targets. L. W. Jones, D. D. Reeder et al. installed their instruments at Echo Lake, Colorado (elevation 3 230 *m*). The apparatus consisted of a liquid hydrogen target, an ionization calorimeter for energy determination and spark chambers to define the direction of the incident particle and the number and directions of secondary charged particles produced in the target. The results of both groups are shown in Fig. 2. The Grigorov et al. data taken alone suggest a very slow logarithmic increase in $\sigma_{pp}^{\text{inel}}$ with energy:

$$\sigma_{pp}^{\text{inel}} = (30.7 \pm 1{,}5)\left[1 + (0.24 \pm 0.12)\lg\frac{E\,(eV)}{10^{11}}\right],\ mb$$

although the fit to a constant cross section (29 ± 2 *mb*) is also very good. The Echo Lake data contain possible systematic error (contamination of pions in the primary beam) but the relative position of points is determined fairly well. The best fit to all the data is consistent with a constant $\sigma_{pp}^{\text{inel}}$ in the region 20 to 1000 *GeV*.

The Echo Lake experiment gave also results on the total inelastic cross section in iron. The results shown in Fig. 3 are consistent with a constant mean free path of protons in iron

$$\lambda_{\text{Fe}} = (124.1 \pm 1.0)\,g \cdot cm^{-2} (\sigma = 747 \pm 6\ mb).$$

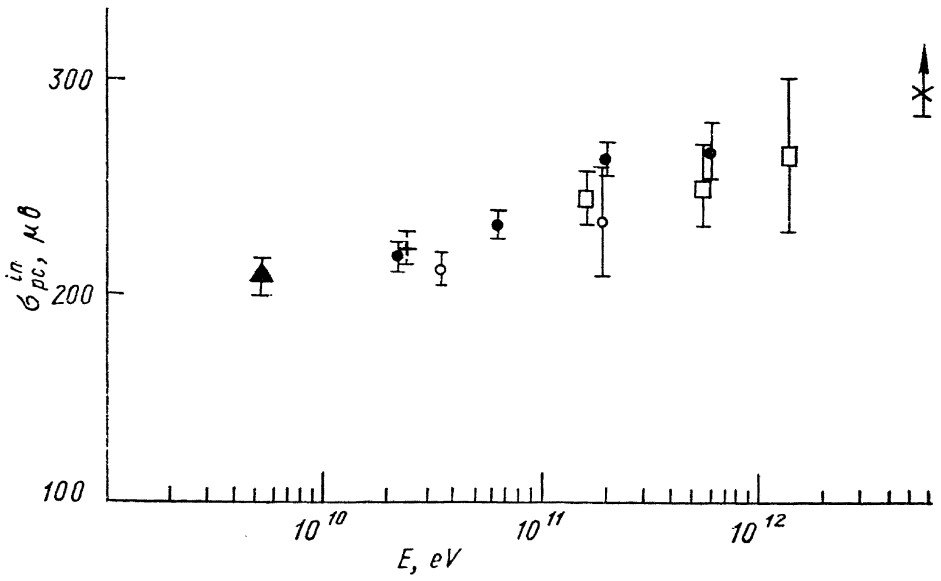

Fig. 4.

The best fit is actually a very slowly rising cross section:

$$\lambda_{Fe} = (132.0 \pm 8.6) - (3.5 \pm 3.8) \lg_{10} E.$$

The data of Grigorov et al. for the total inelastic cross section in carbon shown in Fig. 4 indicate more pronounced increase of σ_{pc}^{inel} with energy:

$$\sigma_{pc}^{inel} = (243 \pm 4) \left| 1 + (0.17 \pm 0.03) \lg \frac{E\,(eV)}{10^{11}} \right|, \; mb.$$

G. B. Yodh et al. [5] analysed the results of Grigorov et al. and the measurements of primary proton spectra and unaccompanied hadron spectra at different atmospheric depths. The authors show that σ_{p-air}^{inel} would increase with energy above 30 *GeV* from 235 *mb* and reach a saturation value of ∞ 350 *mb*, somewhere between 3000 and 10^4 *GeV* if the conventional primary proton spectrum ($\sim E^{-1.67}$) is used. If, on the other hand, the primary proton spectrum steepens above 2000 *GeV* in accord with Grigorov's recent measurements, σ_{p-air}^{inel} would rise to a broad maximum around $2 \cdot 10^3$ *GeV* and then decrease to a plateau value of 280 *mb* around $3 \cdot 10^4$ *GeV*.

It may be noted that a priori the hydrogen and nuclear cross section may not show the same energy dependence. However, it was checked by Balashov and Korenman [6] using Glauber's model that the increase in σ_{pp}^{inel} as suggested by Grigorov et al. is compatible with the observed behaviour of σ_{pc}^{inel}.

We do not have information on the cross sections of pions and kaons in the cosmic ray energy region. I shall only remind you that the measurements at Serpukhov last year gave rather unexpected results that these cross sections do not decrease with energy in the region $30 < E < 70$ *GeV* as expected from the extrapolation of accelerator data at $E < 30$ *GeV*. There is number of theoretical implications of these new facts (see excellent review in Ref. 7).

1.2. STRANGE PARTICLE PRODUCTION BY PIONS

The total cross section for strange particle production in πp and pp interactions increases with energy in the region $E < 30$ *GeV* [8, 9, 10]. In $\pi^- p$ collisions at 25 *GeV/c* the production of strange particles account for $\sim 20\%$ of $\sigma_{\pi^- p}^{inel}$. This increase is due to the rise of $\sigma_{K\bar{K}}$ whereas the probability of proton becoming a hyperon is small and roughly constant ($\sigma_{YK} \approx 1mb$). New results were submitted to this Conference [11, 12, 13]. The Dubna group studied $\pi^- p$ collisions at 5.1 *GeV/c* using the 1 meter propane bubble chamber with relatively high conversion probability of γ-quanta. The ratio $\frac{\sigma(\pi^- p \to \Sigma^0 K + \text{pions})}{\sigma(\pi^- p \to \Lambda^0 K + \text{pions})}$ was found to be close to 0.5 independent of multiplicity. For two body reactions this ratio $\frac{\sigma(\pi^- p \to \Sigma^0 K^0)}{\sigma(\pi^- p \to \Lambda^0 K^0)}$ equals about $^2/_3$ and seems to be independent of energy up to 16 *GeV/c* [12, 13].

1.3. PRODUCTION OF STRANGE ANTIBARYONS BY K^+ MESONS

Data reported to this Conference on the production of strange antibaryons by K^+ mesons [14, 15, 16] revealed several interesting features:

1. The total cross section for the production of $\bar{\Lambda}^0$ in $K^+ p$ interactions increases substantially with energy from 3.8 ± 1.2 μb at 5.0 *GeV/c* to 160 ± 30 μb at 12.7 *GeV/c*.

2. The cross section for $\bar{\Xi}^+$ production at 12.7 *GeV/c* (10 ± 3 μb) is about four times larger than the cross section for Ξ^- production at this energy ($2.5 \pm \pm 1.0$ μb) although the corresponding ratio for $\sigma(\bar{\Lambda}^0)/\sigma(\Lambda^0) \approx 0.4$. In K^-p interactions at 12.6 *GeV/c* the $\Lambda/\bar{\Lambda}$ and $\Xi^-/\bar{\Xi}^+$ production ratios are $\approx {}^{20}/_{1}$.

The Dubna group [12] found also a significant excess of events of the type 0 prongs + Λ^0 + Λ^0. It is not possible to explain this excess in terms of secondary interactions or Ξ^- production and absorption in the carbon nuclei.

1.4. SEARCH FOR QUARKS AND $\overline{He_3}$

There were two contributions to this conference on the fruitless search for quarks. Böhm et al. [66] (Aachen) were looking for fractionally charged particles in high energy air showers. Antipow et al. [25] searched for diquarks (particles of charge $-{}^4/_3$) at Serpukhov. Both groups give fairly low upper limits for production cross-section of these particles. But we are not going to be very unhappy about there results because instead we have the important discovery of antihelium-3 by the Serpukhov group [67] so that the members of antiworld are growing in number.

1.5. TOPOLOGIC CROSS SECTIONS

The topologic cross sections, i. e. the cross sections for a given number of prongs are fairly well known in the energy region below 30 *GeV*. At higher energies we have the recent data of L. W. Jones, D. D. Reeder et al. [2, 3, 4l

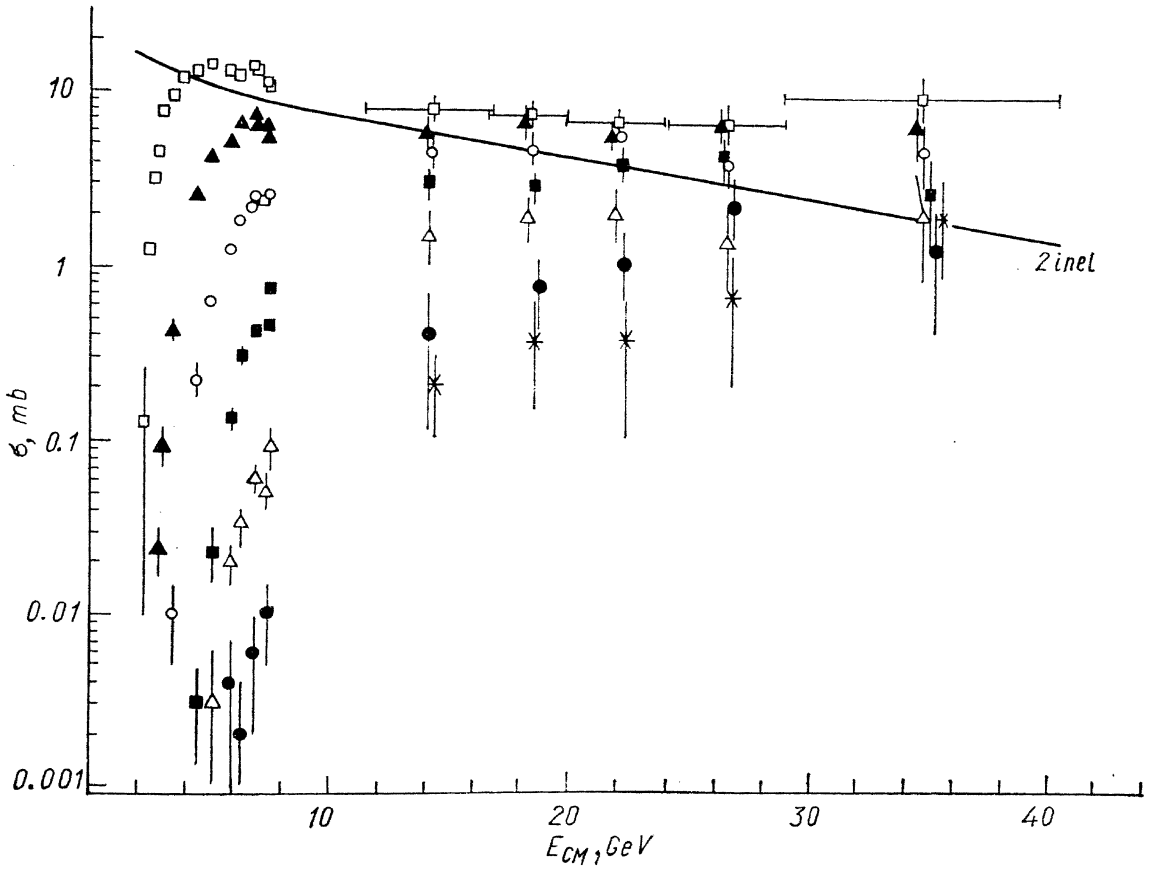

Fig. 5. *pp* interactions.

which replace less reliable data obtained earlier with the use of emulsions exposed to cosmic radiation. Data reported in Ref. [2, 3] are the fraction of events with given number of prongs. Assuming a **constant** inelastic p-p cross section of 29 mb one may calculate pp topologic cross section from these data. The results are shown in Fig. 5 together with the available data at energies below 30 GeV. One may notice a very sharp rise of each topologic cross section near the threshold. Earlier this year a striking regularity was found [17] that the topologic cross section for the production of k pairs of charged particles is 2^{k-1} times smaller than the cross section for the production of one pair of charges at the same c. m. energy per pair. The cosmic ray data do not seem to agree with this rule. Unexpectedly, only two-prong inelastic cross section is seen to fall down with energy, whereas the cross sections for 4, 6, 8, 10 and even 12 prongs are essentially constant in the whole range from 100 to 1000 GeV. The cross sections for higher multiplicities are still rising with energy but it is probable that they also reach a saturation value. Such a behaviour would be in agreement with the hypothesis of limiting fragmentation of Benecke, Chou, Yen and Yang [18].

1.6. ENERGY DEPENDENCE OF CROSS SECTIONS FOR INELASTIC CHANNELS

In this section I shall consider reactions with a given set of secondary particles in the final state, i. e. $\pi p \to p\pi\pi\pi$, $Kp \to pK\pi\pi\pi\pi$ etc. without taking into account possible intermediate states of short-lived resonances.

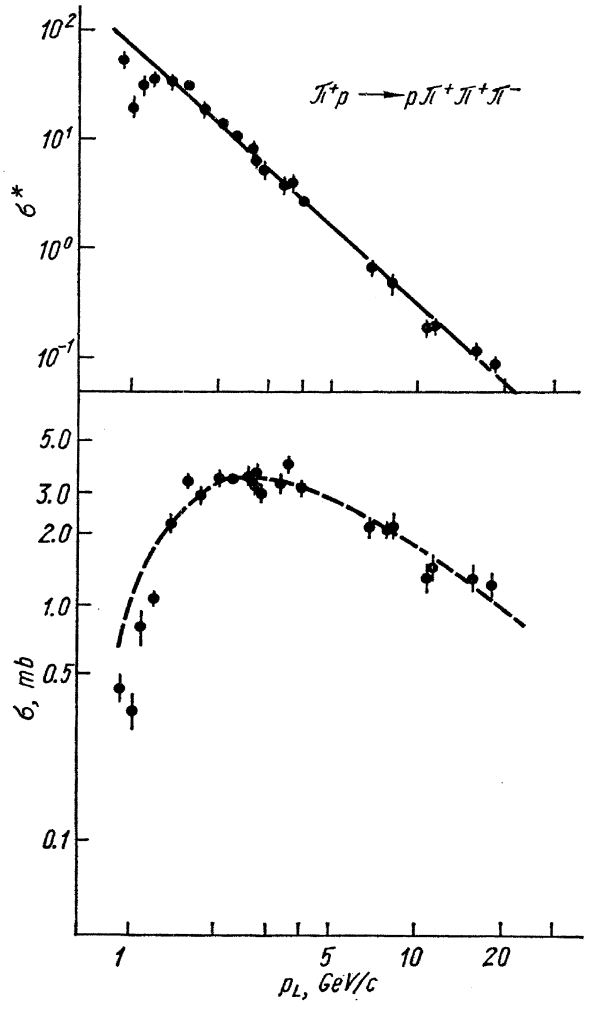

Fig. 6.

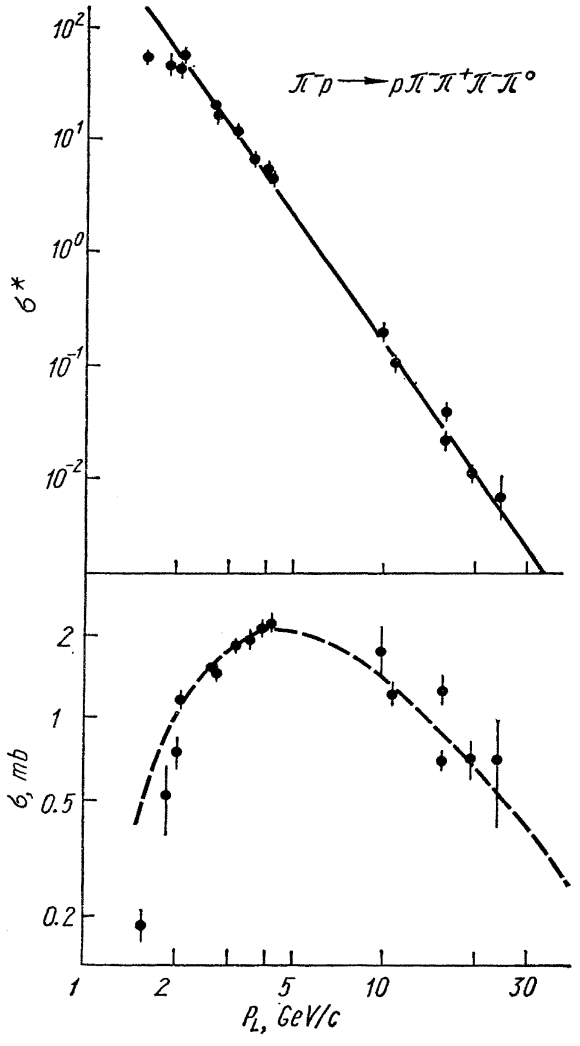

Fig. 7.

The cross section for a given inelastic channel rises from zero at the threshold to a certain maximum and then decreases with increasing laboratory momentum of the primary particle. Such an energy dependence is due to a competition of two factors: a dynamical factor $|T|^2$, where T is a transition matrix element, and a factor depending on the phase space volume available for secondary particles.

The cross section for a channel with N particles in the final state may be written as

$$\sigma_N = |T|^2_{\text{av}} \cdot \frac{\text{LIPS}}{\text{FLUX}}$$

where $|T|^2_{\text{av}}$ is the square of the transition matrix element averaged over all dynamical variables but the incoming energy, FLUX is the flux factor equal to $p_{CM} \cdot \sqrt{s}$ and LIPS — the Lorentz Invariant Phase Space volume is proportional to an integral

$$\int \prod_{i=1}^{N} \frac{d^3p_i}{p_i^0} \delta^4(\Sigma p_i - P).$$

Now, it seems reasonable to study the energy dependence of cross sections normalized to constant flux and phase space volume. It was first done by Muirhead and Poppleton [19] for $\bar{p}p$ annihilations into pions. Their conclusion was that the $|T|^2_{\text{av}}$ for all annihilations falls down approximately as s^{-5}.

T. Hofmokl and the author of this report [20] investigated this question for 40 inelastic channels of πp, Kp, pp and $\bar{p}p$ interactions. We introduced the quantity

$$\sigma^* = \frac{\sigma_N \cdot \text{FLUX}}{\text{LIPS}} \propto |T|^2_{\text{av}}$$

and showed that available data on cross sections may be well fitted by a power law

$$\sigma^* \propto p_{\text{lab}}^{-n},$$

where the values of the exponent, n, increase with the multiplicity of the final

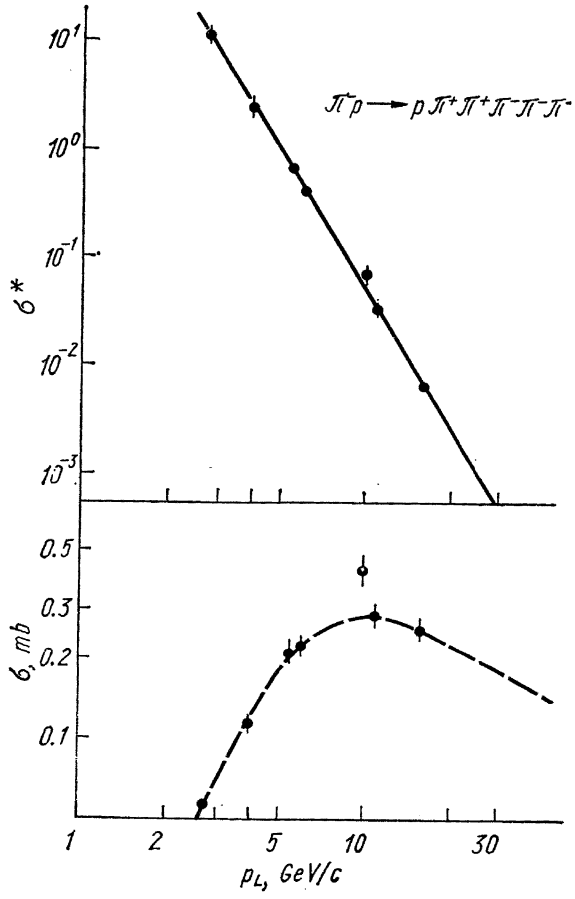

Fig. 8.

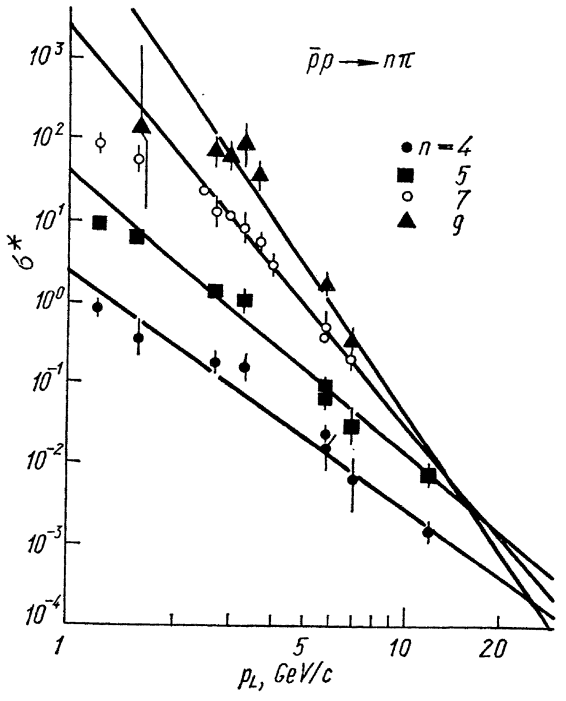

Fig. 9.

state. Figs. 6, 7, 8 show the examples of the fit for πp reactions in the log-log scales. The data fit the straight lines quite well except for the region very near the threshold where the points seem to fit better σ^*-constant lines. In other words, very near the threshold the cross section σ_N increases according to the phase space volume, as already noticed by Bartke and Sosnowski [21]. Investigation of γp reactions was done by Brandt [22] with essentially the same results. The reanalysis [23] of the data for $\bar{p}p$ annihilations into pions (see Fig. 9) showed that also in this case the exponent n depends on the multiplicity, contrary to the original conclusion of Muirhead and Poppleton. The average values of the exponent for different reactions are shown in Fig. 10. It is seen that for all kinds of reactions the exponent n is increasing with multiplicity

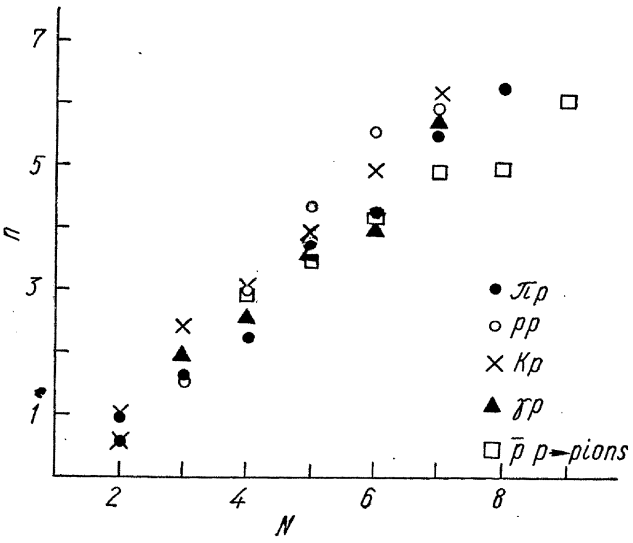

Fig. 10.

$$n = C + N - 2, \qquad (*)$$

where C is between zero and one. Before discussing the results of the next paper which is by Hansen, Kittel and Morrison [24] let me spend a little time discussing the physical meaning of the relation (*).

As it is well known, for $p_{\text{lab}} \to \infty$ the Lorentz Invariant Phase Space volume is proportional to p_{lab}^{N-2} where N is the multiplicity. Therefore the observed dependence of the exponent n on multiplicity N is caused mainly by this dependence of LIPS on the number of particles, N. Now, there is the physical meaning: with increasing p_{lab} the phase space volume is growing but (since transverse momenta are limited) it remains practically empty except for very small region. When we calculate σ^*, i. e. average $|T|^2$ over all (empty) phase space volume, we find that this quantity is rapidly decreasing with the increase in p_{lab}. In other words, even if σ = const we would find $\sigma^* \sim p_{\text{lab}}^{-n}$ with $n = C + N - 2$, $C = -1$.

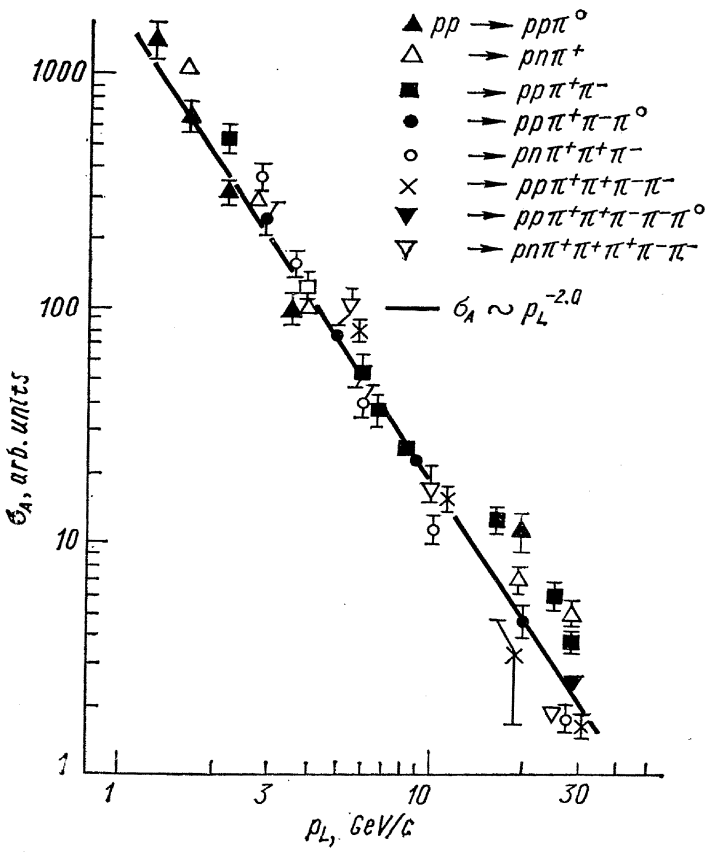

Fig. 11.

What we find in experiment is that the values of the exponent are larger than those expected for σ = = const what means that the $|T|^2$ decreases faster with energy because of some physical mechanism. Therefore it is the sudy of deviations of experimental values of n from those resulting from LIPS behaviovr

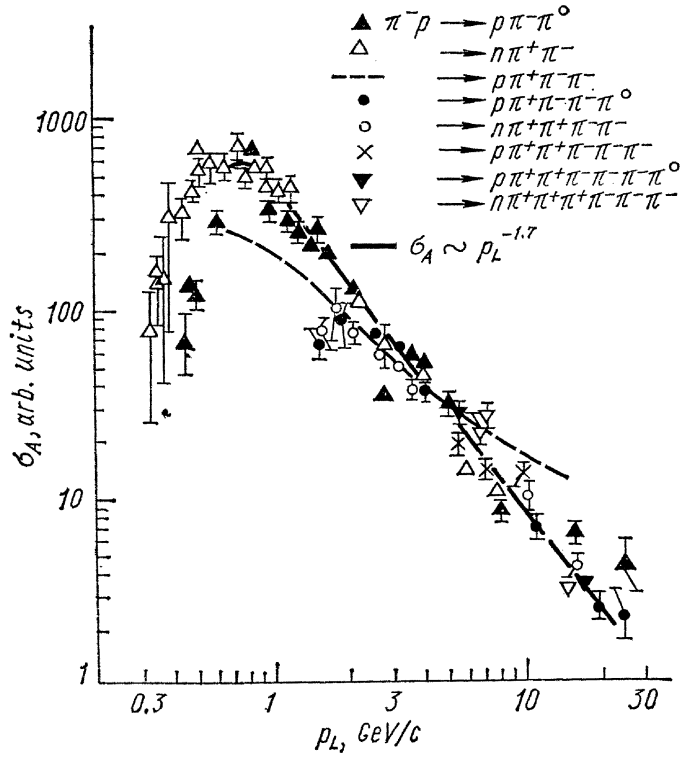

Fig. 12.

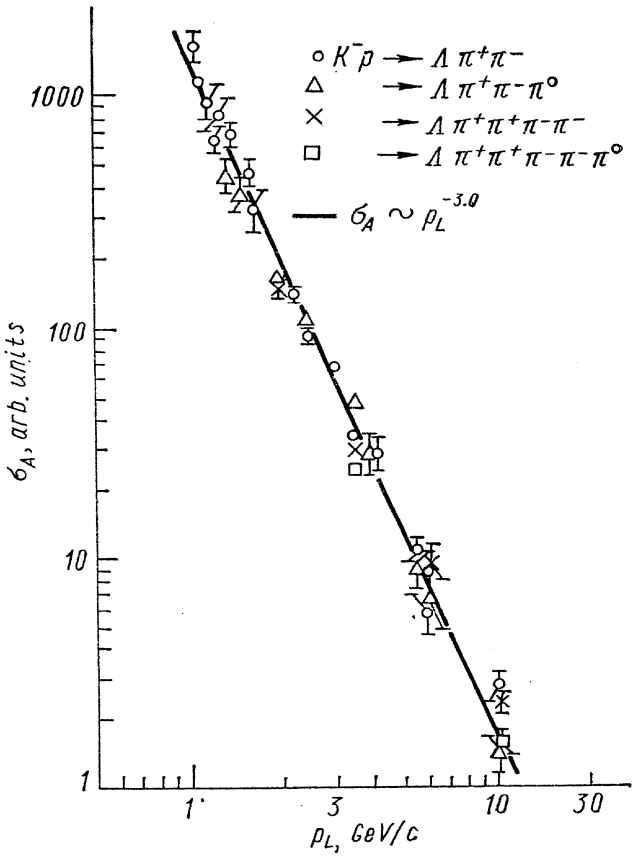

Fig. 13.

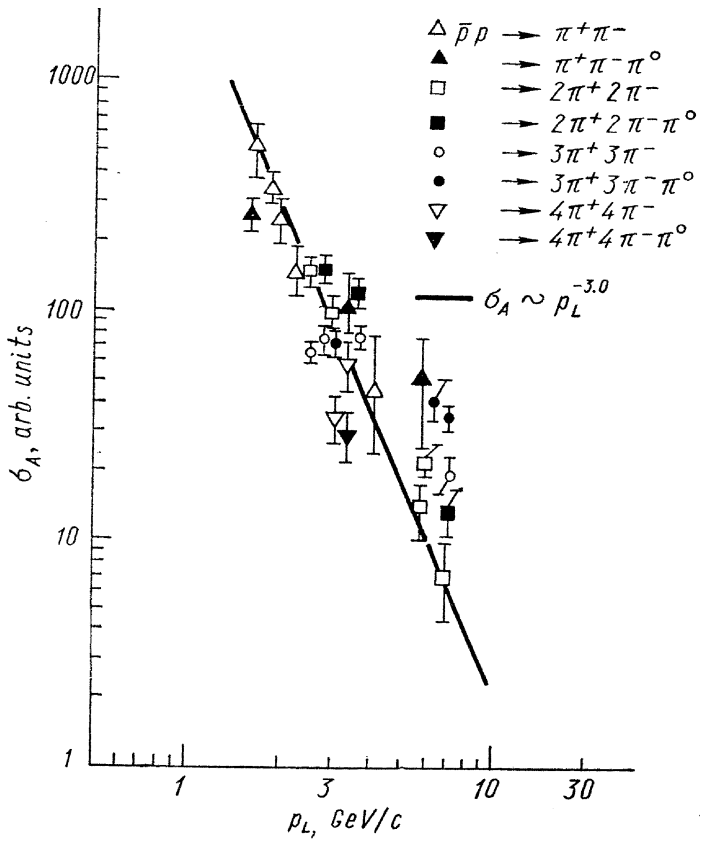

Fig. 14.

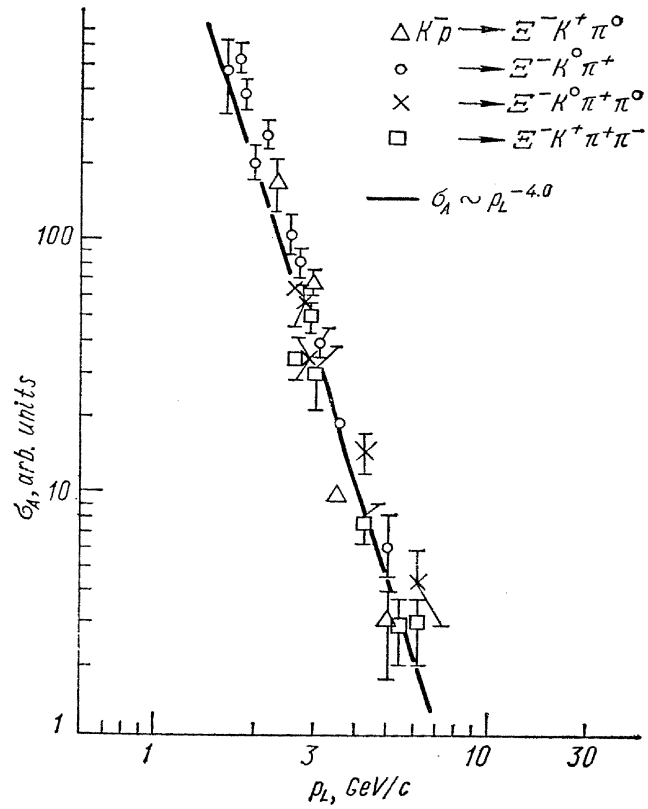

Fig. 15

Two-body		Many-body			
Exchange	n	Reaction	Exchange		n_A
			Dominant	Secondary	
Pomeron	0.2				
S=0 Meson	2.0	$(\pi, K, p)+p \rightarrow (\pi, K, N)+N+$ Pions	S=0 Meson	Pom., Bar	2
S=1 Meson	2.5	$K^- p \rightarrow \Lambda +$ Pions	S=1 Meson	Baryon	3
Baryon	4.0	$K^- p \rightarrow \Xi^- + K +$ Pions	Baryon	S=1 Meson	4

Fig. 16.

what may help understand physical mechanism of reactions. This line of reasoning was accepted by Hansen, Kittel and Morrison in their paper [24] in which they present extensive study of 64 different reactions including those of Y production by kaons.

They introduced the «asymptotic» cross section σ_A:

$$\sigma_A = \sigma_N \frac{p_{\text{lab}}^{N-2}}{LIPS} \cdot \text{const}$$

in which the asymptotic factor in LIPS, p_{lab}^{N-2} was taken into account. Available data could be fitted by the power law:

$$\sigma_A \sim p_{\text{lab}}^{-n_A}$$

where the values of the exponent, n_A, no longer depend on multiplicity but differ for reactions in which different exchange mechanisms dominate in a way similar to the one found of two-body reactions [26]. The results are presented in Figs. 11 — 16. For pion production reactions $n_A \approx 2$ what seems to agree with the simple-minded idea that in these reactions nonstrange meson exchange is expected to dominate with some less important contributions from pomeron and baryon exchange. For the reactions of Λ production by K^- mesons strange-meson exchange is expected to dominate and some baryon exchange is possible, but pomeron and non-strange meson exchange are impossible, hence a value of $n_A \approx 3$ is not unreasonable. Finally, the production of Ξ^- by K^- mesons requires baryon exchange, thus $n_A \approx 4$ like in the case of similar two-body reactions [26]. Now, one may question the word «asymptotic» that the authors of Ref. [24] use for σ_A and n_A. In the region $E < 30$ *GeV* in general many mechanisms contribute to many body reactions. We believe that diffraction dissociation, i. e. Pomeron exchange, which at present energies accounts for only part of a cross section will dominate many reactions at higher energies

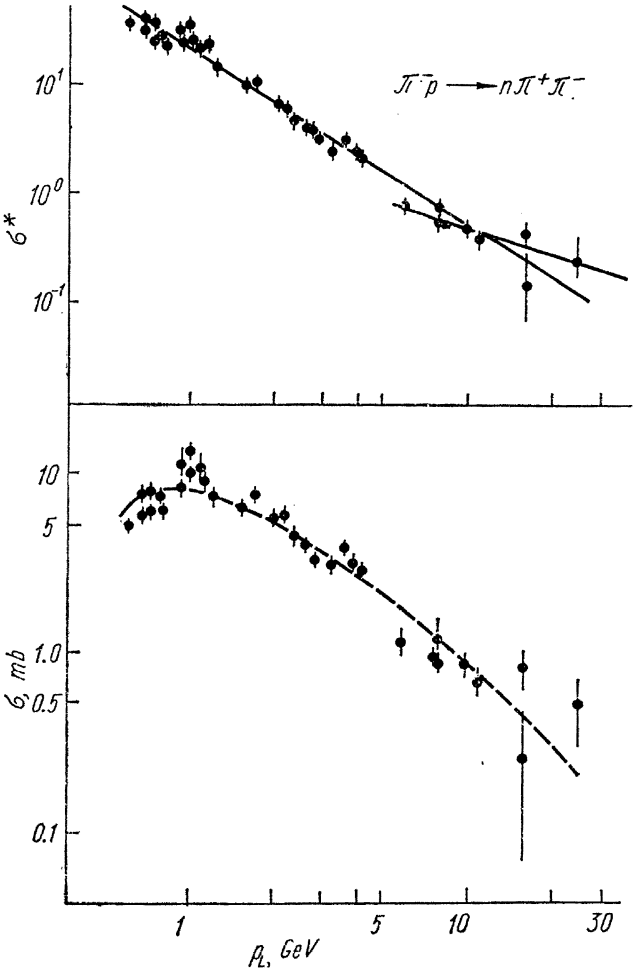

Fig. 17.

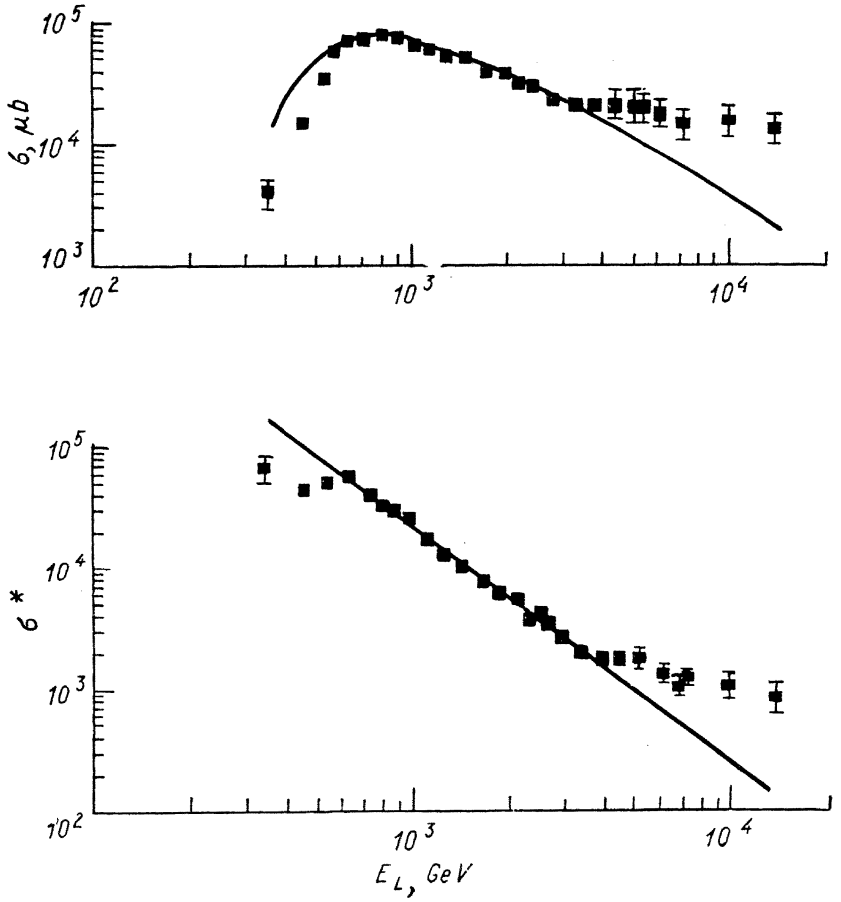

Fig. 18. $\gamma p \to p\pi^+\pi^-$, $E_{\min} = 0.60$, $\chi^2 = 40.423$, $E_{\max} = 3.00$, $N = -1.94 \pm 0.02$.

and if so, the cross sections for these reactions will become constant, independent of incident energy. There is already substantial experimental evidence that in three-, four- and even five body reactions Pomeron exchange, whenever possible, plays an important role. I will give you the details later. So one may speculate that for all those reactions where Pomeron exchange is not forbidden we shall have the asymptotic values:

$n = N - 3$ (Hofmokl — Wróblewski parametrization)

$n_A = 0$ (Hansen — Kittel — Morrison parametrization)

for the fit in high energy region only, because in the formula

$$\sigma^*_{(A)} \sim p^{n\,(A)}_{\text{lab}}$$

the exponent will be a decreasing function of energy.

Two examples are shown in Figs. 17 and 18 where you may see deviations from $n = \text{const}$ assumption at higher energies. To conclude the section on cross sections I should like to comment on a recent experimental check of a simple statistical model (I-spin dominance model). In such a model it is assumed that for a given number of produced pions, the relative probabilities of different charge configurations depend only on I and I_3. Tables of these probabilities have been given by Cerulus [27] and Shapiro [28]. Bartke [29] and Bartke and Czyzewski [30] have successfully applied such a model to high multiplicity πp interactions below 10 *GeV*. Firstly they checked the predictions of the model for the cross sections for fitted channels and secondly, they used fitted channels to calculate the «true» cross sections σ_k for the production of k pions (irrespectively of charge) and have reproduced the total inelastic cross section $\sigma^{\text{calc}}_{\text{inel}} = \Sigma\sigma_k \approx \sigma^{\text{exp}}_{\text{inel}}$. However, with in-

crease in incoming energy the cross sections for fitted channels are falling down, the percentage of no fit events (multiple π^0 production) is increasing and the disagreement with the predictions of a simple statistical model grows larger. Already at 16 *GeV/c* $\pi^- p$ $\sigma_{\text{inel}}^{\text{calc}}$ and $\sigma_{\text{inel}}^{\text{exp}}$ differ by about 20%. Let me quote few other examples:

1. Elbert et al. [31] found large disagreement with the predictions of the statistical model in π^0 production in 25 *GeV/c* $\pi^- p$ interactions (see Fig. 19).

2. Bar — Nir et al. [32] found very large differences in σ^{calc} and σ^{exp} for $\bar{p}p$ annihilations at 6.99 *GeV/c*.

3. Budagov et al. [33] measured cross sections for reactions $\pi^- p$ + neutral pions at 5 *GeV/c*. Also in this case experimental values differ considerably from those which may be predicted from fitted channels assuming *I*-spin independence.

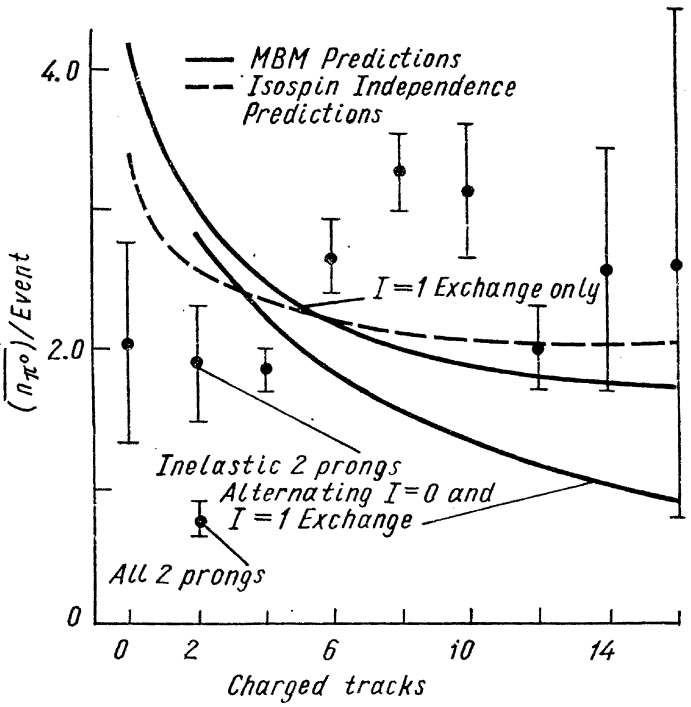

Fig. 19.

2. Multiplicity

2.1. MULTIPLICITY DISTRIBUTION

There have been many formulae proposed for the distribution of the number of charged prongs in high energy interactions. Some of them are listed here:

1. Brandt [34] has proposed to use the usual Poisson formula

$$P(n_\pm) = \frac{\langle n_\pm \rangle^{n_\pm}}{n_\pm!} \exp[-\langle n_\pm \rangle].$$

This formula was used for example by the ABBCCHW Collaboration [35] and by the Scandinavian Collaboration [36].

2. Wang [37] has proposed two models:

I. $\pi^+\pi^-$ are produced only in pairs («local charge conservation») so the Poisson formula governs the distribution of the number of **pairs** of charged pions **produced** (Wang model I):

$$P(n_\pm) = \frac{\left(\frac{1}{2}\langle n_\pm - \alpha \rangle\right)^{\frac{1}{2}(n_\pm - \alpha)}}{\frac{1}{2}(n_\pm - \alpha)!} \exp\left[-\frac{1}{2}\langle n_\pm - \alpha \rangle\right],$$

where α is the number of charged particles in the initial state.

II. The Poisson formula governs the distribution of the number of charged pions **produced** (Wang model II):

$$P(n_\pm) = \frac{\langle n_\pm - \alpha \rangle^{n_\pm - \alpha}}{(n_\pm - \alpha)!} \exp[-\langle n_\pm - \alpha \rangle].$$

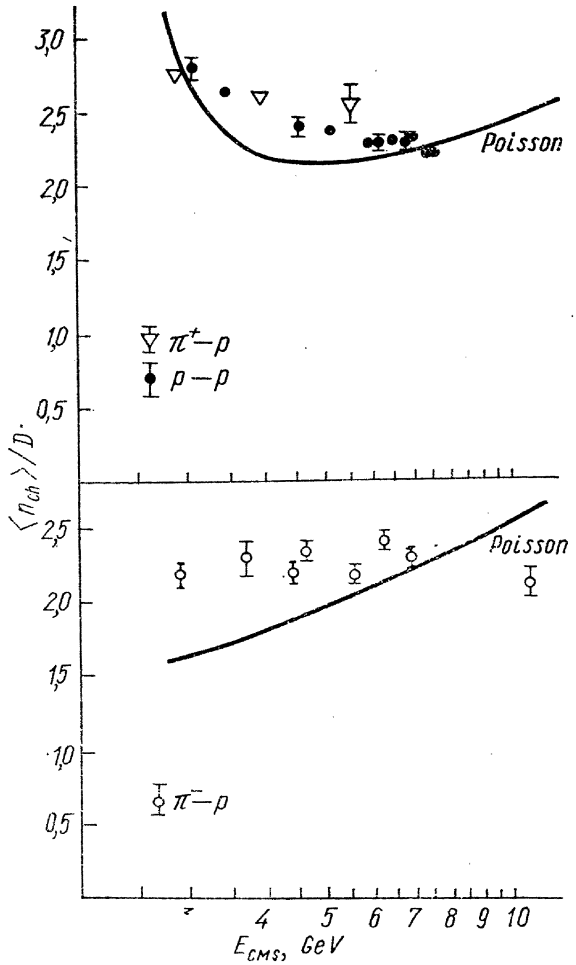

Fig. 20. Ratio of the average to the dispersion of the prong-number distribution.

3. In the multiperipheral model of Chew and Pignotti [38] it is assumed that the Poisson formula describes the distribution of the number of pions produced (irrespective of charge). Using additional assumptions, for example that there are only $I = 1$ and $I = 0$ exchanges alternating along the multiperipheral diagram one can obtain the distribution of charged prongs. In the following I will show you evidence that really no one of these formulae agrees with the data. In the paper submitted to this Conference Czyzewski and Rybicki [39] propose to use a parameter which is the ratio of the average multiplicity to the dispersion of the distribution of charged prong number. It is a very good characteristic integral measure of deviations of experimental data from the predicted distribution. As shown in Fig. 20 the experimental data are in general inconsistent with the predictions of the Poisson distribution.

Figs. 21 and 22 show the distribution of $n_\pm$ for pp interactions studied in Echo Lake experiment [2, 3, 4]. Wang model II is clearly excluded by the data and also Chew — Pignotti model gives rather bad agreement since it predicts too few many prong events. Wang model I seems to be the best choice. Let me mention also the paper of Elbert et al. [31] in which various models were compared to the experimental data of 25 *GeV/c* $\pi^- p$ interactions.

The authors found that:

a) Wang model II disagrees with data.

b) Wang model I gives fairly good fit for pion production but disagrees with data on the multiplicity of events with strange particles.

c) Chew — Pignotti model gives a good fit to the data if 0-prong events are excluded.

To conclude I will show you a slide (Fig. 23) in which I compared new experimental data with the predictions of Wang model I following the idea suggested by Czyzewski and Rybicki [39]. It is seen that in general Wang model I does not pass the test proposed by these authors. Czyzewski and Rybicki [39] were studying the distribution of charged prongs using the following new variables:

$$x = \frac{n_\pm - \langle n_\pm \rangle}{D},$$

$$y = D \cdot P(n_\pm),$$

where $D = [\langle n_\pm^2 \rangle - \langle n_\pm \rangle^2]^{1/2}$ is the dispersion of the experimental distribution.

Fig. 24 shows the experimental data in these variables for $\pi^- p$, $\pi^+ p$ and pp interactions. It is seen that all the data (including 0-prong events) follow the same curve which represents the universal distribution of the number of charged prongs. This curve can be well approximated by the following formula

$$y = 2d \cdot e^{-d^2} \frac{d^{2(dx+d^2)}}{\Gamma(dx + d^2 + 1)}$$

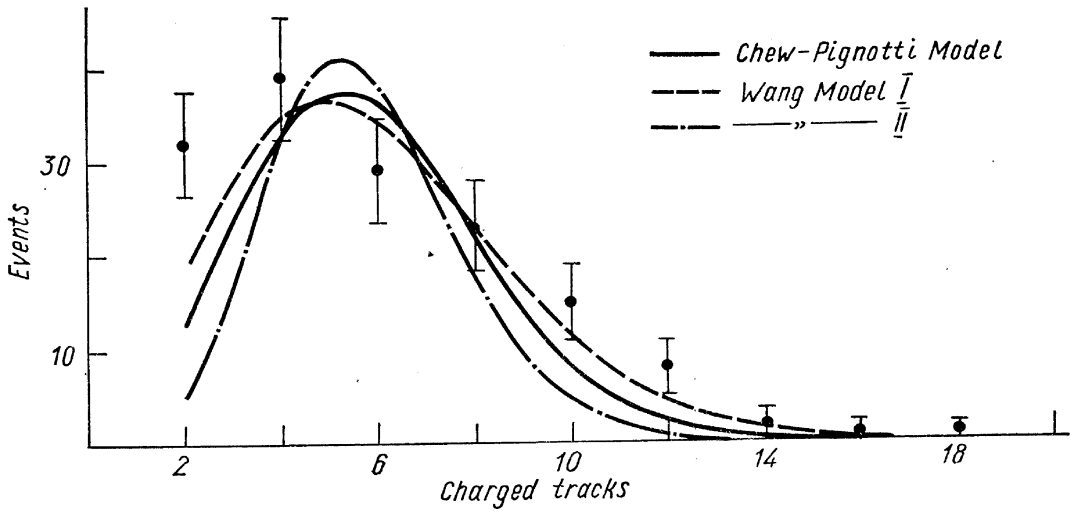

Fig. 21. pp charged multiplicity distribution. $71 \leqslant E \leqslant 146$ GeV (150 events).

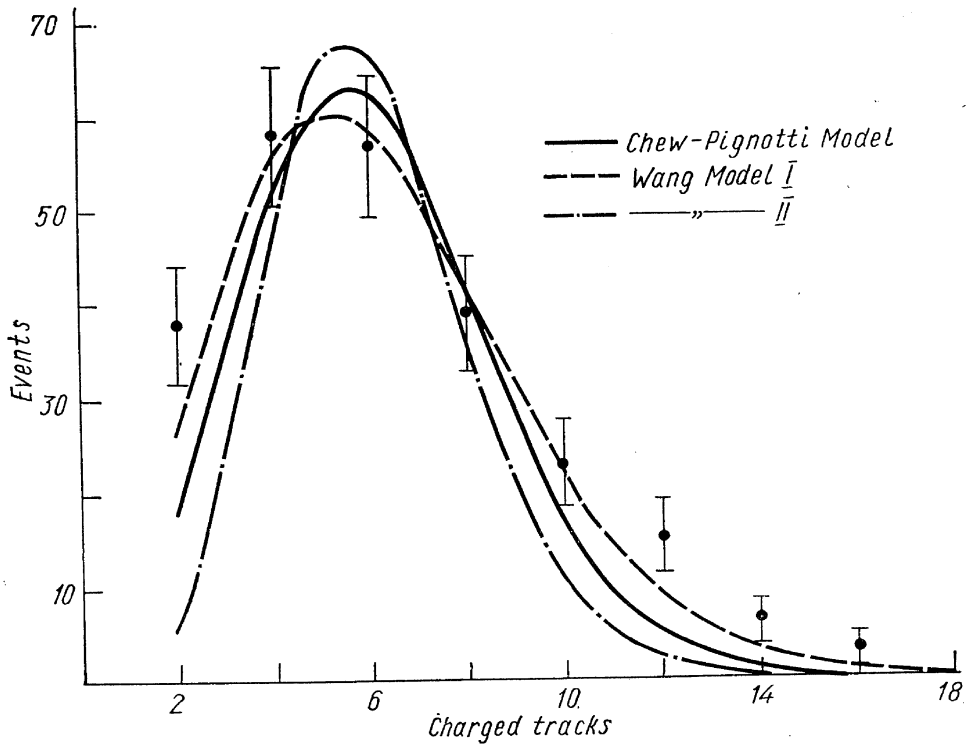

Fig. 22. pp charged multiplicity distribution. $146 \leqslant E \leqslant 211$ GeV (239 events).

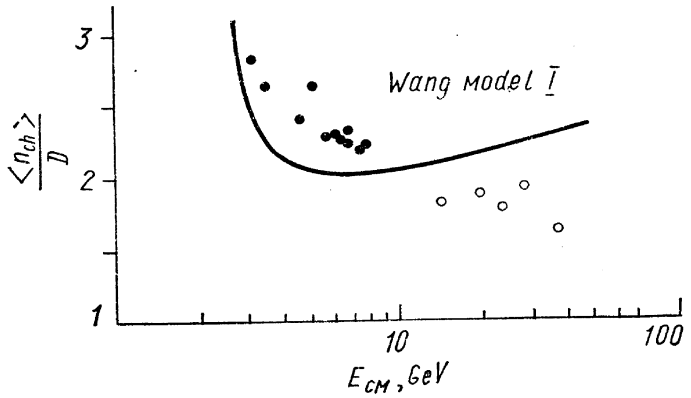

Fig. 23.

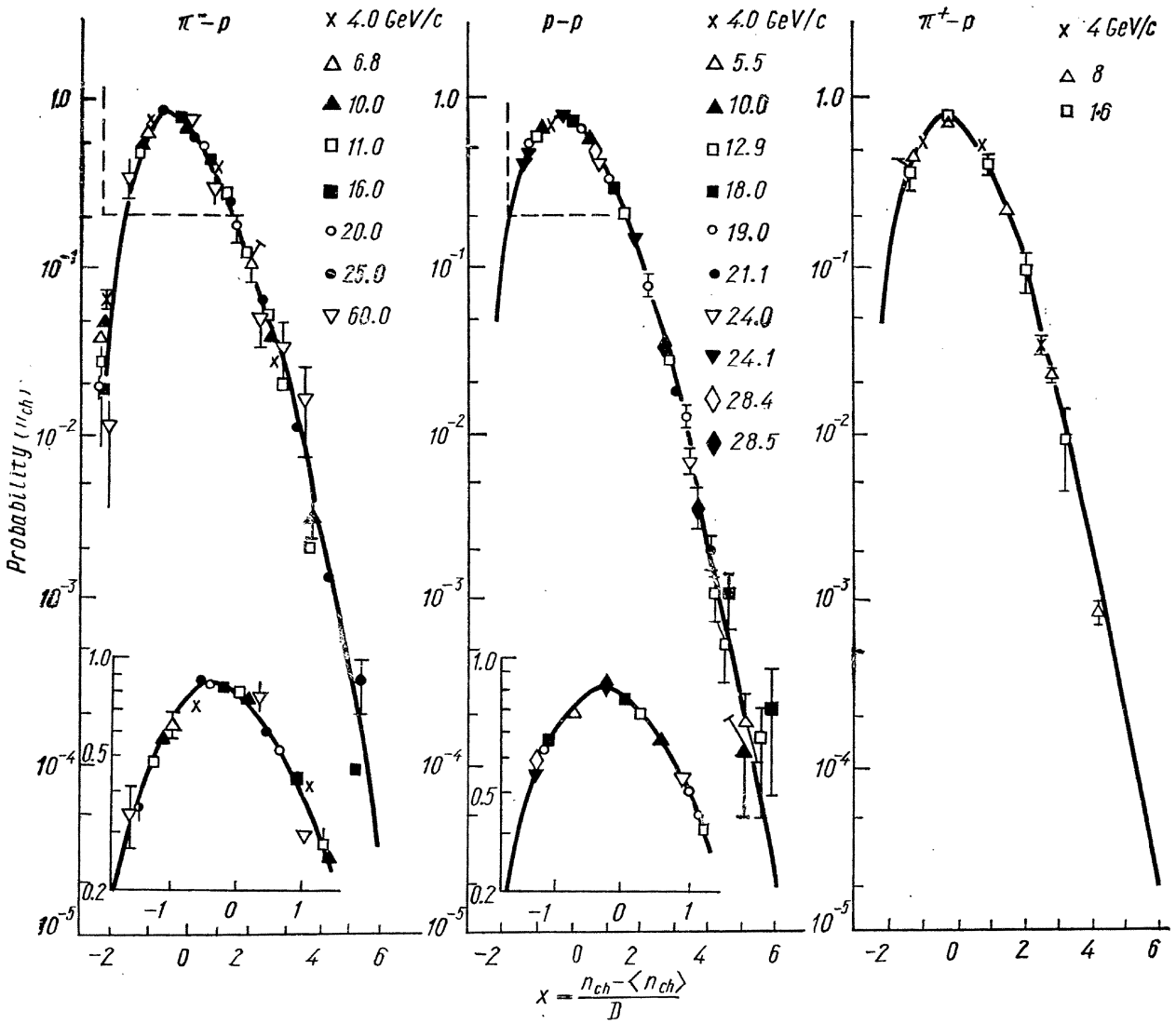

Fig. 24.

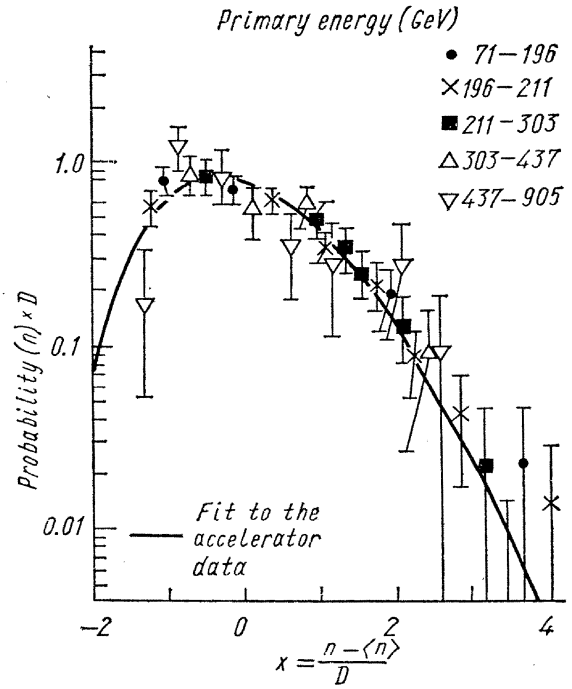

Fig. 25. $pp \to n$ charged particles (Jones et al.).

where d is the only parameter to be fitted. The curve shown in Fig. 24 was drawn for $d = 1.8$. Fig. 25 shows the cosmic-ray data for pp interactions [2, 3, 4]. This curve is the same as in Fig. 24. The formula of Czyzewski and Rybicki gives a good fit to all experimental data *.

2.2. AVERAGE MULTIPLICITY OF CHARGED PARTICLES

The average multiplicity of charged particles and its dependence on energy are very important since it may distinguish between various models of multiple production. Let me remind you that the models of statistical type predict a power dependence

$$\langle n_{\pm} \rangle = bE^{a}.$$

Whereas multiperipheral models [38] favour a logarithmic dependence

$$\langle n_{\pm} \rangle = C \log E + d.$$

Fig. 26 shows the results of Jones, Reeder et al. [2, 3, 4] for pp interactions together with the results of fits to various models. There is a definite preference for a logarithmic dependence over the power law suggested by statistical models.

Fig. 27 shows the same cosmic ray data together with a complete set of data at lower energies [39]. It is seen that the logarithmic fit to cosmic data (solid line) does not accomodate points below 20 *GeV*. Dashed line shows the logarithmic fit to accelerator data alone [39]. One may comment that the observed slow increase of the average multiplicity is connected with the behaviour of pp topologic cross sections. As discussed in the previous section topologic cross sections for 4, 6, 8, 10 and 12 prongs remain practically constant up to 1000 *GeV*. These cross sections account for about 75% of the total inelastic cross section. The increase of the average multiplicity results from the slow decrease in $\sigma^{\text{inel}}_{\text{2prongs}}$ and from the increase of cross sections for higher multiplicities.

We do not have such a good data for πp interactions. Fig. 28 shows experimental results for $\pi^- p$ interactions. Included are the results obtained in emulsions

* It may be remarked that this formula is a generalization of the Poisson distribution for noninteger parameter x in which case the factorial has to be replaced by a Γ-function.

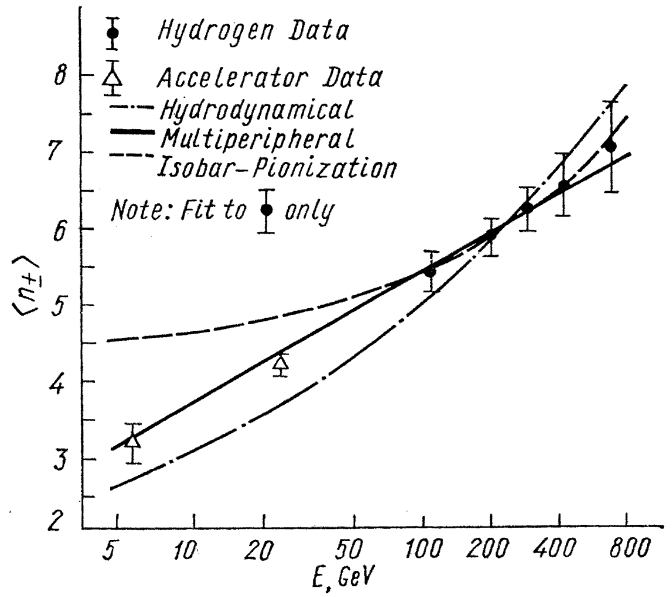

Fig. 26.

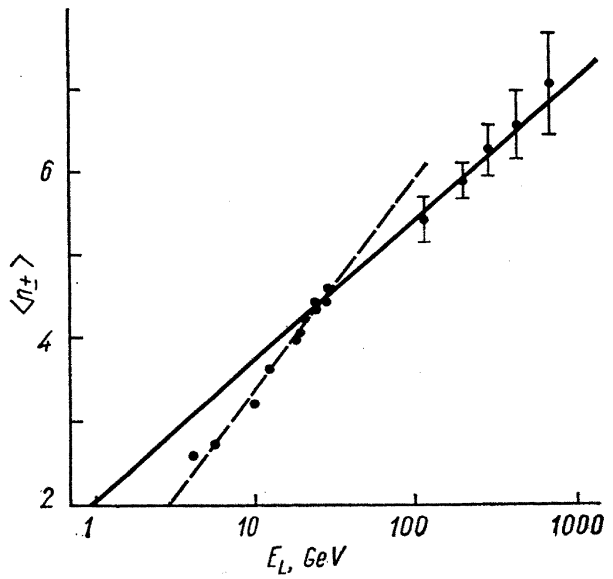

Fig. 27.

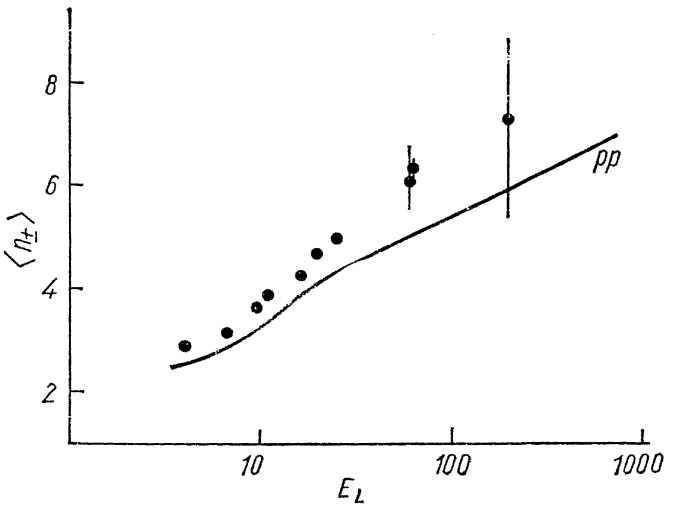

Fig. 28. $\pi^- p$ interactions.

at 60 *GeV/c* [40, 41] and 200 *GeV/c* [42]. Solid line is a hand drawn curve through the *pp* points of Fig. 27. Points for $\pi^- p$ interactions lie higher than the curve for *pp* but it is largely due to the fact that in *pp* collisions there is less c. m. energy available for pion production than in πp collisions at the same E_{lab}. If one accounts for the nucleon mass which can not be spend for pion production the results for *pp* and $\pi^- p$ are closer to each other (Fig. 29). To conclude this section I should like to mention new results for the average multiplicity in the interactions with nuclei. Fig. 30 shows the results of Echo Lake experiment [2, 3, 4] for *p*-Carbon interactions together with older data of Dobrotin et al. [43]. The average multiplicity is not very much higher than this for proton interactions.

Dalkhazav et al. [41] studied π^--interactions at 60 *GeV/c* in emulsion enriched in hydrogen as well as in normal one. By comparing results with these two kinds of emulsion they found average multiplicity of interactions with different nuclei. The results are:

Nucleus	$\langle n_s \rangle$
H	6.3 ± 0.2
C, O	7.4 ± 0.3
Ag, Br	9.9 ± 0.7

These results do not include obvious evaporation tracks.

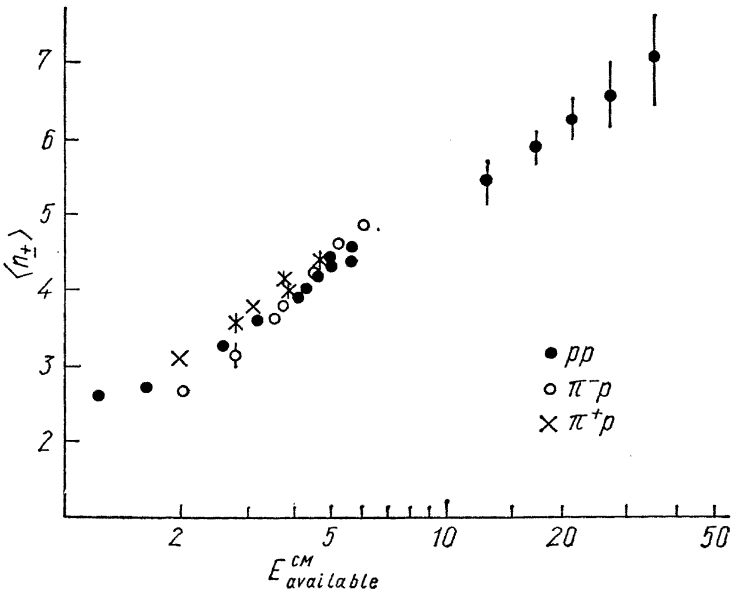

Fig. 29.

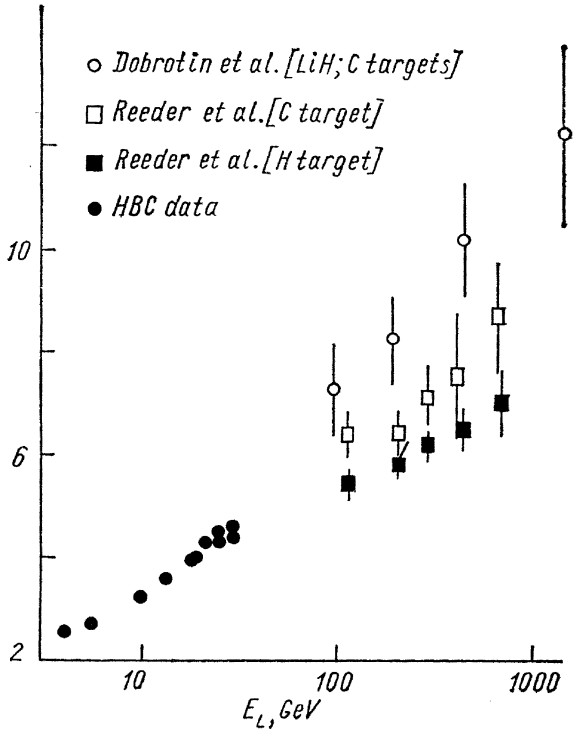

Fig. 30.

3. Single Particle distributions

3.1. ANGULAR DISTRIBUTIONS

Before reporting new results presented to this Conference I would like to show you three slides. The first two (Fig. 31 and 32) show angular distributions of protons and pions for constant multiplicity (six prong events $\pi^- p \to p 3\pi^- 2\pi^+$) and different incoming energy. The third (Fig. 33) shows angular distributions for constant energy (60 *GeV* π^--interactions [40]) and different multiplicities. The figures illustrate well known fact that anistropy of angular distribution increases with the increase of the average c. m. energy per particle.

Cosmic ray physicists use other representations for angular distributions. The first one is the distribution of the quantity

$$\lambda = \log \tan \theta_{\text{lab}} = \log \tan \frac{\theta_{CM}}{2} - \log \gamma_c$$

the second is so called Duller — Walker plot of $\log \frac{F(\theta_{\text{lab}})}{1 - F(\theta_{\text{lab}})}$ vs. λ ($F(\theta_{\text{lab}})$ is the fraction of particles emitted at angle smaller than θ_{lab}). All three ways of presenting data are compared in Fig. 34. Isotropic c. m. angular distribution corresponds to a Gaussian distribution in λ with $\sigma = 0.36$ and to a straight line of slope 2 in the Duller — Walker plot. Fig. 35 shows data of Fig. 33 in the λ coordinate. Fig. 37 shows selected data for highly anisotropic jets. A two-maximum structure is visible.

Let us pass now to the data from Echo Lake [2, 3, 4]. Fig. 36 shows the Duller-Walker plot for energy bin 146—211 *GeV*. There is a clear two-branch structure corresponding to a nonisotropic distribution. The author fit the data to the distribution of the form $A + B \cos^M \theta_{CM}$. The fit is relatively insensitive to the power of $\cos \theta_{CM}$ but M is at least as large as 2. The degree of anisotropy B is well specified: $B \approx 0.55$ at $\sim$ 185 *GeV* and 0.7 at $\sim$ 400 *GeV*.

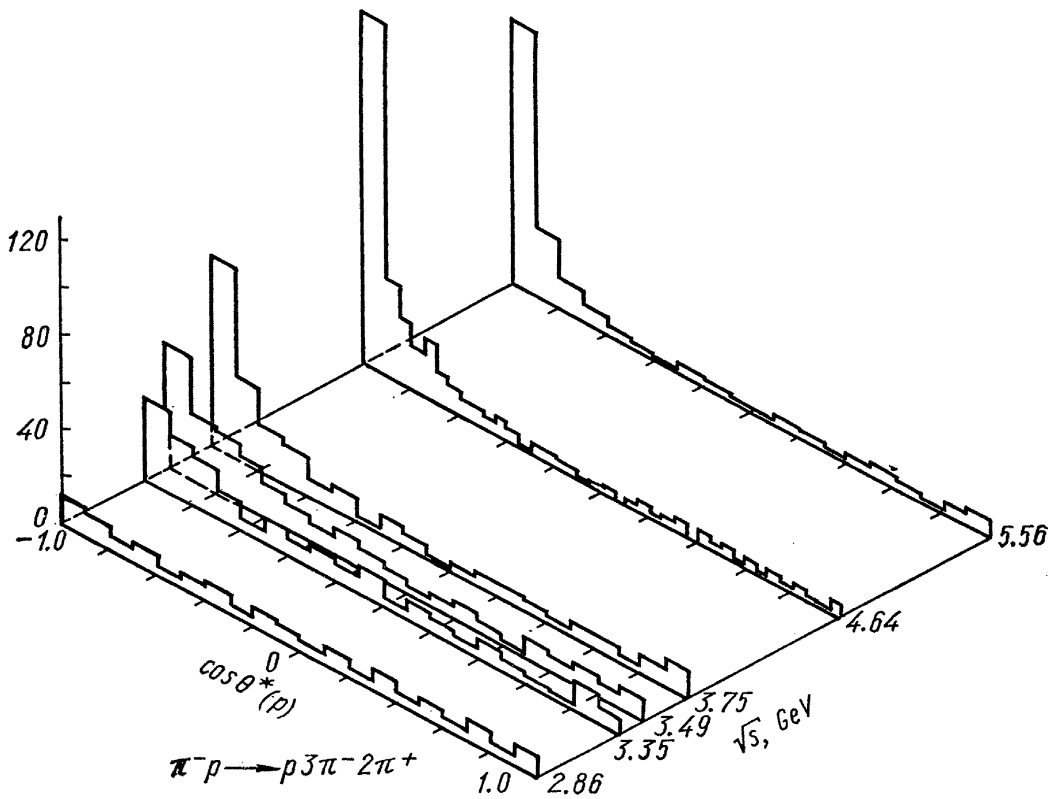

Fig. 31.

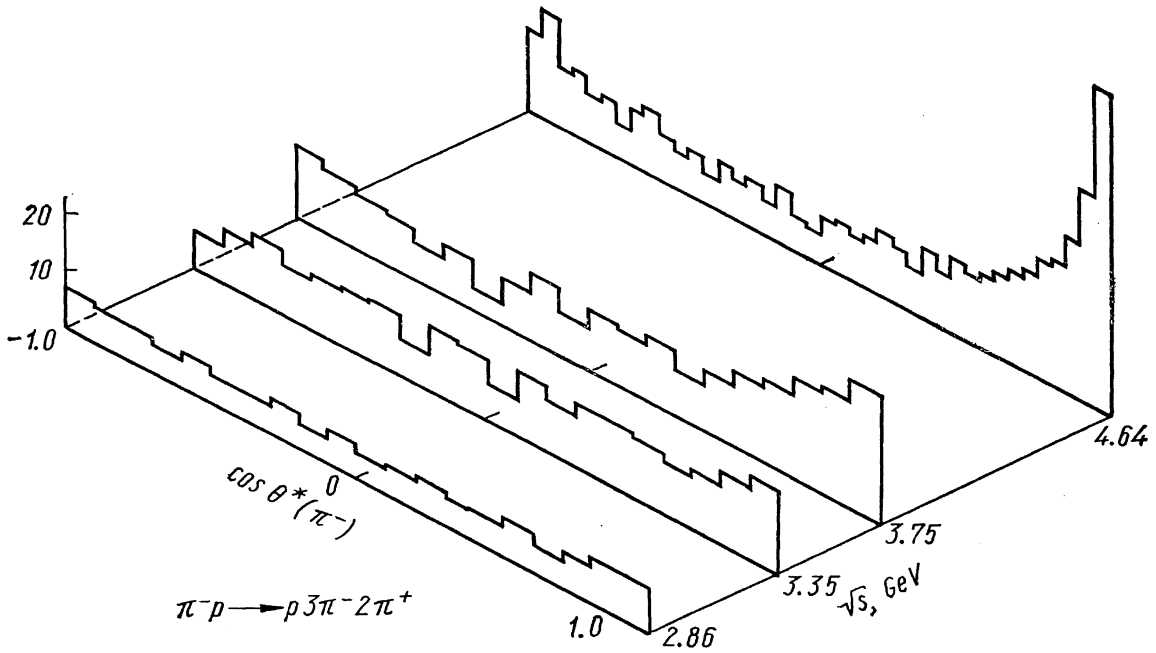

Fig. 32.

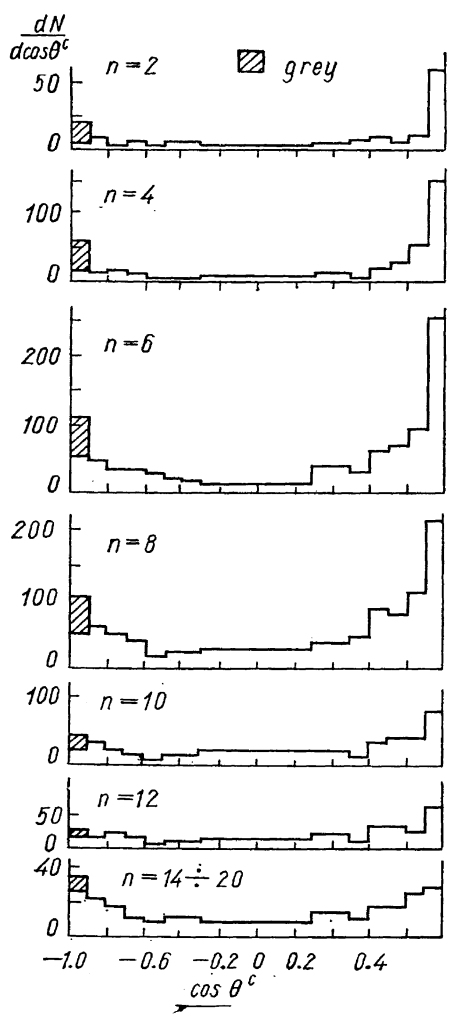

Fig. 33.

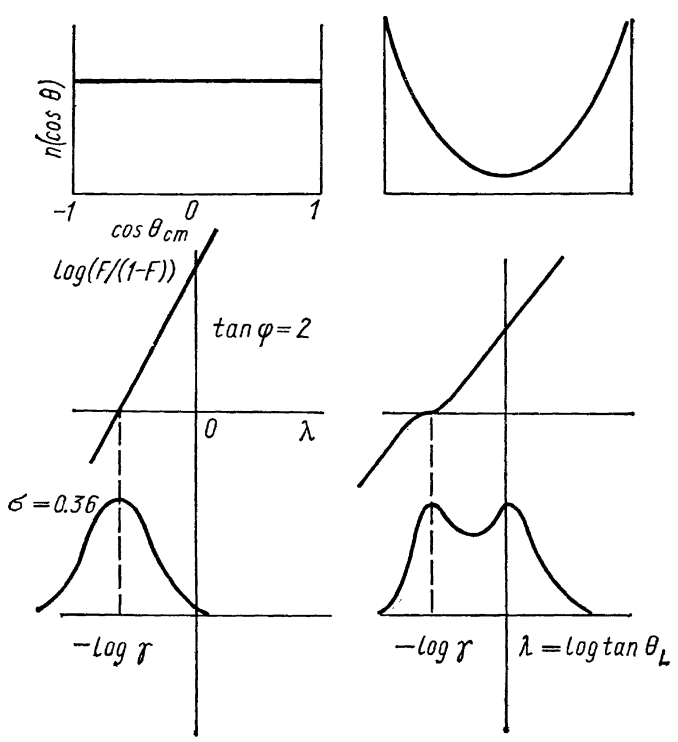

Fig. 34.

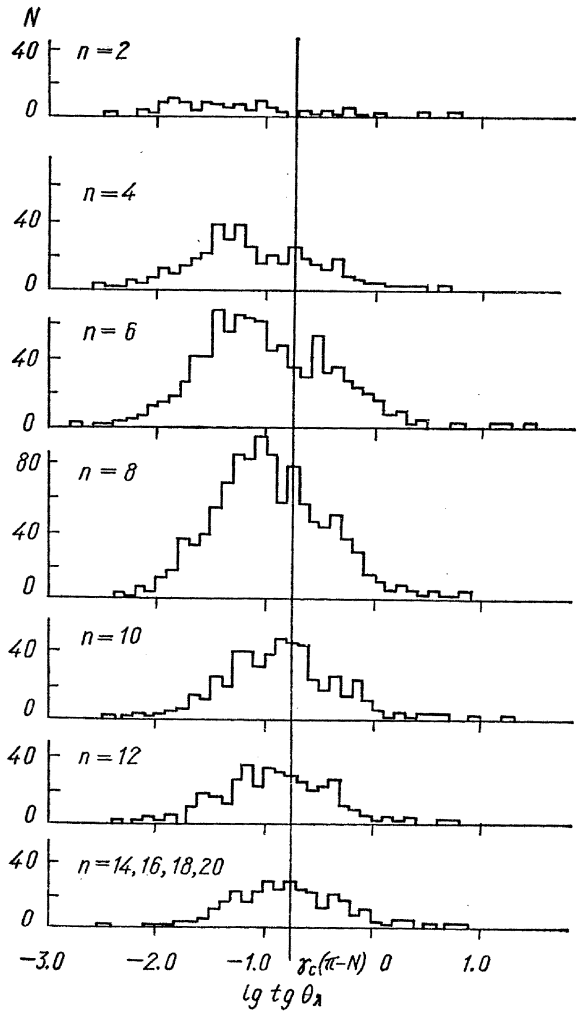

Fig. 35.

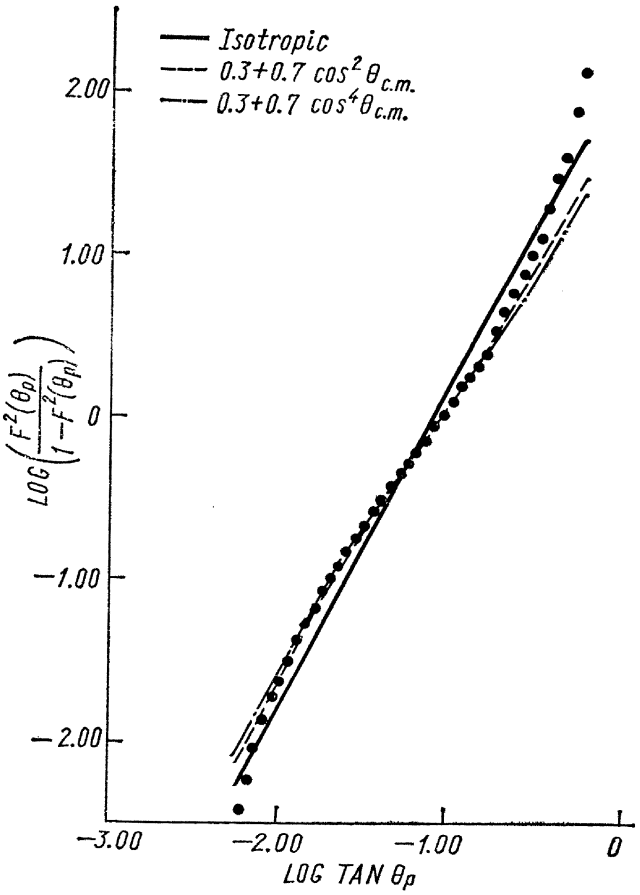

Fig. 36. Hydrogen data. 146—211 *GeV* (192 events).

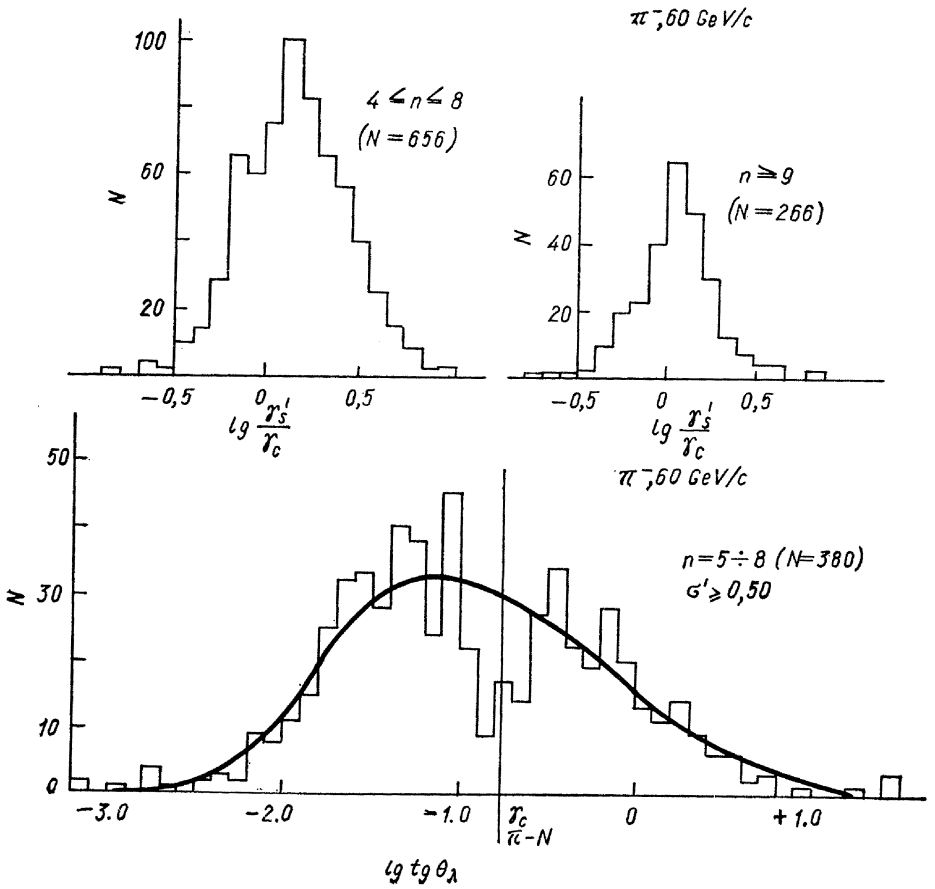

Fig. 37.

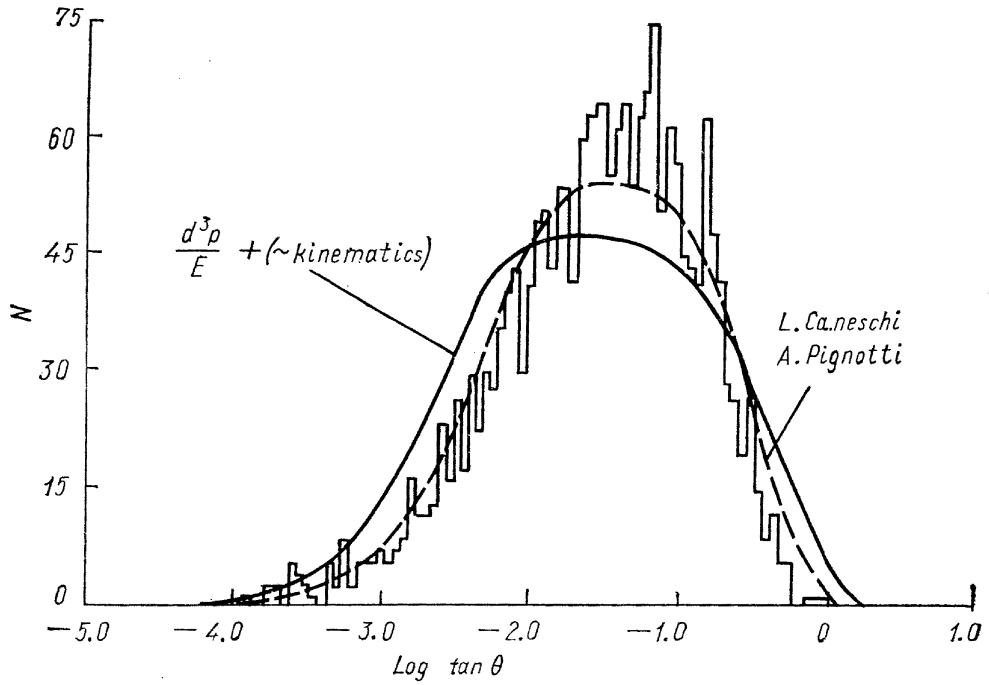

Fig. 38. Number of charged tracks (192 events at 175 *GeV*).

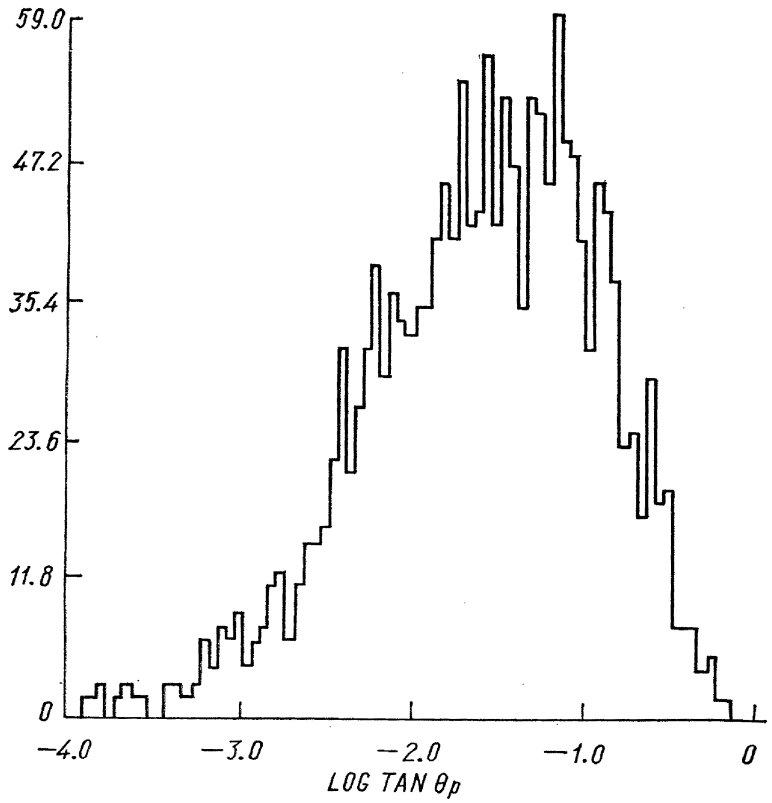

Fig. 39. Number of charged tracks. Hydrogen data. 211—303 *GeV* (132) events.

Figs. 38 and 39 show the results from Echo Lake in λ coordinate for two energy bins. The data shown were recently analyzed by Caneschi et al. [44] who showed that the multiperipheral model of Caneschi and Pignotti [45] gives good description of the data although the parameters fitted were the same as used at 30 *GeV*.

3.2. MOMENTUM DISTRIBUTIONS

Fig. 40 shows the average values of the transverse momentum for different multiplicities in 16 *GeV/c* $\pi^- p$ interactions [35]. Experimental $\langle p_\perp \rangle$ does not agree with the value predicted by LIPS for low multiplicities but for higher multiplicities the two values get closer. This is simply another manifestation of already mentioned fact that for small enough $\langle E_{CM} \rangle$ per particle the interactions are becoming «phase space like». In the paper submitted to this conference O. Balea et al. [46] propose a new parametrization for $\langle p_\perp \rangle$. They introduce a quantity

$$A_{ij} = \frac{\langle p_\perp^{LIPS} \rangle_i - \langle p_\perp \rangle_i^{\exp}}{p_j^{CM}},$$

where i denotes particular channel with n particles and j — incoming energy; p_j^{CM} is the total c. m. momentum at given energy.

It appears that A_{ij} is a simple exponential function of $B_{ij} = \Sigma m_i / E_j^{CM}$ where Σm_i is the sum of masses of secondary particles:

$$A_{ij} = \exp [- a_j (B_{ij} - B_{ij}^0)].$$

This may be a useful parametrization of experimental data (Fig. 41). The distributions of $p_\perp$ and p_L^{CM} were studied in many papers submitted to this Conference [47, 48, 49, 50, 51, 36]. The results are essentially the same as those found previously [52, 53]. The distributions are well fitted by formulae:

$$dN(p_L^{CM}) \sim \exp(- a p_L^{CM})\, dp_L \quad (*)$$

$$dN(p_\perp) \sim p_\perp^{3/2} \exp(- b p_\perp)\, dp_\perp \quad (**)$$

$$dN(p_\perp^2) \sim$$

$$\sim \exp[- c p_\perp^2 + d p_\perp^4]\, dp_\perp^2 \quad (***)$$

where the coefficients a, b, c and d depend both on multiplicity and incoming energy. It is interesting that formula (**) seems to be still valid at $\sim 2 \cdot 10^5$ *GeV* [65]. The value of $\langle p_\perp \rangle$ determined at this energy is 0.60 ± 0.05 *GeV/c*. The compilation of $\langle p_\perp \rangle$ determinations at cosmic ray energy given in [65] shows that $\langle p_\perp \rangle$ log E_{lab}. N. N. Biswas et al. [50] studied $\pi^\pm p$ interactions at 18.5 *GeV/c*

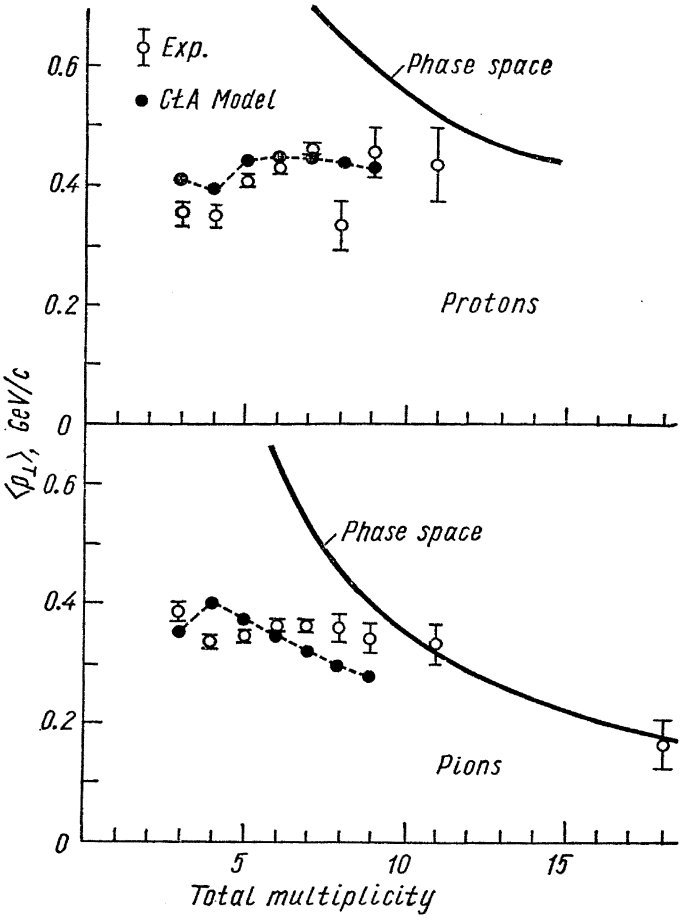

Fig. 40. $\pi^- p$ interactions at 16 *GeV/c*.

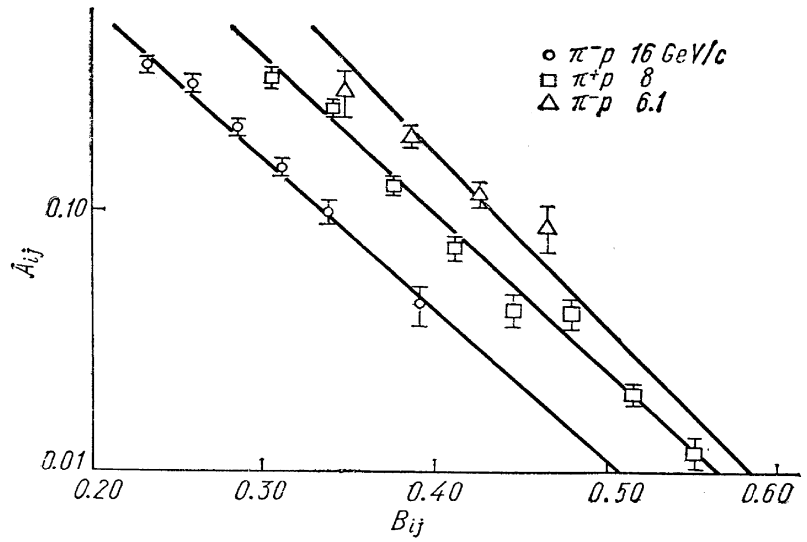

Fig. 41.

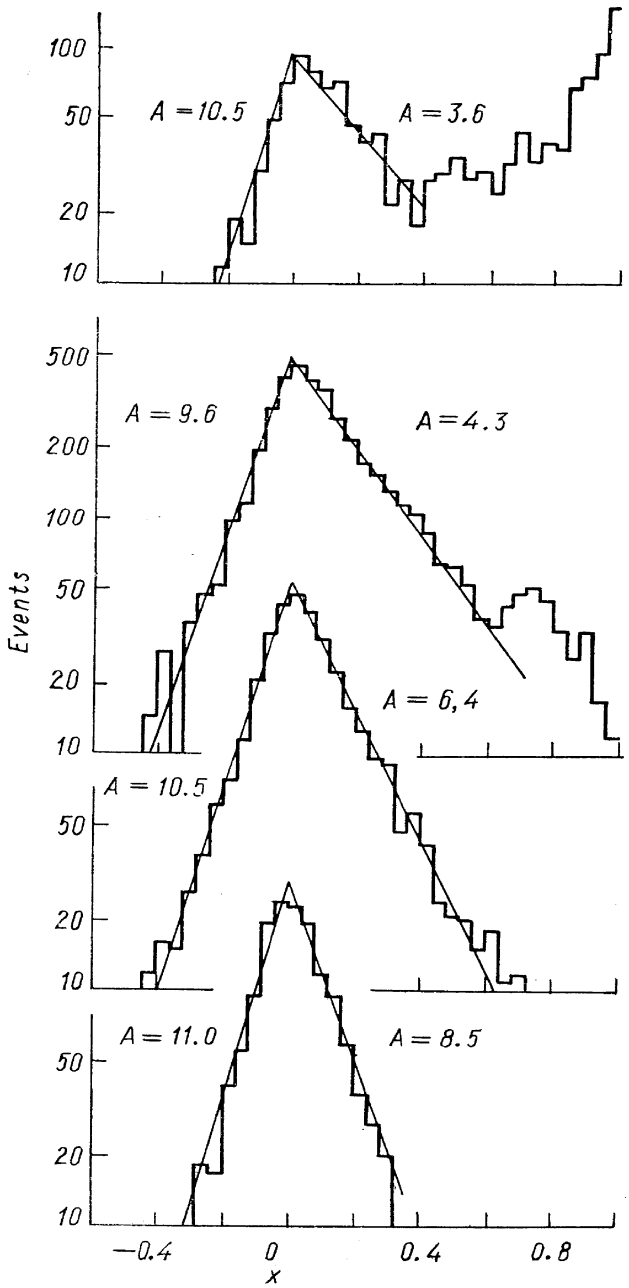

Fig. 42.

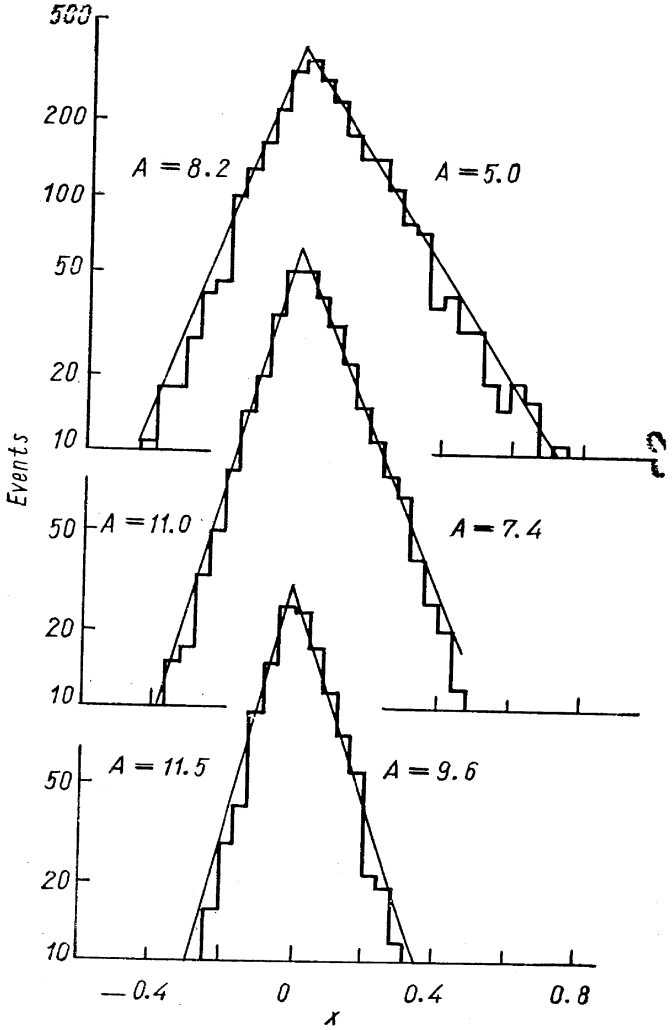

Fig. 43.

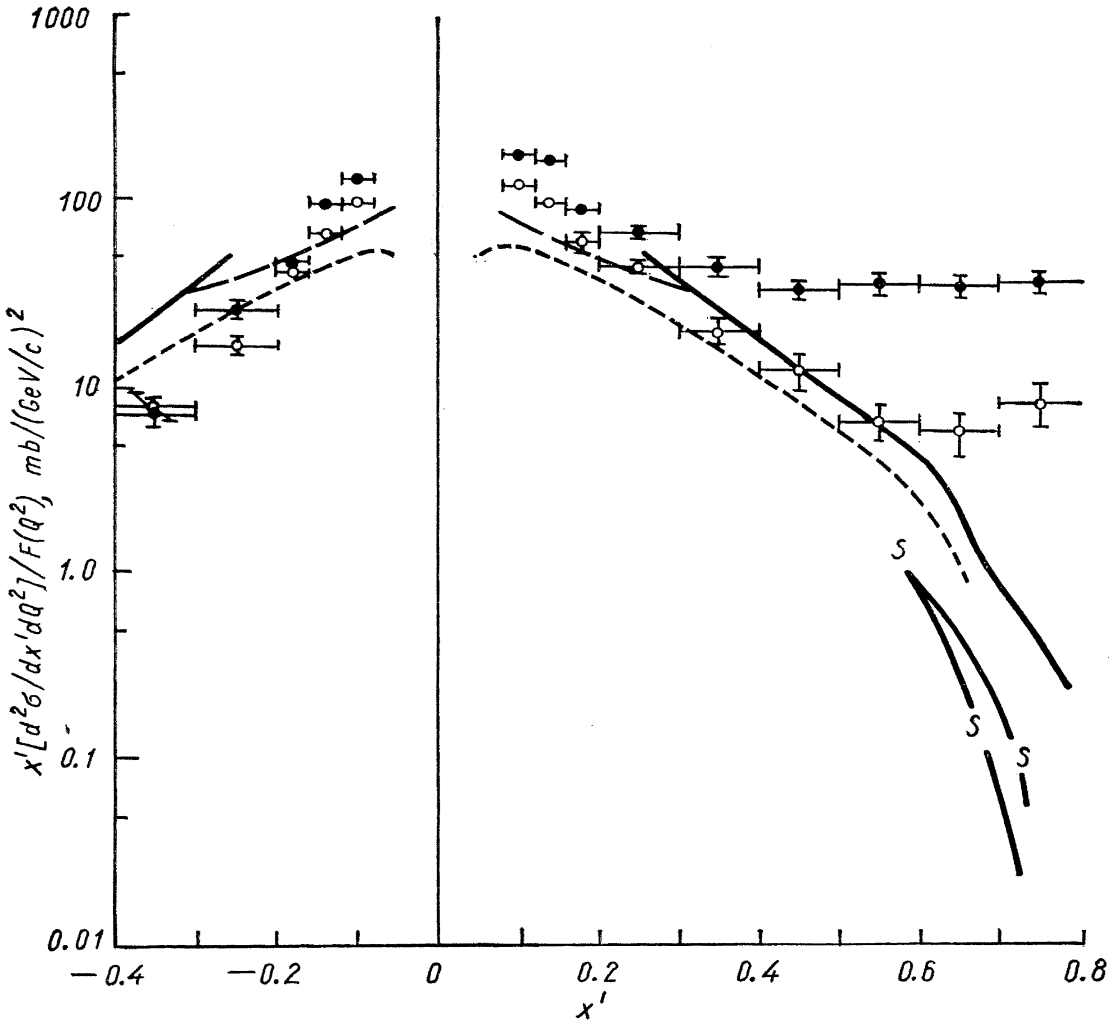

Fig. 44.

and measured about 10 000 negative tracks from 2, 4, 6 and 8 prong events. The reactions studied

$$\pi^- p \to \pi^- + \text{anything}$$
$$\text{and } \pi^+ p \to \pi^+ + \text{anything}$$

represent, in the terminology of Feynman [54], «inclusive» processes. The authors used Feynman's variables

$$Q \equiv p_1, \quad X = \frac{p_L^{CM}}{W}.$$

W being the maximum possible value of p_L^{CM}. Representative results are shown in Figs. 42 and 43. The distribution in x for all multiplicity is well fitted by a simple exponential

$$dN(x) \sim \exp(-A(x))$$

with $A = 10.3$ for $x < 0$ (backward) and $A = 7.0$ for $x > 0$ (forward). Finally (Fig. 44) the $\pi^{\pm} p$ results are compared with pp data [55]. The agreement is only qualitative. Undoubtedly, more extensive studies are needed before we are to conclude on the similarity of global features of pp and πp interactions.

3.3. INELASTICITY

The results of the Echo Lake experiment [2, 3, 4] show that inelasticity in pp collisions is ~ 0.4 independent on energy (~ 0.7 in p-carbon collisions). W. N. Akimov et al. [56] reports value 0.37 for cosmic ray jets at $\langle E \rangle = 250$ *GeV* studied in the cloud chamber with ionization calorimeter. Similar results were reported for pp interaction at lower energy [48, 36]. This new results confirm previous conclusions.

3.4. FOUR-MOMENTUM TRANSFER DISTRIBUTIONS

The experimental t-distribution $D_{\text{exp}}(t)$ results from two factors: a dynamical factor $|T|^2$ where T is a transition matrix element and a factor depending on the available phase space. It is more instructive to know the t-dependence of $|T|^2$ and not the $D_{\text{exp}}(t)$. To get rid of the phase space factor Bialkowski and Sosnowski [57] introduced the $F(t)$ function defined as

$$F(t) = A \frac{D_{\text{exp}}(t)}{D_{\text{LIPS}}(t)}$$

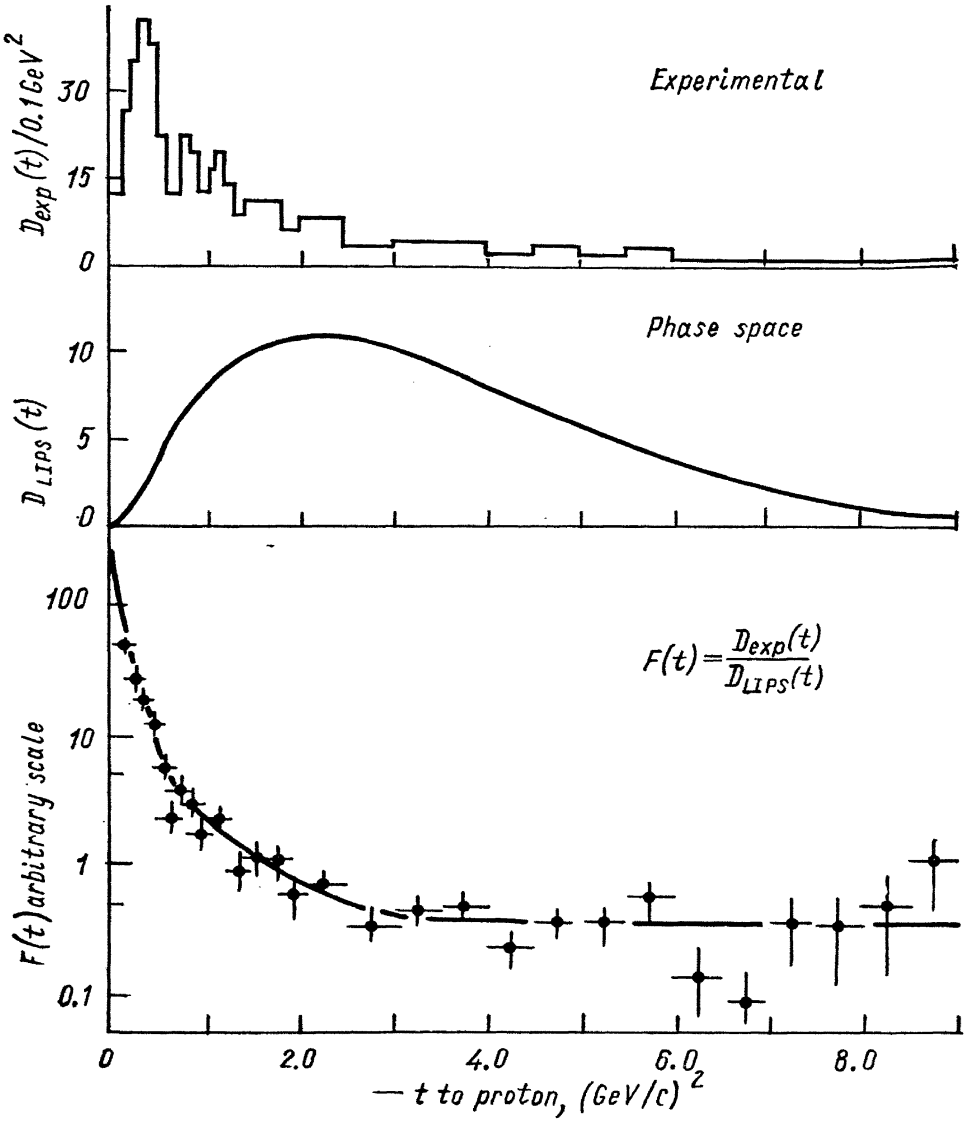

Fig. 45. $\pi^+ p \to p\pi^+\pi^+\pi^+\pi^-\pi^-$ at 8 *GeV/c*.

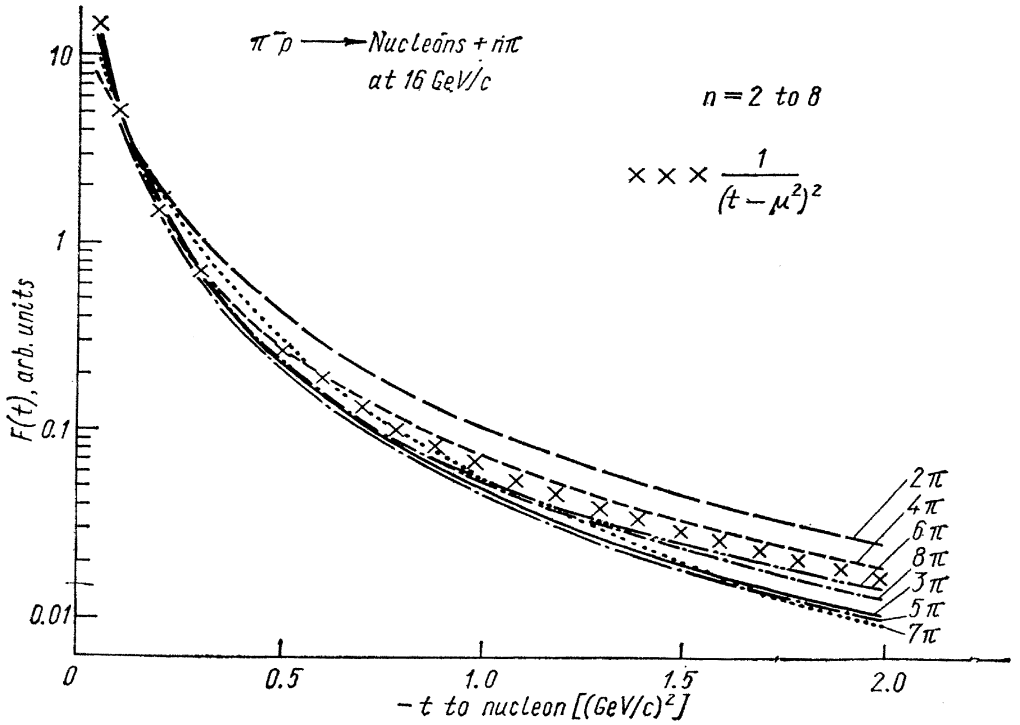

Fig. 46.

where D_{LIPS} is the t-distribution predicted by the Lorentz invariant Phase Space. It follows from the definition that $F(t)$ function represents the dependence of the matrix element squared on t after the averaging over all the other variables in the available phase space has been carried out. Fig. 45 illustrates the definition of $F(t)$ function. In a paper submitted to this conference by Aachen — Berlin — Bonn — CERN — Cracow — Heidelberg — Warsaw Collaboration [58] the $F(t)$ distributions were studied for fitted channels of $\pi^- p$ interactions at 16.2 *GeV/c*. The reactions studied were

$$\pi^- p \to p + k\pi \qquad k = 2, 3, 4, 5, 6, 7, 8;$$

$$\pi^- p \to n + k\pi \qquad k = 2, 4, 6, 8.$$

For each reaction the $F(t)$ function in the t-range from 0.01 GeV^2 to 2 GeV^2 was approximated by the formula

$$F(t) = \frac{N}{(-t + a)^b}$$

Fig. 46 shows the fits to the $F(t)$ distributions for all pion multiplicities. The curves are normalized to the same area in the + region from 0.05 GeV^2 to 2 GeV^2. The shape of all distributions (except for 2 pions in the final state) is very similar to the shape of the pion propagator, also plotted in this figure. The conclusion is that in spite of differences in experimental t-distributions of nucleons produced in various multiplicity channels at 16.2 *GeV/c* (Fig. 47) the dynamics of these interactions has some common features. At 8 *GeV/c* [59] $F(t)$ seemed to depend on multiplicity and perhaps with increasing energy becomes identical for all channels at a given energy. The Dubna — Zeuthen group [68] studied $F(t)$ and $F(t')$ functions for 6-*prong* $\pi^- p$ interactions at 5 *GeV/c*. The $F(t)$ function used as a transition matrix element gave, in general, a better description of the data than $F(t')$ function though this approximation was checked to be too crude to describe the data completely.

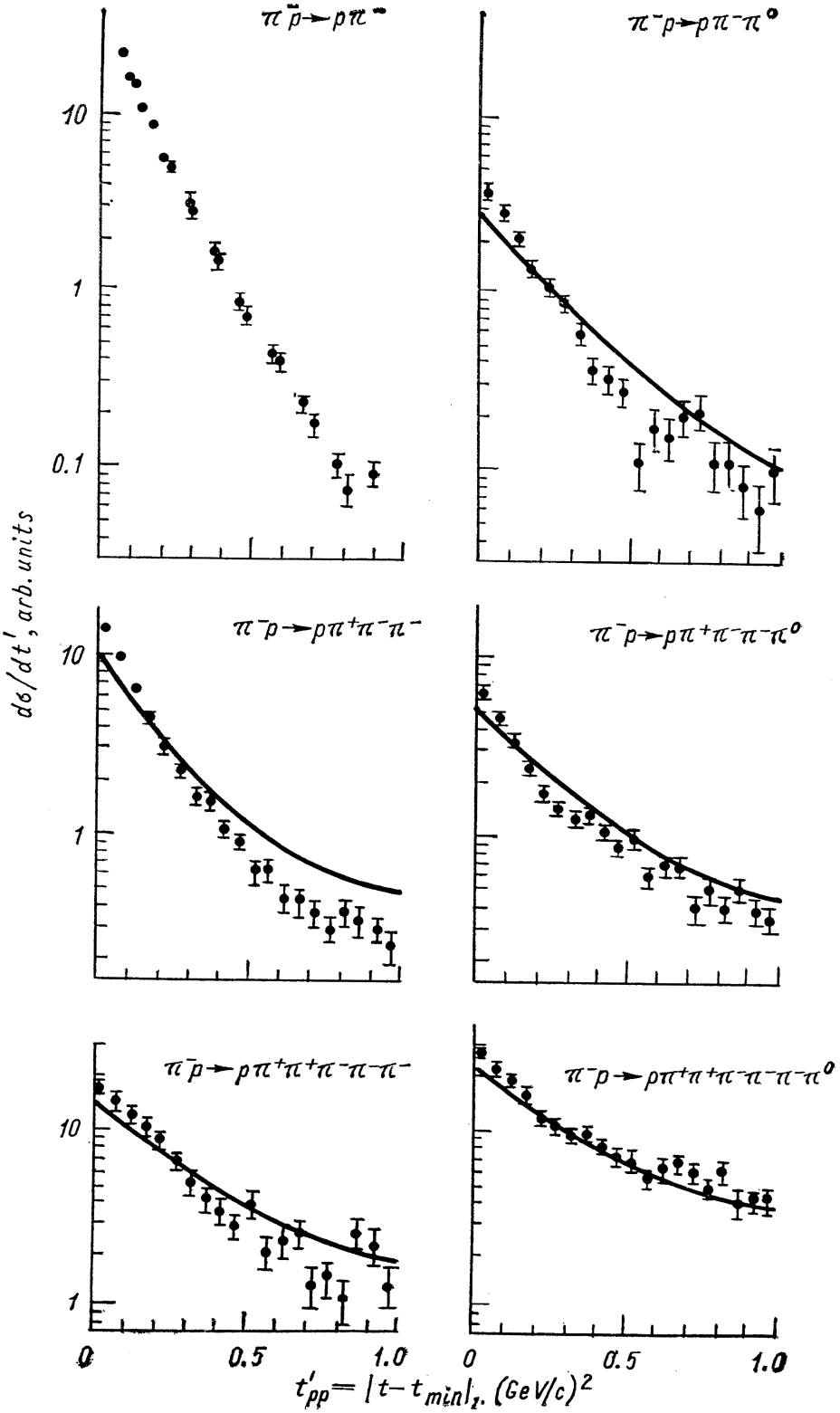

Fig. 47. $\pi^- p$ collisions at 16 *GeV/c*.

4. Resonance production

There have been many papers submitted to this conference on production of resonances in many-body channels [68—75]. Instead of reporting individual results I shall try to present some more general conclusions.

Let me first show you a slide (Fig. 48) which illustrates difficulty in studying or even recognizing resonances in many-body channels. The curves were calculated for 5 *GeV* πp interaction with the assumed 100% of ρ^0 production. In eight-body channel the number of combinations is so large that the ρ^0 peak is barely visible. Fig. 49 shows ρ^0 production in six-body channels at different energies.

One may try to answer few general questions:

1. What is the energy dependence for resonance production in many body processes. Since we know fairly well (see Section 1.) the energy dependence for inelastic channels we may look not for cross sections but for percent of resonances in different multiplicities. The results for πp interactions for which we have most complete data are shown in Figs. 50, 51 and 52. The conclusions are not easy to draw but perhaps there is a correlation between percentage of resonances and multiplicity and also that at higher energies one may expect less ω and Δ^{++} but not ρ for which the percentage seems to stay constant or increase with energy.

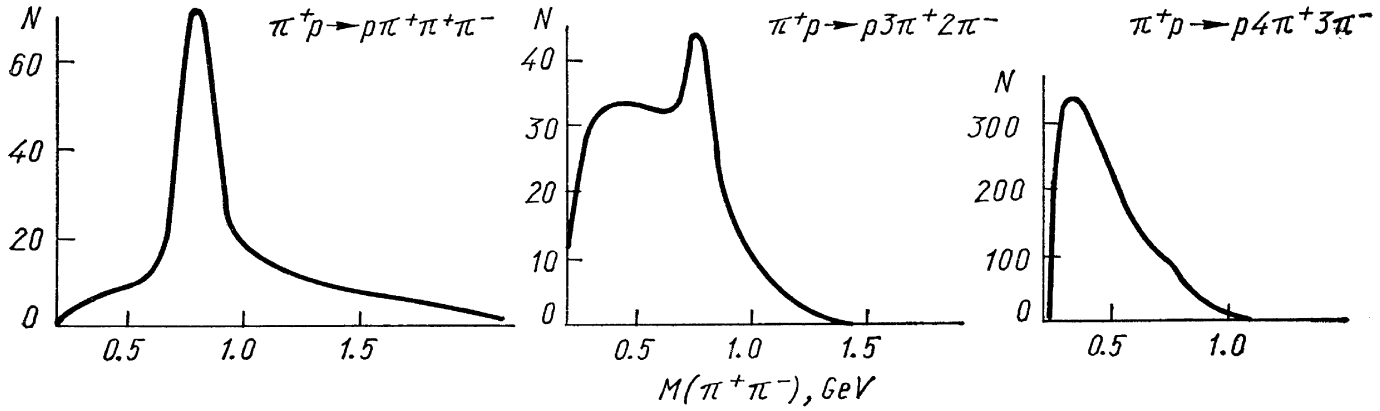

Fig. 48.

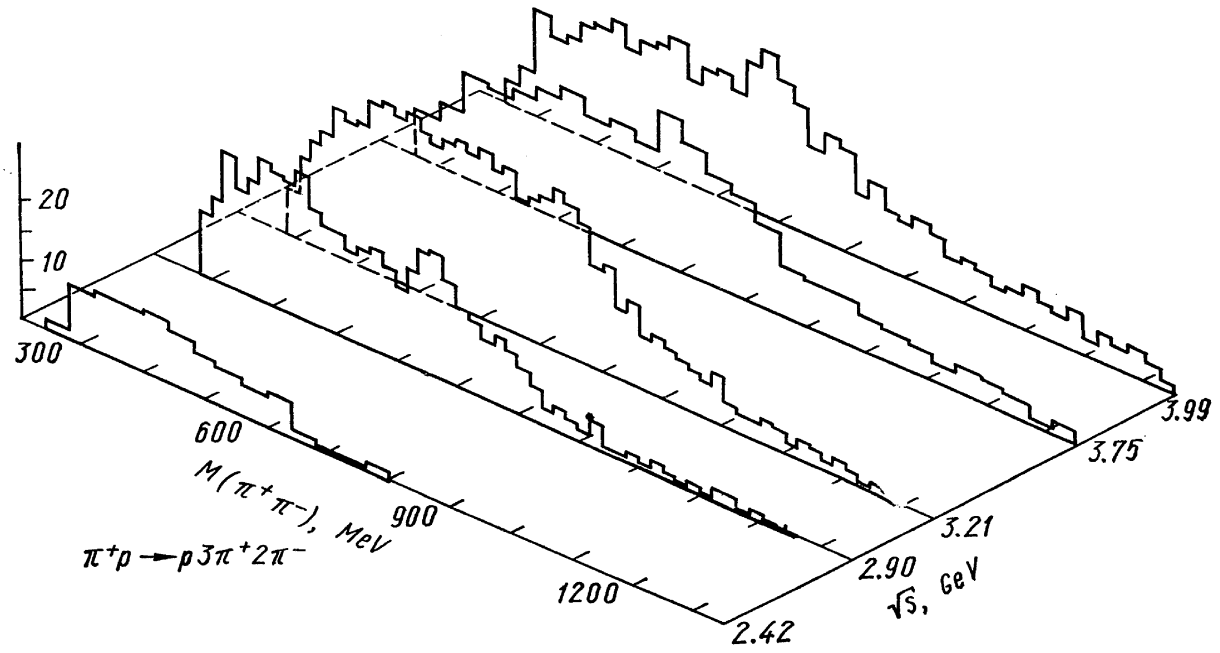

Fig. 49.

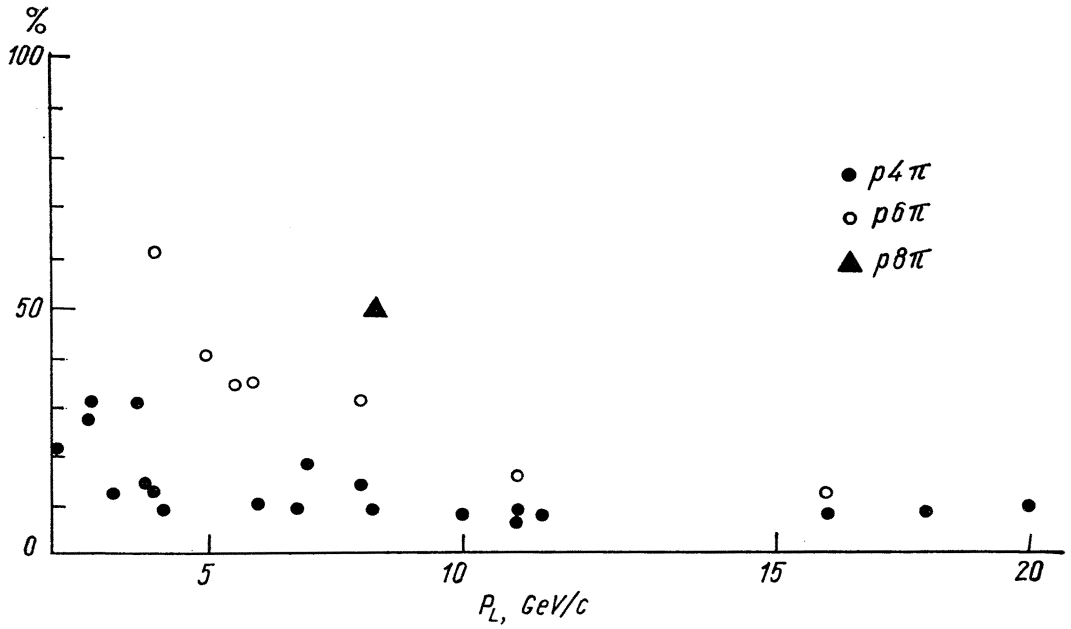

Fig. 50. Percent of ω^0 in πp interactions.

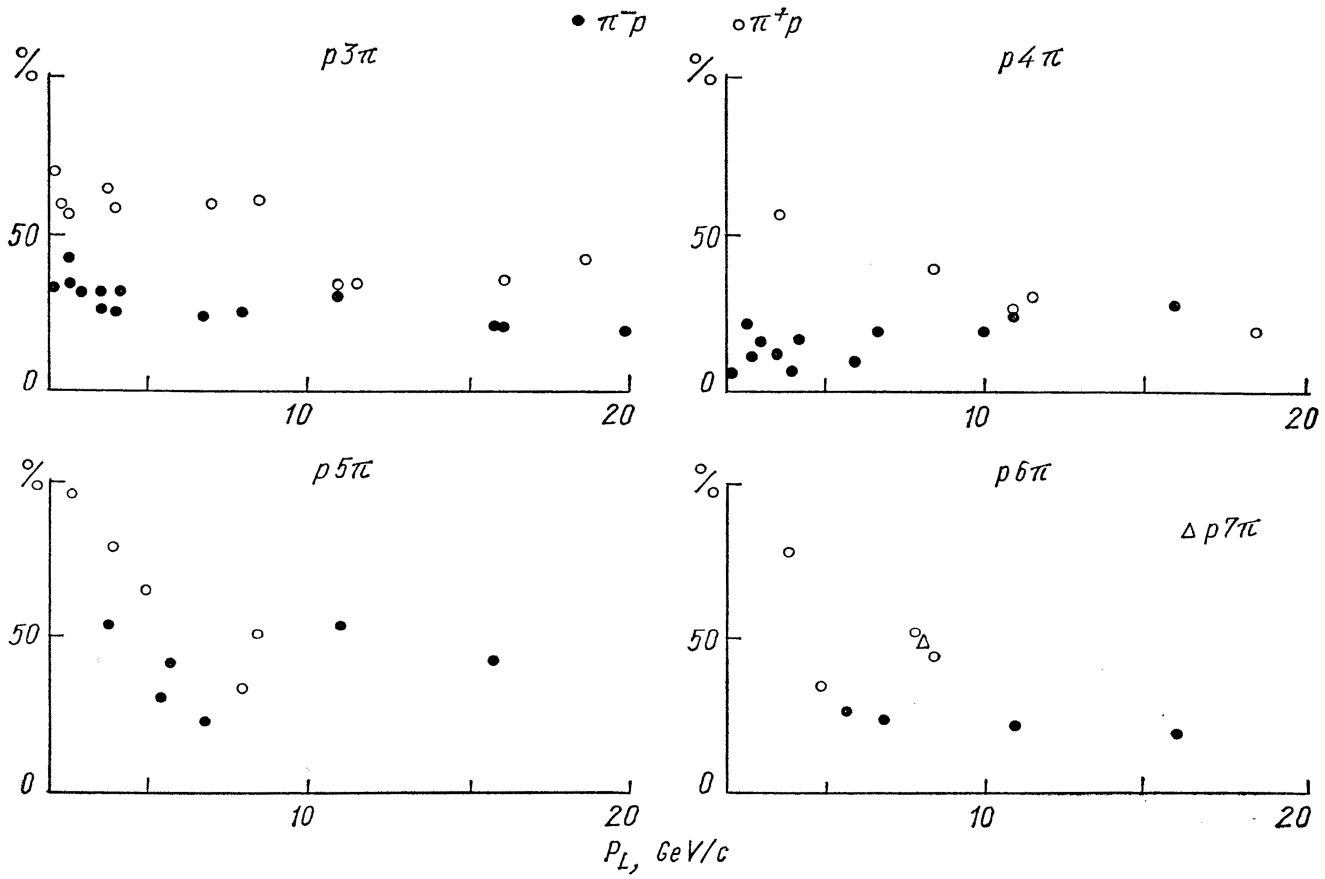

Fig. 51. Percent of Δ^{++} in $\pi^{\pm}$ interactions.

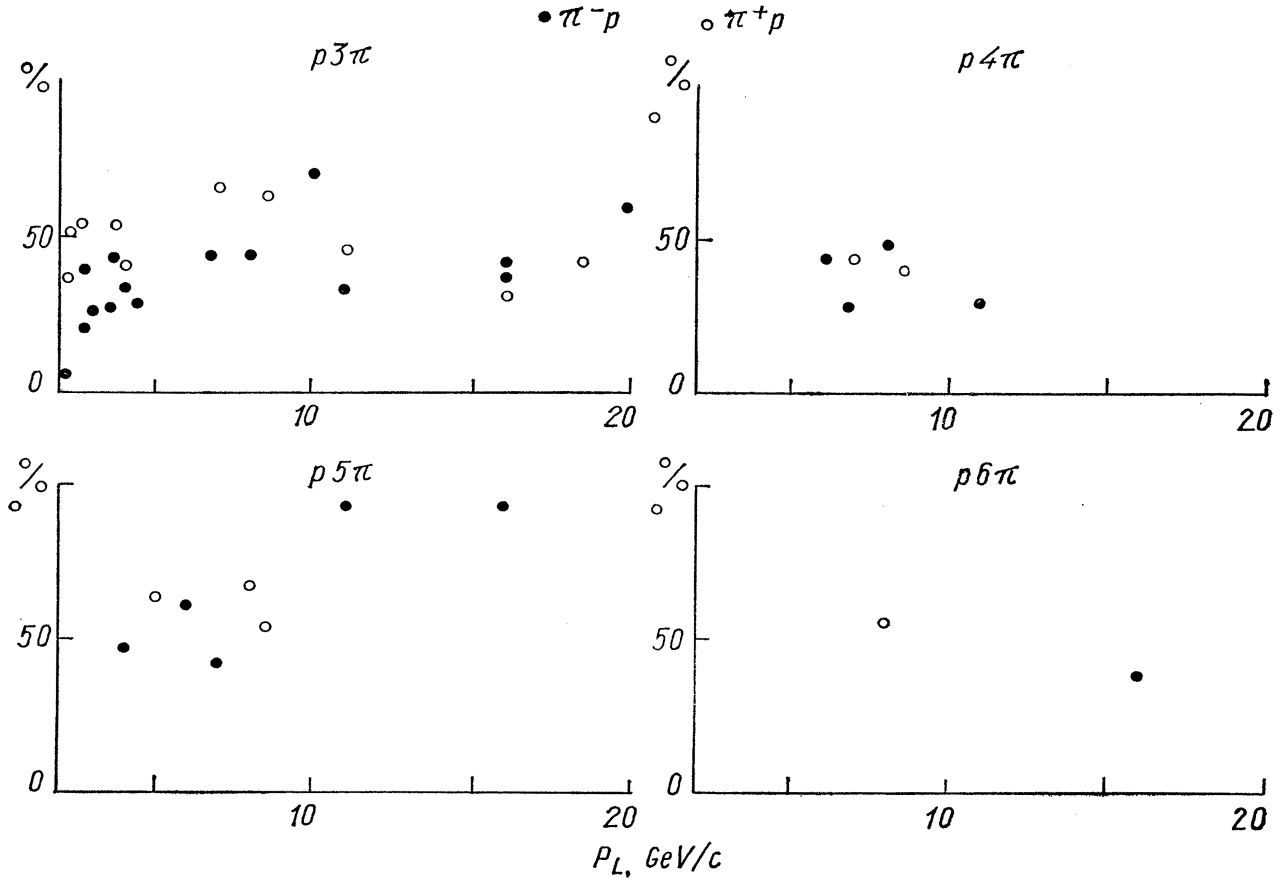

Fig. 52. Percent of ρ in $\pi^{\pm}$ interactions.

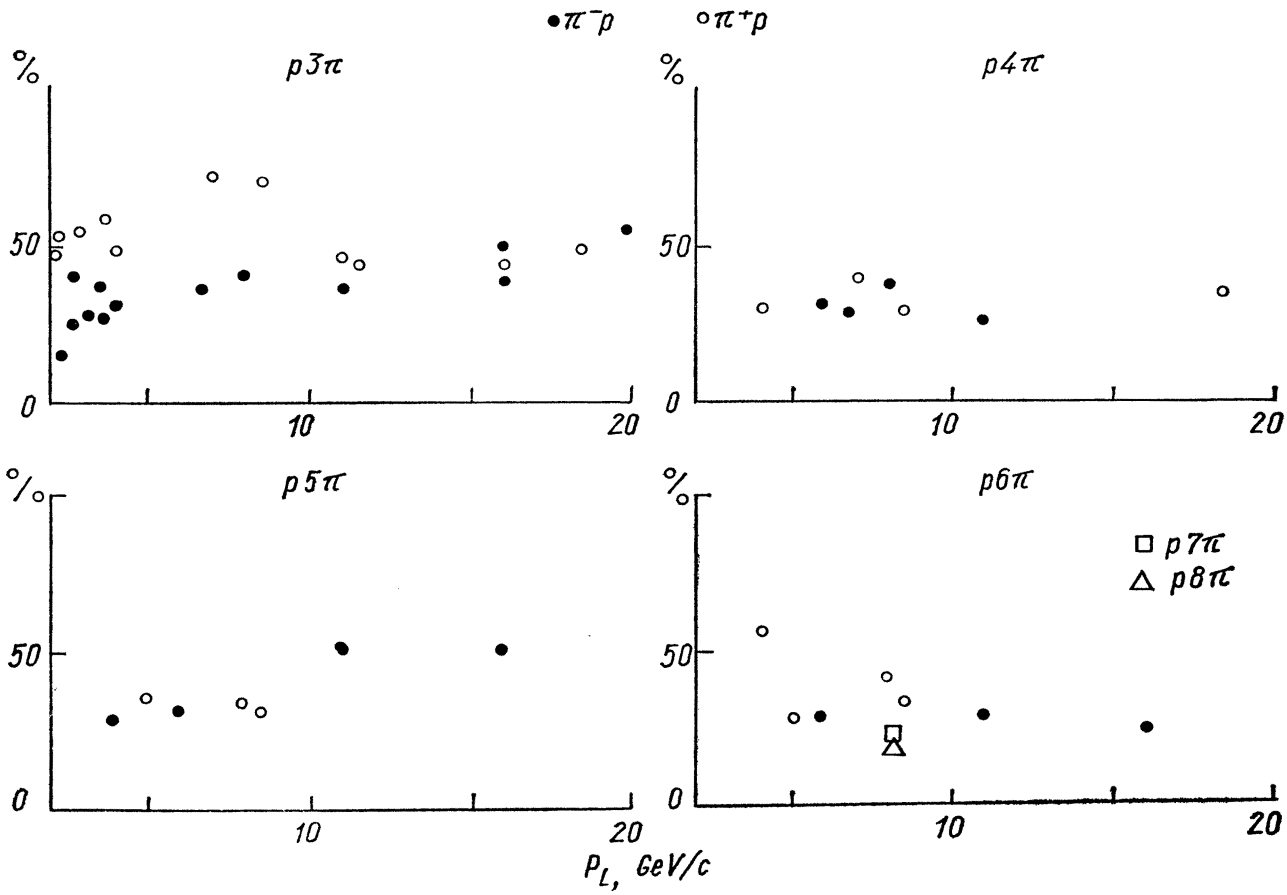

Fig. 53. Percent of pions in resonances in πp interactions.

2. Is the production of resonances in channels with neutron the same as with proton? The answer is relatively certain: channels with neutron have less resonances.

3. What percent of pions is produced through resonances? The results of compilation for πp interactions are shown in Fig. 53. The points represent of course only lower limits because only «good» resonances like ρ, f, ω, η, Δ^{++} (seen in every experiments) were taken into account and all minor effects like B, A_2, A_3, higher nucleon isobars, were neglected. Also there might be wide resonances produced with small cross section, difficult to resolve.

There seems to be a tendency that for higher multiplicity less pions are produced through resonances.

4. Are resonances produced mainly singly or in association with one another, is the associated production of resonances stronger than expected for «statistical» coincidence?

This question is very difficult to answer. The study of associated production of resonances in 4-body channels may be done by fitting density of points in a triangular mass plot. In 6-body channels we need a fit to a density of points in three dimensions. This has been done by the Warsaw groups [76] for interactions at 8 *GeV/c*.

The results are:

6 body channel	$\pi^- p \to p5\pi$	«Independent
uncorrelated p	5π $49.0 \pm 12.1\%$	production»
$\Delta^{++}\rho^0\rho^0$	$10.5 \pm 5.4\%$	26.6%
7 body channel	$\pi^- p \to p6\pi$	4.3
uncorrelated $p6\pi$	$29.7 \pm 8.2\%$	20.5
$\Delta^{++}\omega^0\rho^0$	$7.0 \pm 2.3\%$	6.6

Obviously the data are not accurate enough to draw definite conclusion.

The data for Kp or pp interactions are still less complete.

5. Correlations

5.1. GGLP EFFECT

The best known is the angular correlation between pions discovered by Goldhaber et al. [77] — so called GGLP effect. Most often this correlation is expressed in terms of the coefficient γ which is the ratio of the number of pion pairs with $\theta_{ij} \geqslant 90°$ to the number of pairs with $\theta_{ij} < 90°$, where θ_{ij} is the angle, in the reaction c. m. system, between two pions. For both $p\bar{p}$ annihilations and πp collisions the parameter γ for like pions (γ_L) was found to be smaller than for unlike pions (γ_u):

$$\gamma_L < \gamma_u \text{ (LIPS predicts } \gamma_L = \gamma_u)$$

The difference $\gamma_u - \gamma_L$ is found to decrease with increasing pion energy. The GGLP effect was studied recently in many papers [60, 51, 64]. Let me quote some results:

1. No GGLP effect was found in many-prong pp interactions at 13.1 *GeV/c* [51]. The effect is observed to be rather weak in many-prong $\pi^+ d$ interactions at 5.1 *GeV/c* [60].

2. H. Hulubei et al. [64] studied GGLP effect in $\pi^\pm p$ interactions producing strange particles at 4, 7.5, 8 and 20 *GeV/c*. The authors study the influence of resonances and of the peripheral character of interactions on angular correlations.

3. W. De Baere et al. [61] studied angular correlations in K^+p many-body interactions at 5 *GeV/c*. The usual GGLP effect for pions ($\gamma_u > \gamma_L$) was observed, whereas no difference in γ was found for $K^+\pi^+$ and $K^+\pi^-$ pairs.

The authors use several model to explain observed correlations. Resonance production alone does not explain the GGLP effect since the removal of events in the resonance region does not alter the characteristics of the angular correlations. Also simple uncorrelated model with experimental single particle distributions does not work. The global GGLP effect is best reproduced if in addition to single particle distributions and resonances (K^* (890), Δ^{++}), the Bose — Einstein symmetrization is introduced.

4. G. Alexander et al. [62] also find that resonances alone do not explain the GGLP effect observed in six-prong $\bar{p}p$ annihilations at 6.94 *GeV/c*.

I can easily agree with the conclusion of [61] that for a more detailed understanding of the GGLP effect a better knowledge of the reaction mechanism is needed, in particular outside the resonance region.

5.2. BCCKLMKZAEJKZ EFFECT [63]

Since this is too difficult to pronounce I shall simply call it the three-pion correlation. Fig. 54 shows the definition of parameters which have been used by the Cracow group [63].

One may use the solid angle Ω within the pyramid formed by the directions of the three momenta or the angle $\alpha_{(AB)C}$ between the momentums vector of pion C and the bisectrix of the angle between the momenta of two pions A and B. The authors introduce a parameter

$$\beta = \frac{n(2\pi > \Omega > \pi/2)}{n(\Omega < \pi/2)}$$

which is to a certain extent analogous to the parameter γ, since the median value of Ω for isotropic distribution equals $\pi/2$.

Fig. 55 shows the values of β for all charge combinations in the channel $\pi^+p \to p4\pi^+3\pi^-\pi^0$ at 8 *GeV/c*. The greatest difference is observed between the Ω distributions corresponding to $(- - -)$ — (lowest β) and $(+ - 0)$ — highest β.

Fig. 56 shows the correlation between the γ_3 values (defined in the usual sense for the angle $\alpha_{(AB)C}$) and the total charge of the AB group (or alternatively the total charge of the 3-pion group).

The nature of these correlations is unfortunately not yet known, since the authors did not check whether they are new or only due to the reflection of the two-pion correlations (the usual GGLP effect).

5.3. THE $\langle p_\perp \rangle - p_L^{CM}$ DEPENDENCE

There have been many papers submitted to this conference in which the dependence of $\langle p_T \rangle$ on p_L^{CM} was studied [56, 47, 48, 78, 79]. As an example I will show you a slide (Fig. 57) with the results from cosmic ray jets at average energy ~ 250 *GeV* [56]. In this experiment all momenta of secondary particles (in the backward hemisphere) were measured and the incoming energy was determined by a calorimeter. In the lower part of the figure you see the usual $p_T - p_L^{CM}$ plot (Peyrou plot) and in the upper part the average values of p_T for different intervals of p_L^{CM}.

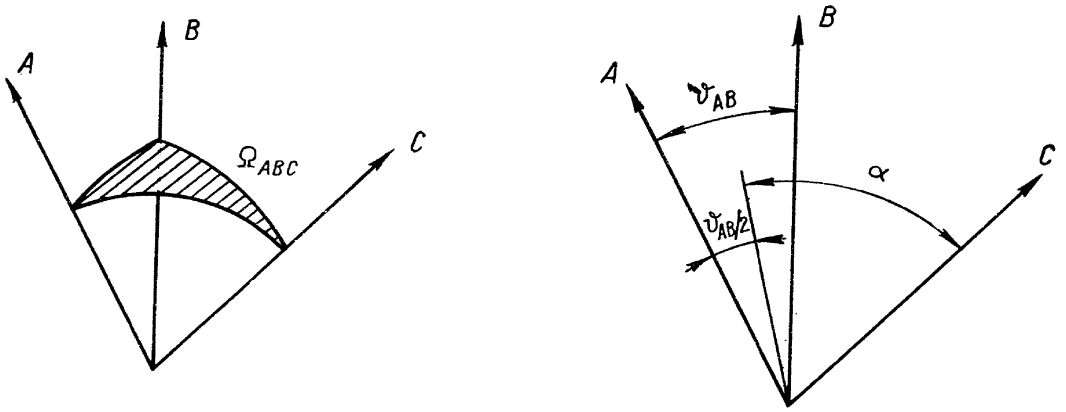

Fig. 54.

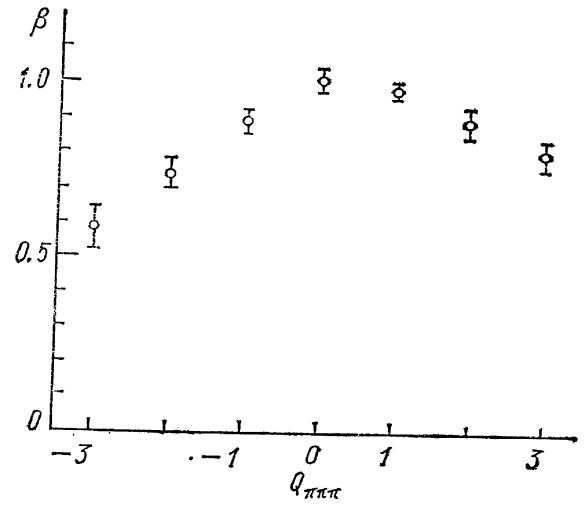

Fig. 55. $\pi^+ p \to p 4\pi^+ 3\pi^- \pi^0$ at 8 *GeV/c*.

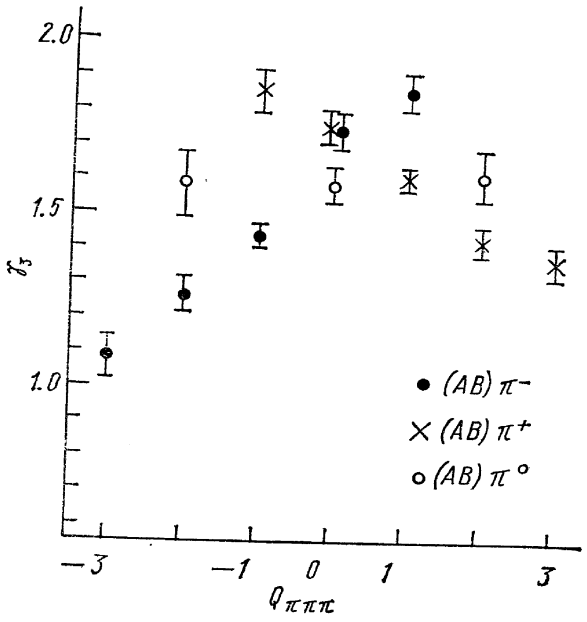

Fig. 56. $\pi^+ p \to p 4\pi^+ 3\pi^- \pi^0$ at 8 *GeV/c*.

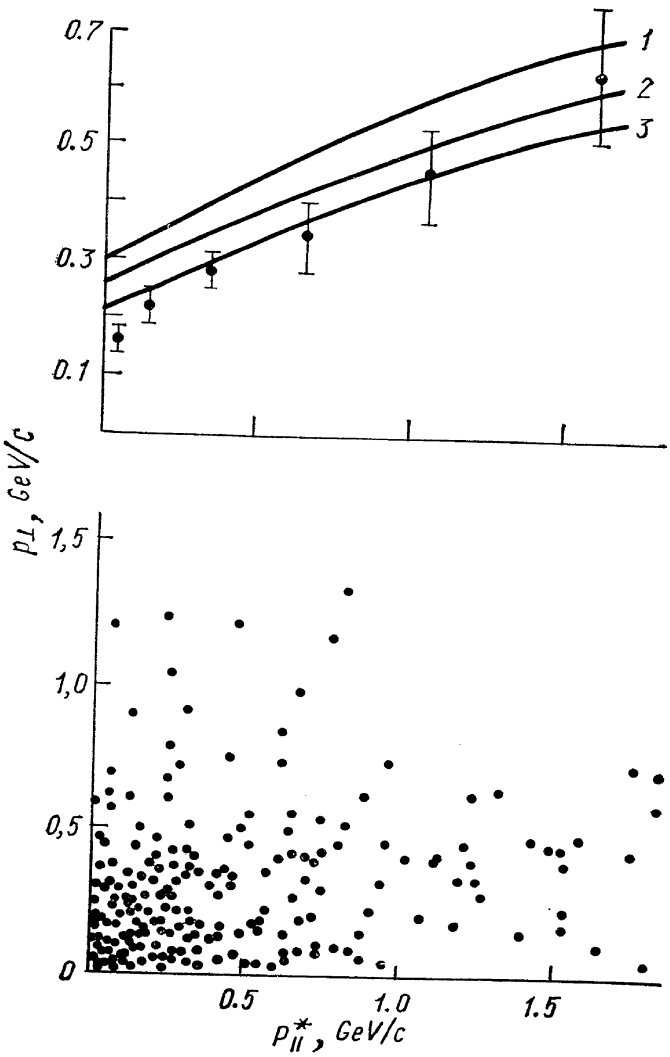

Fig. 57.

The $\langle p_T \rangle - p_L^{CM}$ dependence was discovered by the Warsaw group [81] in 1963 and soon it was proven [82] that the general shape of this dependence agrees with the predictions of LIPS although the experimental values of $\langle p_T \rangle$ are lower than those resulting from LIPS. When the predictions from LIPS are corrected for the experimental fall-off of transverse momenta good agreement with data can be achieved. It is interesting to see that the effect is still observed at such high energy.

5.4. CORRELATIONS BETWEEN MOMENTA OF SECONDARY PARTICLES

Akimov et al. [56] studied the cosmic ray jets of average energy ~ 250 *GeV*. For study of correlations they took only those events in which a slow (backward) proton was identified. Then they calculated the four momentum transfer t from the target proton to the group consisting of a slow proton and m pions ($m = 0, 1, 2 \ldots$) from backward hemisphere. The pions were ordered according to their laboratory momenta. The results for representative events are shown in Fig. 58. The authors claim that the observed correlation between t and m is what may be expected from a fireball model also shown in the figure.

The group from Georgia [78] studied the correlations between the values of longitudinal momentum of pions ordered according to increasing p_L. This ordering may correspond to a certain extent to positions of particles in the multiperipheral ladder. No correlations other than those resulting from statistical distribution were found (Fig. 59).

5.5. THE LONGITUDINAL PHASE SPACE (LPS) ANALYSIS OF VAN HOVE

The best method to test the global correlations between all secondary particles of a given event is that proposed by Van Hove [83]. He pointed out that many dynamic features of high energy interactions can be studied by considering only longitudinal momenta since the transverse momenta of all secondary particles are limited to small values compared to incident momentum. Each event can be represented as a point in longitudinal phase space (Fig. 60). The variable characterizing each event in the LPS plot is the polar angle ω, which is counted counter-clockwise from the line $q_1 = 0$. Because all transverse momenta of final particles remain small at high energy, the single angle ω essentially determines the complete longitudinal configuration of an event.

The ω distribution of events was studied in many papers submitted to this conference [85, 86, 87, 71]. Striking features found were those observed previously [88]: occurence of pronounced maxima in the ω distribution of events for reactions where Pomeron exchange is allowed.

In order to get more quantitative results, a commonly used parametrization for the dependence of cross sections on incident momentum was generalized to the following expression

$$\frac{d\sigma}{d\omega} = C(\omega) \cdot p_{\text{lab}}^{-n(\omega)}.$$

The effective exponent $n(\omega)$ determined in different ω intervals was found to be close to zero for these regions of the ω plot which correspond to Pomeron exchange (Fig. 61).

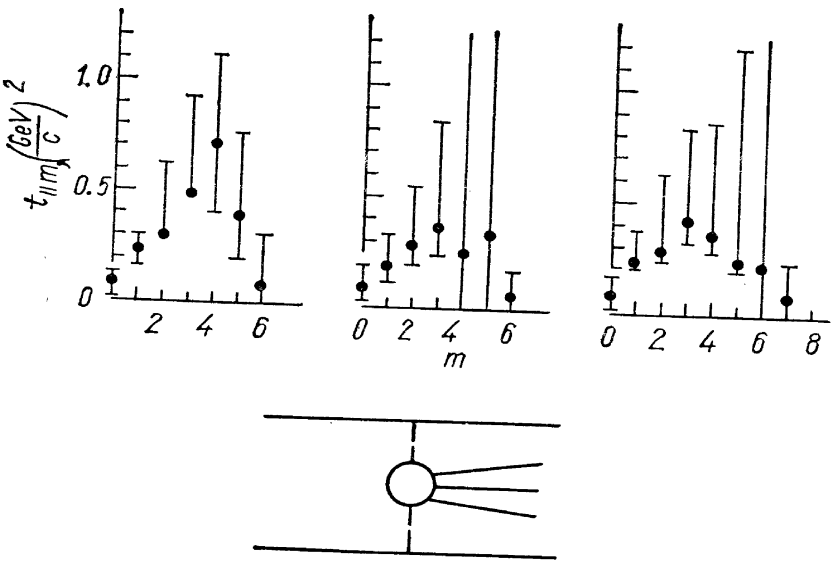

Fig. 58.

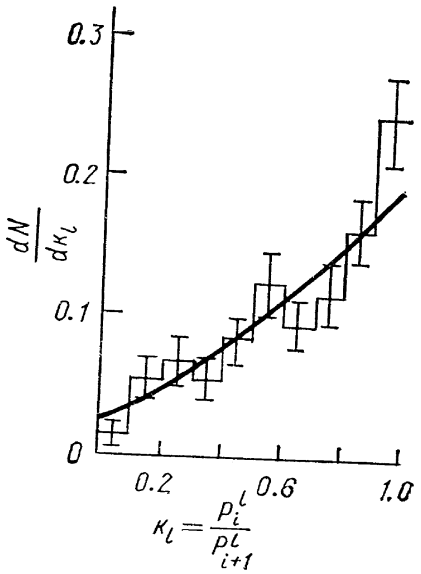

Fig. 59.

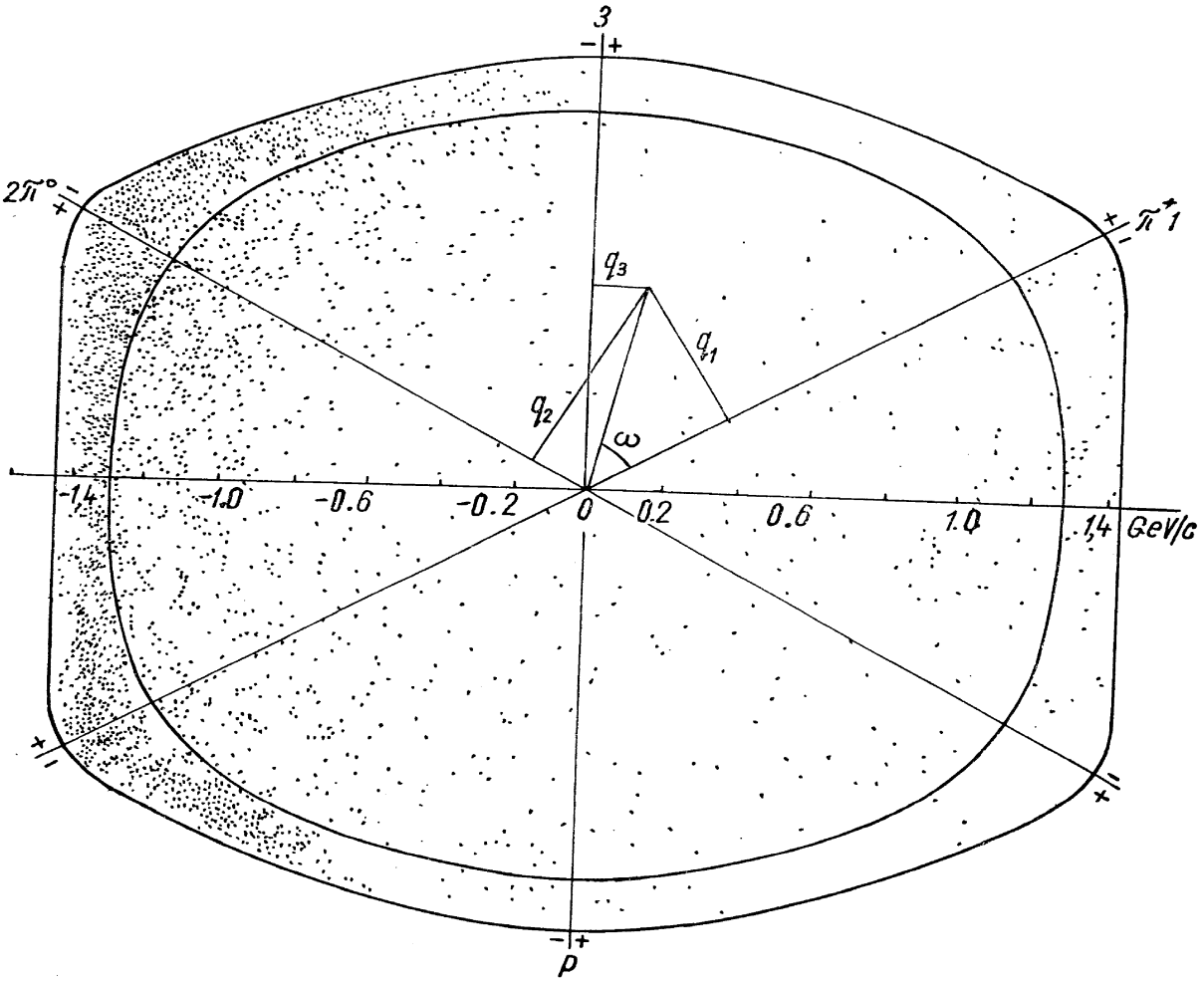

Fig. 60. $\pi^+\pi^0 p$ at 5 *GeV/c*.

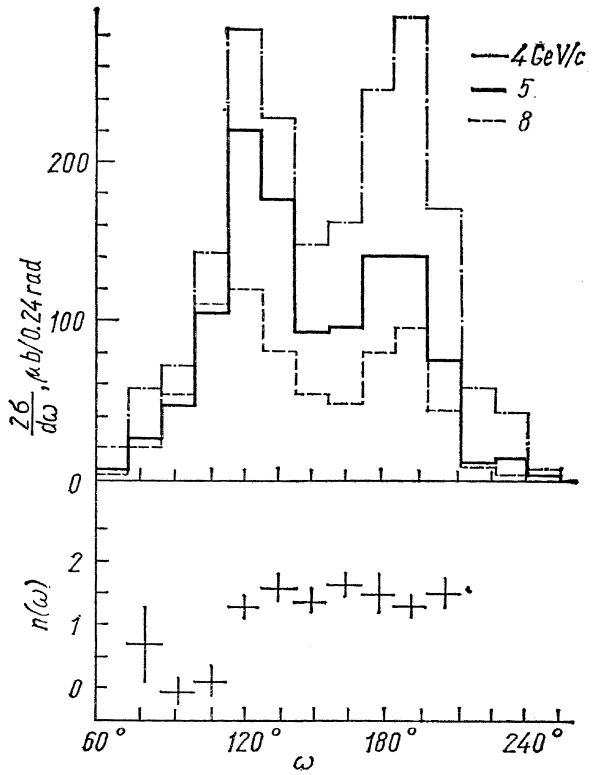

Fig. 61.

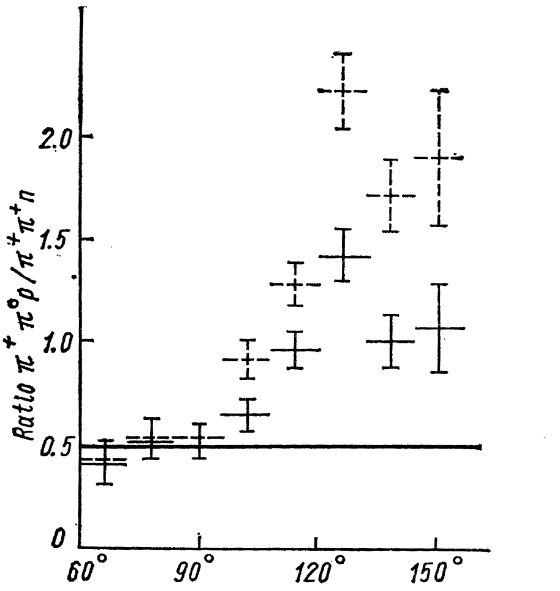

Fig. 62.

Moreover, it was proved that for these configurations which correspond to Pomeron exchange the ratio of $\sigma(\pi^+p \to p\pi^+\pi^0)$ to $\sigma(\pi^+p \to n\pi^+\pi^+)$ equals 0.5 (Fig. 62) as it should be for the decay of a pure $I = \frac{1}{2}$ state [89].

For the case of four-body final state the LPS is a cuboctahedron (Fig. 63). Fig. 64 shows the distribution of points in different sides of a cuboctahedron together with diagrams describing configurations of particles in each side. Kittel, Ratti and Van Hove studied the reactions $\pi^-p \to p\pi^-\pi^+\pi^-$ and $\pi^-p \to p\pi^+\pi^-\pi^-\pi^0$ at 11 and 16 *GeV/c*. Fig. 64 shows the distribution of events in different parts of the LPS. Comparison of the 11 and 16 *GeV/c* distributions shows two clear maxima corresponding to the two diffraction dissociation processes:

$$\pi^-p \to (2\pi^-\pi^+)\,p;$$

$$\pi^-p \to \pi_f^-\,(\pi_s^-\pi^+p).$$

Comparison of the 11 and 16 *GeV/c* distributions (Fig. 65) shows that the dominance of diffraction dissociation becomes more pronounced with increasing energy and that its bulk (central part of the maxima) is nearly independent of s as expected for Pomeron exchange. Fig. 66 shows the exponent n in the formula $\sigma \sim p_{\text{lab}}^{-n}$ for different parts of the LPS.

The same authors show also evidence for diffraction dissociation processes in 5-body reaction

$$\pi^-p \to (\pi^-\pi^-\pi^+\pi^0)\,p$$
$$\pi^-p \to \pi^-\,(\pi^-\pi^+\pi^0p)$$

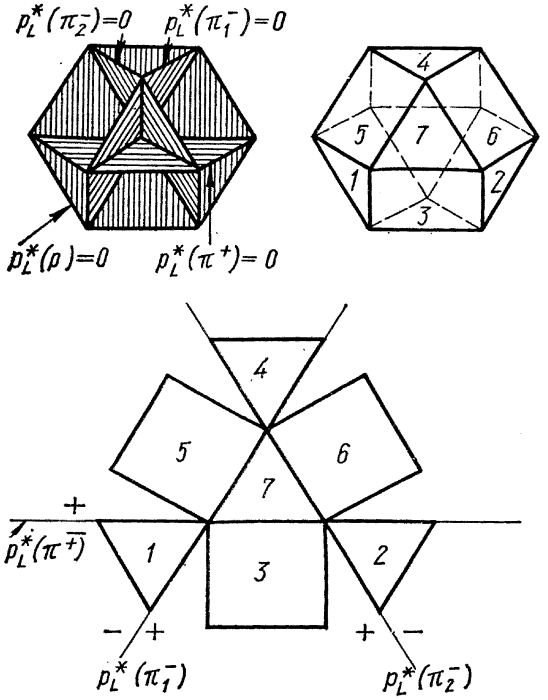

Fig. 63. $\pi^-p \to p\pi^+\pi_1^-\pi_2^-$ at 16 *GeV/c*. Cuboctahedron plot.

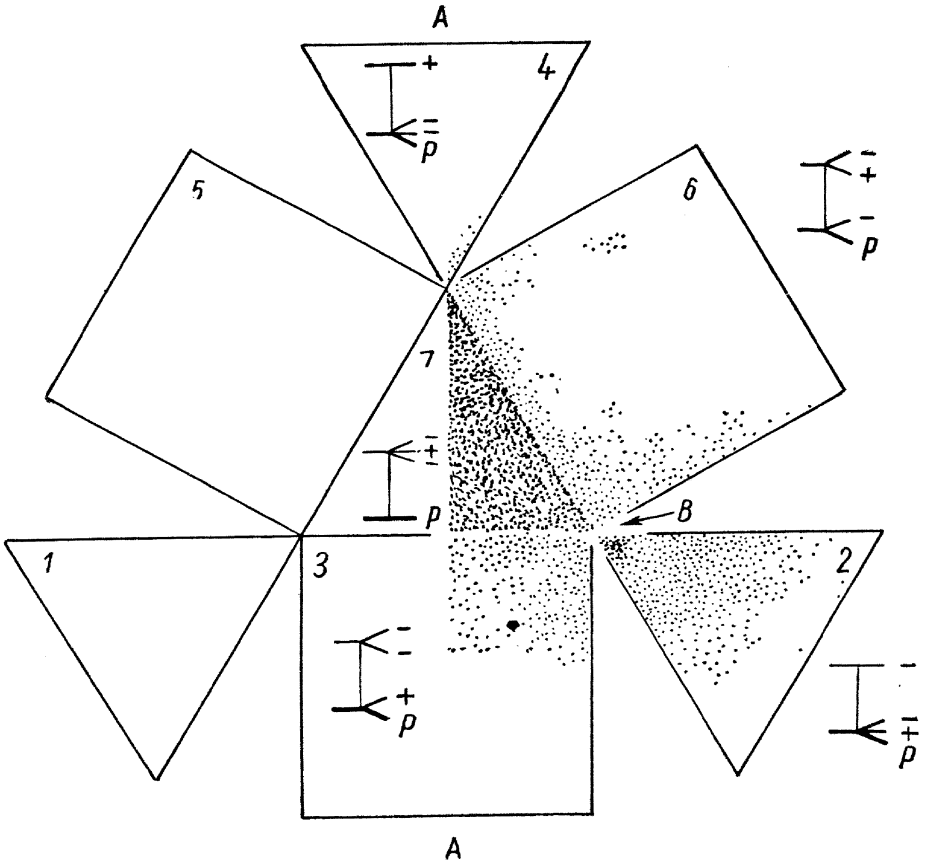

Fig. 64. $\pi^- p \to p\pi\pi\pi$ at 16 *GeV/c*. Longitudinal momenta projected on cuboctahedron faces.

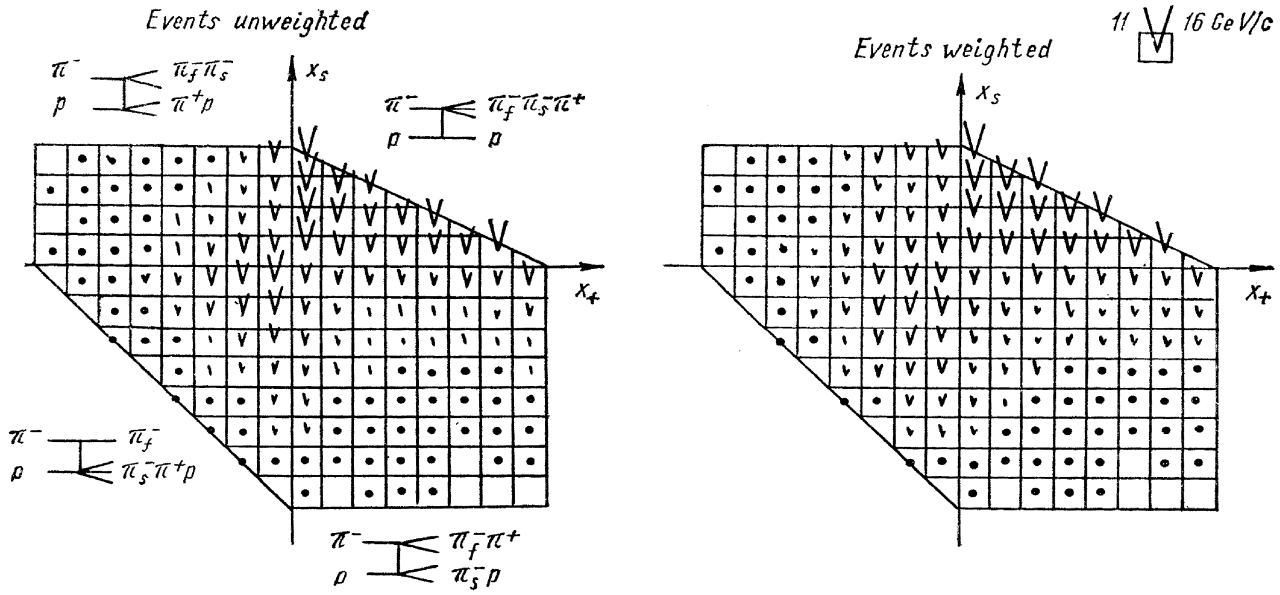

Fig. 65. $\pi^- p \to \pi_f^- \pi_s^- \pi^+ p$. 11 and 16 *GeV/c*.

and double dissociation process

$$\pi^- p \to (2\pi^-\pi^+)(\pi^0 p).$$

For such a process the ratio of cross sections for processes $\pi^- p \to (\pi^-\pi^-\pi^+)\ (p\pi^0)$ and $\pi^- p \to (\pi^-\pi^-\pi^+)\ (\pi^+ n)$ should be equal 0.5 [89].

J. Ballam et al. [84] used the OPE model of Wolf to fit distributions of events in each sector of the LPS separately. The conclusion is that the OPE model cannot account for all the observed features.

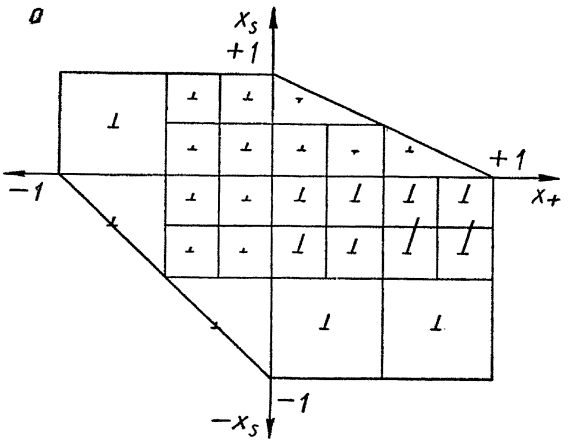

Fig. 66. $\pi^- p \to \pi_f^- \pi_s^- \pi^+ p$. 11 and 16 *GeV/c*.

The table 1 shows the comparison of cross sections in each LPS region with the corresponding absolute predictions for the studied reactions at 16 *GeV/c*.

Table 1

LPS region	$\pi^- p \to p\pi^-\pi^+\pi^+$		$\pi^+ p \to p\pi^+\pi^+\pi^-$	
	$\sigma^{exp}(\mu b)$	OPE (μb)	σ^{exp} (μb)	OPE (μb)
Total	1080±120	980	1280±150	1150
7	477±53	415	490±60	419
2	261±29	176	258±30	170
6	207±23	202	400±17	470
3	128±14	181	80±9	80
4	7±1	6	26±13	10

The cross sections for regions 7 and 2 and those for regions 6 and 3 tend to compensate so that the total cross sections agree with the OPE values.

6. Comparison with models

I will comment shortly only on various papers submitted to this conference in which specific reactions were compared with models.

6.1. DOUBLE-REGGE MODEL

The following reactions were studied:

$K^- n \to K^-\pi^- p$ at 5.5 *GeV/c* [91]
$K^- n \to K^-\pi^- p$ at 12.6 *GeV/c* [92]
$\pi^- p \to \rho^0\pi^- p$ at 4.45 *GeV/c* [93]
$\pi^- p \to \rho^0\pi p$ at 7 *GeV/c* [94]
$\pi^- p \to \rho\pi\Delta$ at 7 *GeV/c* [94]
$\pi^+ p \to \rho^0\pi^+ p$ at 13.1 *GeV/c* [95]
$\pi^+ p \to \pi^+\pi^-\Delta^{++}$ at 13.1 *GeV/c* [96].

An example of the analysis of reaction is shown in Figs. 67, 68, 69.

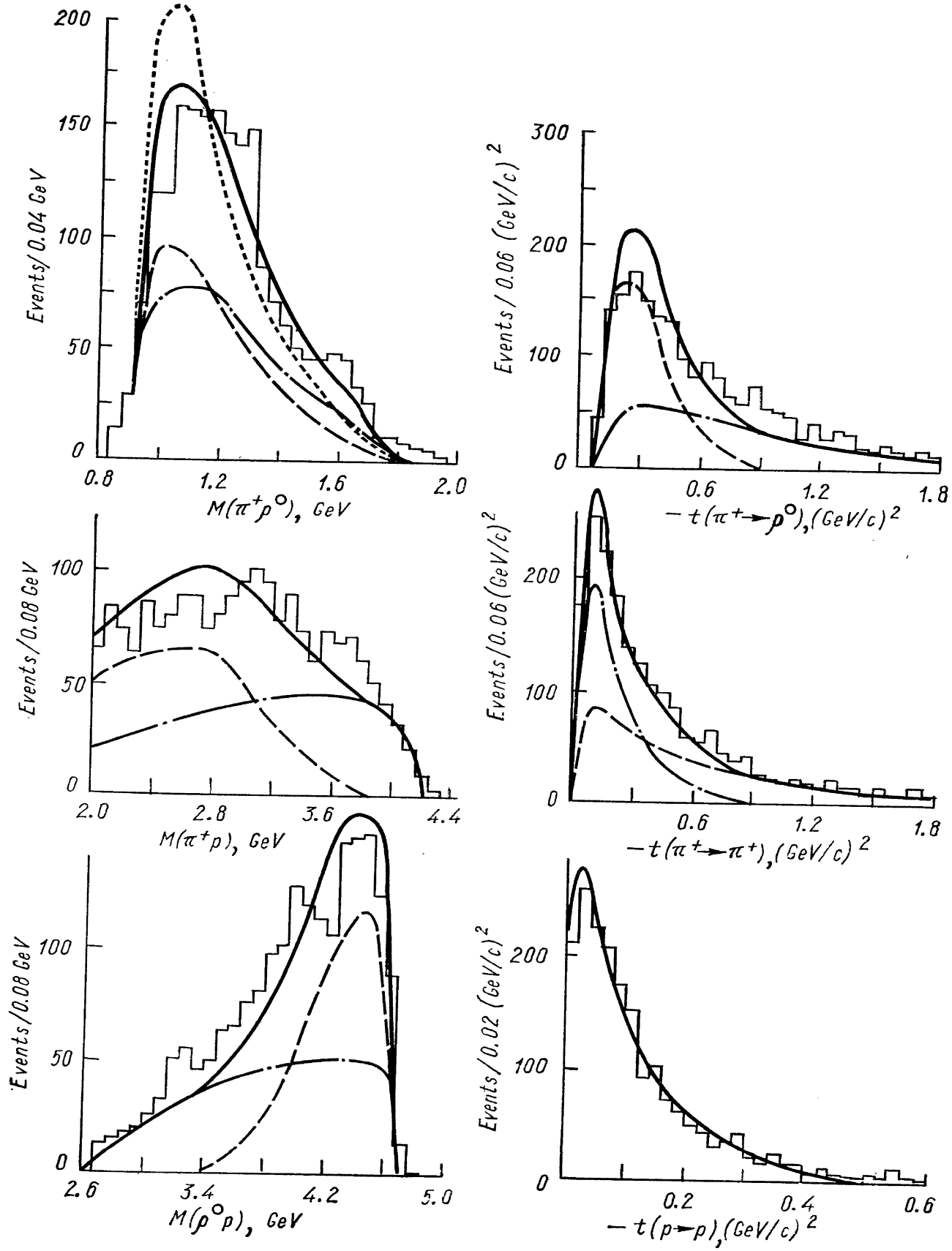
Events/0.04 GeV
200
150
100
50
0
0.8
1.2
1.6
2.0
M(π⁺p°), GeV
Events/0.06 (GeV/c)²
300
200
100
0
0.6
1.2
1.8
−t(π⁺→p°), (GeV/c)²
Events/0.08 GeV
100
50
0
2.0
2.8
3.6
4.4
M(π⁺p), GeV
Events/0.06 (GeV/c)²
200
100
0
0.6
1.2
1.8
−t(π⁺→π⁺), (GeV/c)²
Events/0.08 GeV
100
50
0
2.6
3.4
4.2
5.0
M(p°p), GeV
Events/0.02 (GeV/c)²
200
100
0
0.2
0.4
0.6
−t(p→p), (GeV/c)²

Fig. 67.

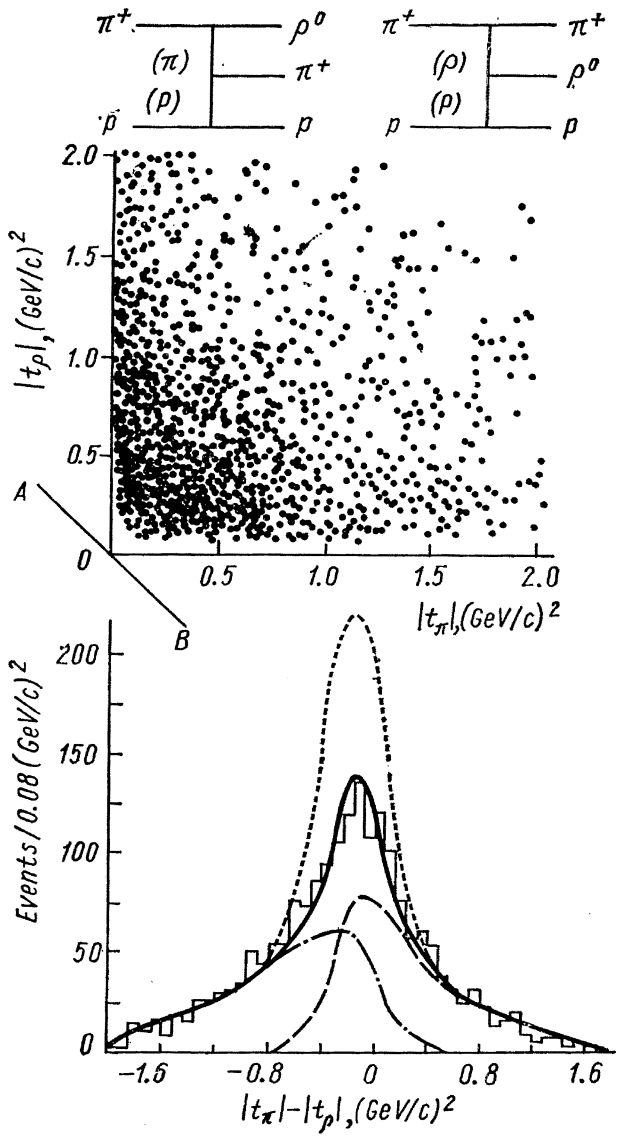

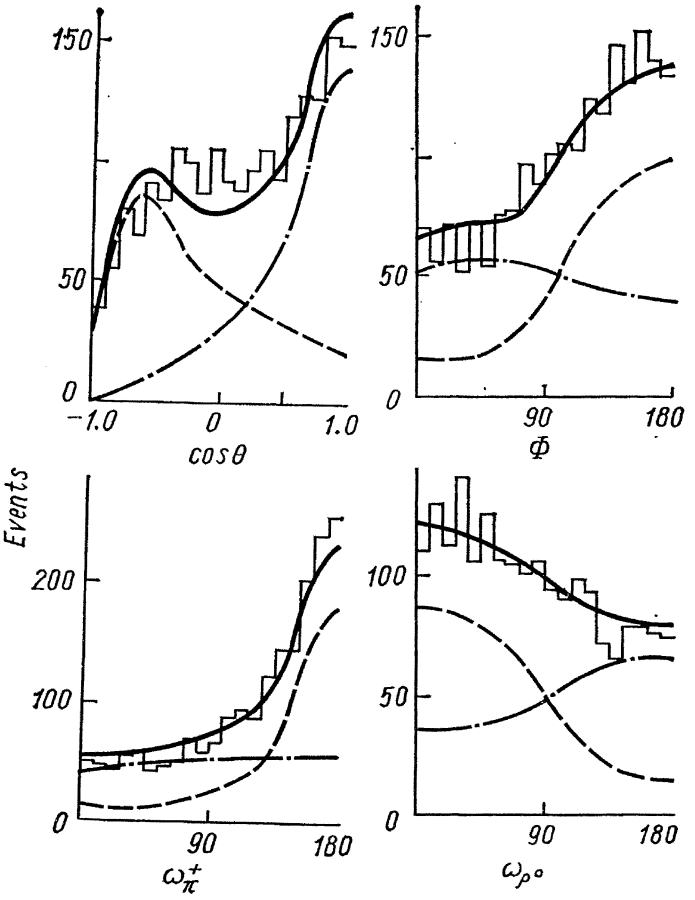

Fig. 69.

Fig. 68.

6.2. MULTI-REGGE MODEL

The Multi-regge model was applied to the reaction $\pi^+ n \rightarrow$ $\rightarrow p\pi^+\pi^-\pi^0$ at 13 *GeV/c* [96].

6.3. VENEZIANO MODEL

The following reactions were studied:

$\bar{p}n \rightarrow \bar{\Delta}^{--}\pi^0 p$ at 7 *GeV/c* [97]

$K^+ p \rightarrow \bar{\Lambda} pp$ at 8.25 *GeV/c* [98]

$K^+ p \rightarrow \bar{\Lambda} pp$ at 10 *GeV/c* [99]

$K^- p \rightarrow \Lambda K^+ K^-$ at 3.3 *GeV/c* [100]

$\bar{p}p \rightarrow K_1^0 K^\pm \pi^\mp$ at 1.1, 2.5 and 5.7 *GeV/c* [101]

$K^- p \rightarrow \bar{K}^0 p\pi^-$ at 5.5 *GeV/c* [102]

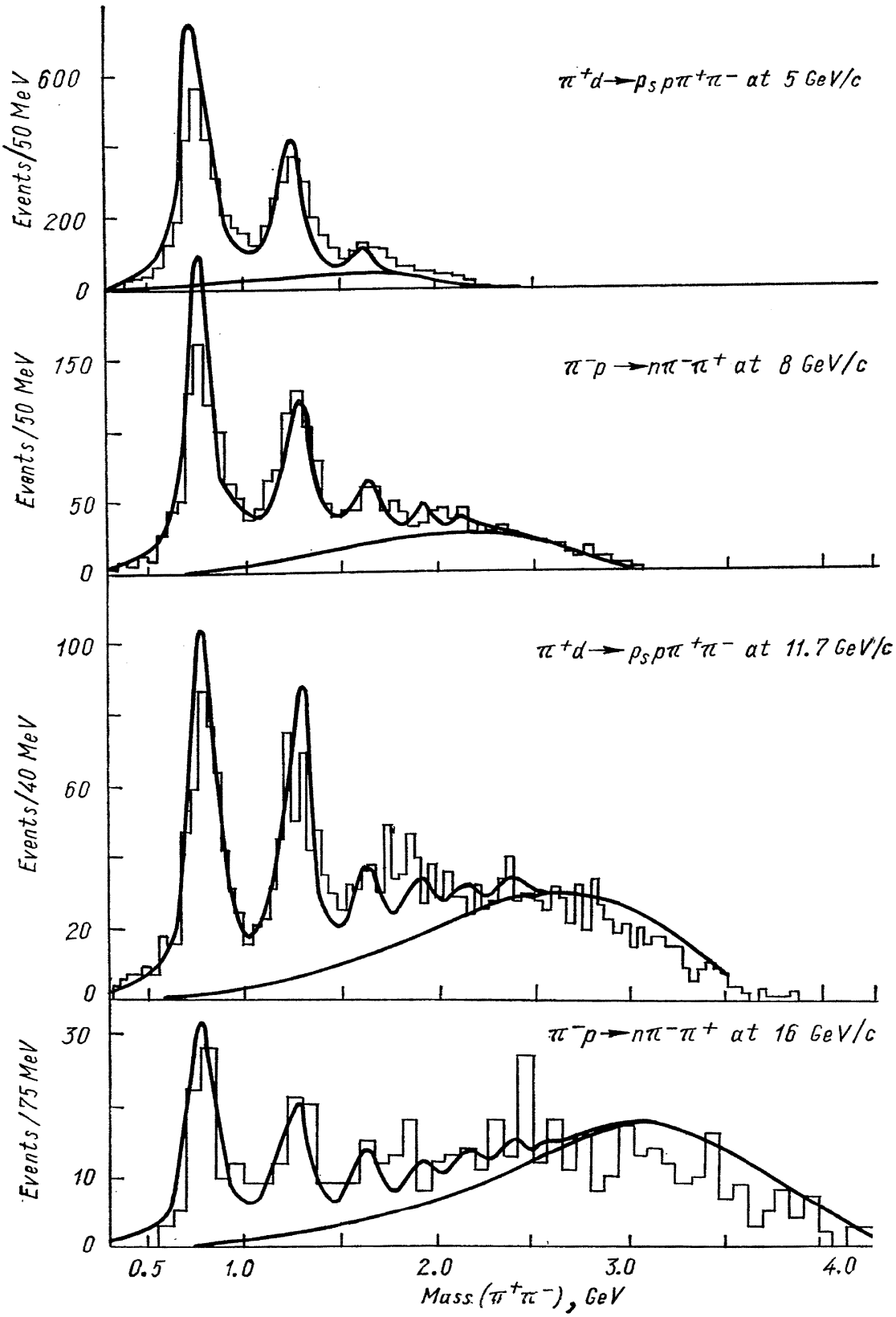
Events/50 MeV
600
200
0
$\pi^+ d \to p_s p \pi^+ \pi^-$ at 5 GeV/c
Events/50 MeV
150
50
0
$\pi^- p \to n \pi^- \pi^+$ at 8 GeV/c
Events/40 MeV
100
60
20
0
$\pi^+ d \to p_s p \pi^+ \pi^-$ at 11.7 GeV/c
Events/75 MeV
30
10
0
$\pi^- p \to n \pi^- \pi^+$ at 16 GeV/c
0.5
1.0
2.0
3.0
4.0
Mass $(\pi^+ \pi^-)$, GeV

Fig. 70

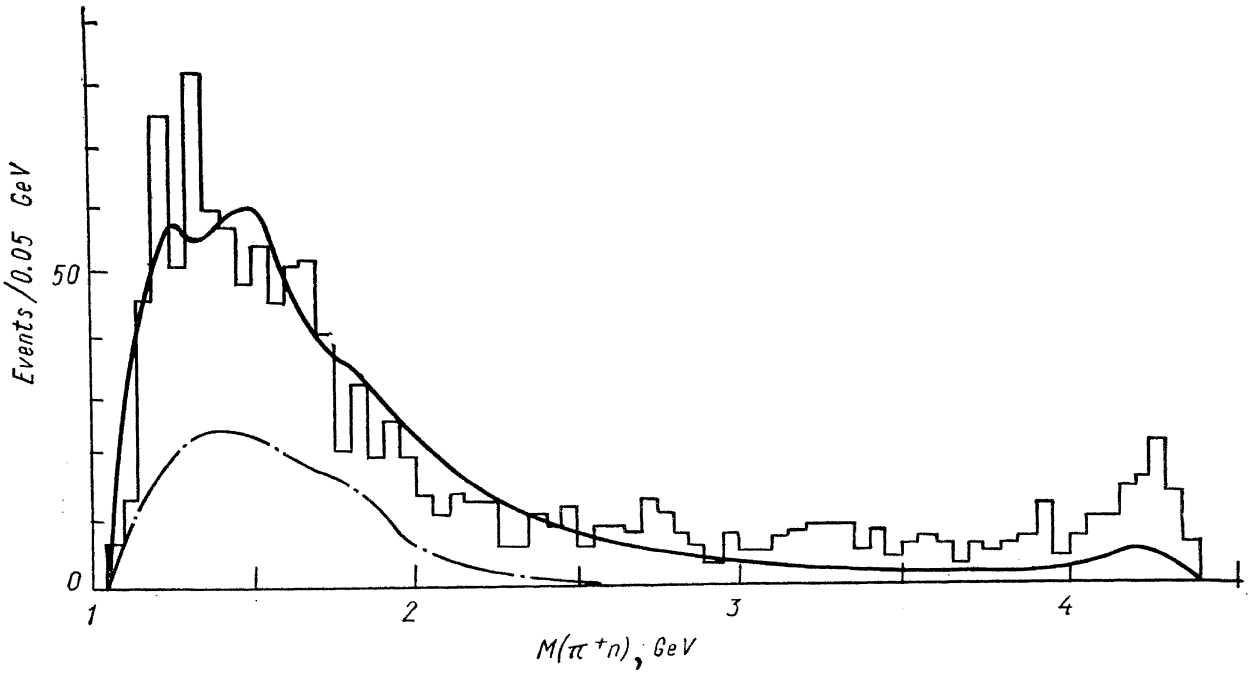

Fig. 71. $\pi^- p \to \pi^+ \pi^- n$ at 11 *GeV/c*.

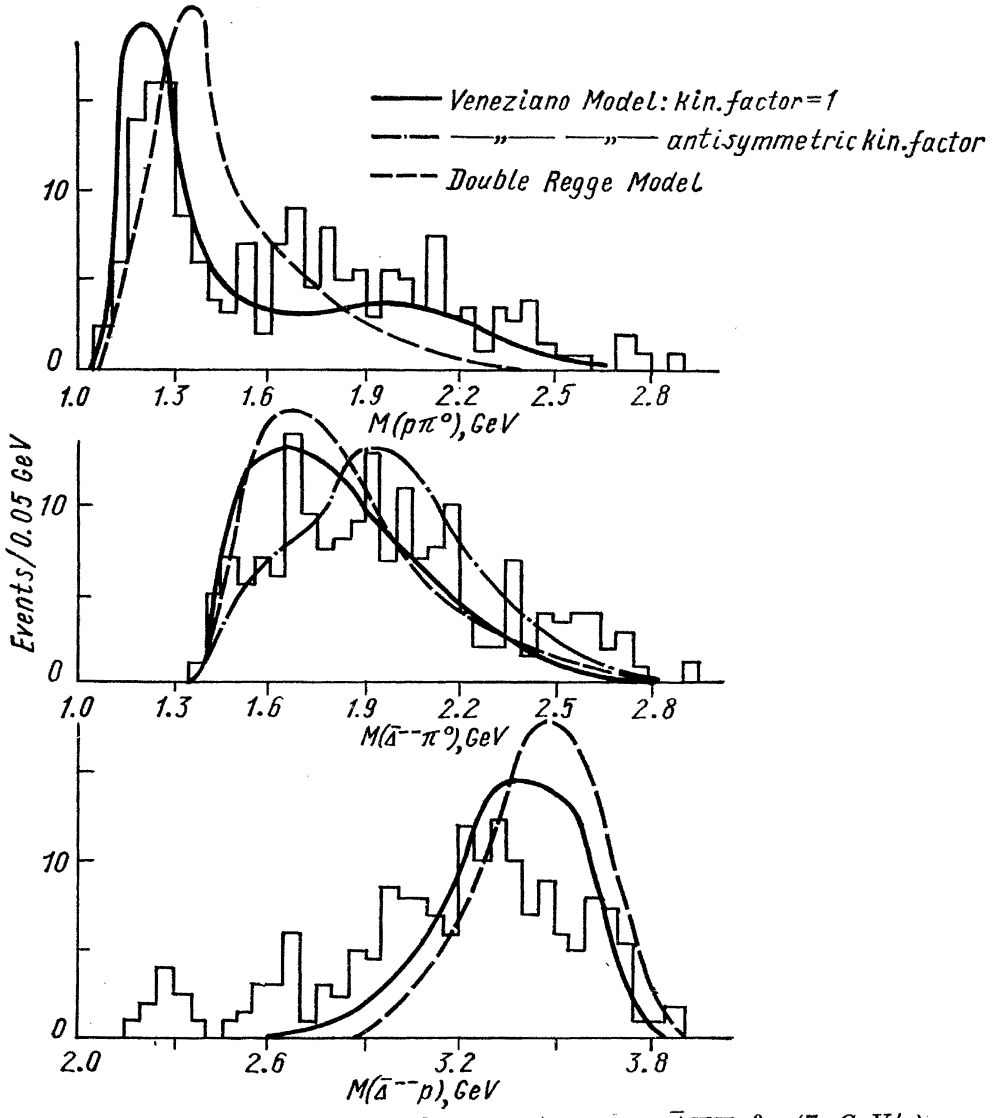

Fig. 72. Invariant mass distributions for $\bar{p}n \to \bar{\Delta}^{--}\pi^0 p$ (7 *GeV/c*).

$\pi^+n \to p\pi^+\pi^-$
$\pi^+p \to \Delta^{++}\pi^+\pi^-$ } at 13 *GeV/c* [103]

$\pi^+n \to p\pi^+\pi^-$
$\pi^-p \to n\pi^+\pi^-$ } at 5, 8, 11.7, 16 *GeV/c* [104]

$\pi^-p \to \pi^-\pi^+n$
$\pi^+p \to \pi^+\pi^-\Delta^{++}$
$K^-p \to K^-\pi^+n$
$K^+p \to K^+\pi^-\Delta^{++}$ } 5 — 16 *GeV/c* [105]

I will shortly comment on the method in which Pomeron contribution is taken into account. The authors of Ref. [104] used a noncoherent sum of amplitudes corresponding to the following diagrams

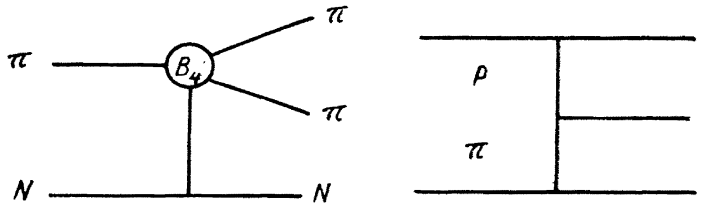

whereas in Ref. [105] the authors used a sum of the B_5 function and Pomeron exchange diagram. Figs. 70, 71 and 72 show examples of the comparison of model prediction with experimental data.

These models were applied only to specific reactions and no correlations between secondary particles were studied. However, as shown in a recent paper [106] it is a study of correlations which gives a strongest test of any model even if it can satisfactorily reproduce single particle distribution. Moreover, as it was pointed out by E. Berger in one of the parallel sessions of this Conference one should not be satisfied if some distributions fit the model, but one should try to find a specific distribution which would be the strongest test of the model.

7. Interactions with nuclei

7.1. COHERENT PRODUCTION ON DEUTERIUM

I would like to comment shortly on the papers submitted to this Conference on the subject of coherent production on deuterium. The reactions studied were:

$\pi^+d \to d\pi^+\pi^+\pi^-$ at 7 *GeV/c* [107]

$\bar{p}d \to d\bar{p}\pi^+\pi^-$ at 7 *GeV/c* [108]

$K^+d \to dK^+\pi^+\pi^-$ at 3.8 *GeV/c* [109]

$\pi^+d \to d\pi^+\pi^+\pi^-$ at 11.7 *GeV/c* [110].

Fig. 73 shows the total cross section for coherent production on deuterium for various incoming particles and energy.

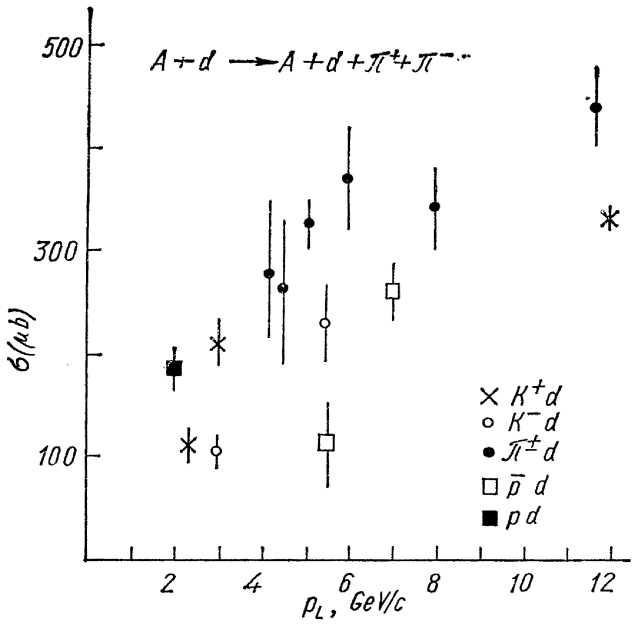
A + d → A + d + π⁺ + π⁻ ...
500
300
100
σ(μb)
2
4
6
8
10
12
p_L, GeV/c
K⁺d
K⁻d
π±d
p̄ d
p d

Fig. 73.

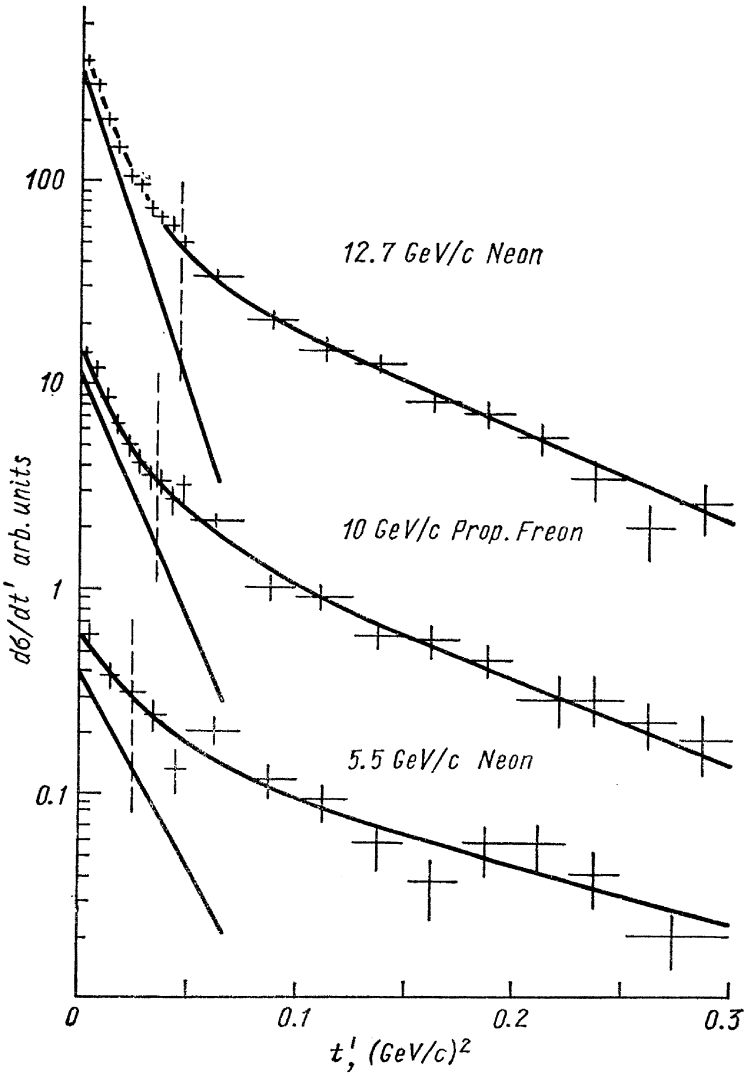
100
10
1
0.1
dσ/dt' arb. units
12.7 GeV/c Neon
10 GeV/c Prop. Freon
5.5 GeV/c Neon
0
0.1
0.2
0.3
t', (GeV/c)²

Fig. 74.

The coherent production on deuterium is usually described in terms of a graph

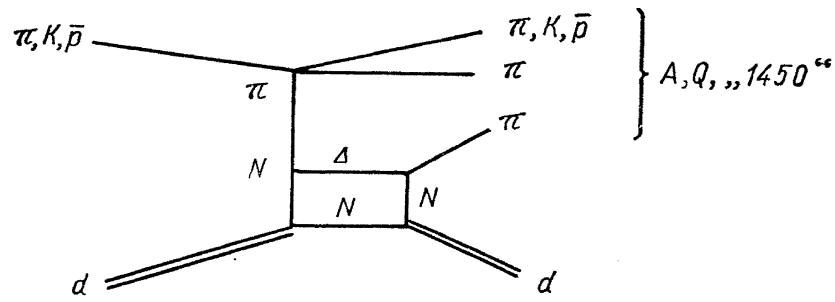

The pion produced in the dissociation of the incoming particle is scattered elastically off the deuteron. This results in the formation of a Δ (1238) by one of the nucleons in the deuteron. The Δ then subsequently decays in a way which leaves an intact deuteron in the final state. This model explains the d^* enhancement at about $m_N + m_\Delta = 2170\ MeV$. Also other experimental features observed in coherent production on deuterium are in agreement with this π exchange model.

7.2. COHERENT PRODUCTION ON HEAVIER NUCLEI

Coherent production of pions by K^+ mesons in the HLBC at 10 *GeV/c* was studied in [111]. Coherent production of $K\pi\pi$ and $K\pi\pi\pi$ systems was observed, the latter having the cross section (0.21 ± 0.08 *mb*) about ten times smaller than the former (2.20 ± 0.35 *mb*).

The total interaction cross section of Q^- in nuclear matter was determined in the study of K^- coherent interactions in HLBC and Ne — H mixture [112] (Fig. 74). The method consisted of measuring the rate for coherent production of Q^- on nuclei and using a model which relates these results to Q^- production on protons and deuterons in terms of Q^--nucleon scattering. The result

$$\sigma_{Q^-} = 21 \pm 8mb$$

is similar to the value of total Kp or πp cross section. If Q enhancement were not a resonance but a noninteracting system of K^* and π travelling independently through the nuclear matter, the expected value of Q-nucleon cross section would be about twice as large.

Similar result for A enhancement defined as having a mass in the region 1.0 — 1.2 *GeV* were obtained in [113]. In this experiment 15.1 *GeV/c* π-beam was used to study coherent production on various nuclei ranging from beryllium to lead. Fig. 75 shows

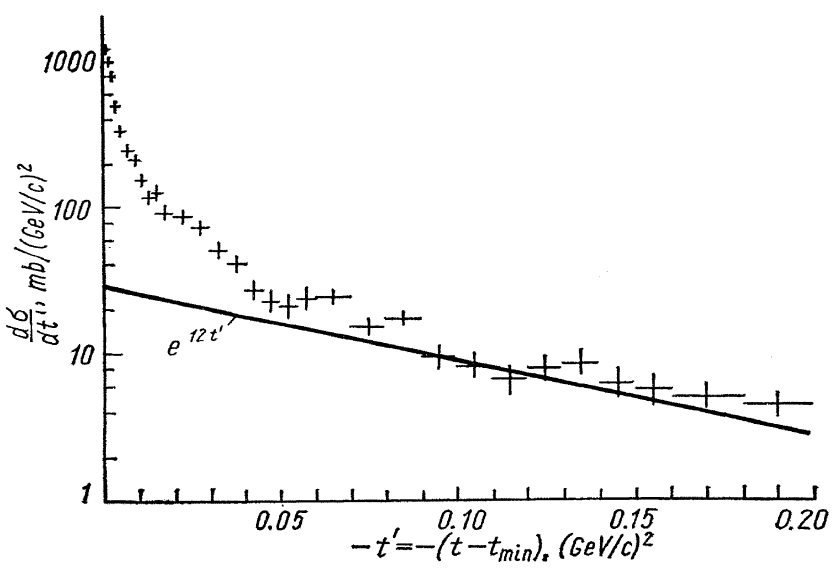

Fig. 75. t' distribution of $\pi^+\pi^-\pi^-$ produced by π^- on Ag at 15.1 *GeV/c*.

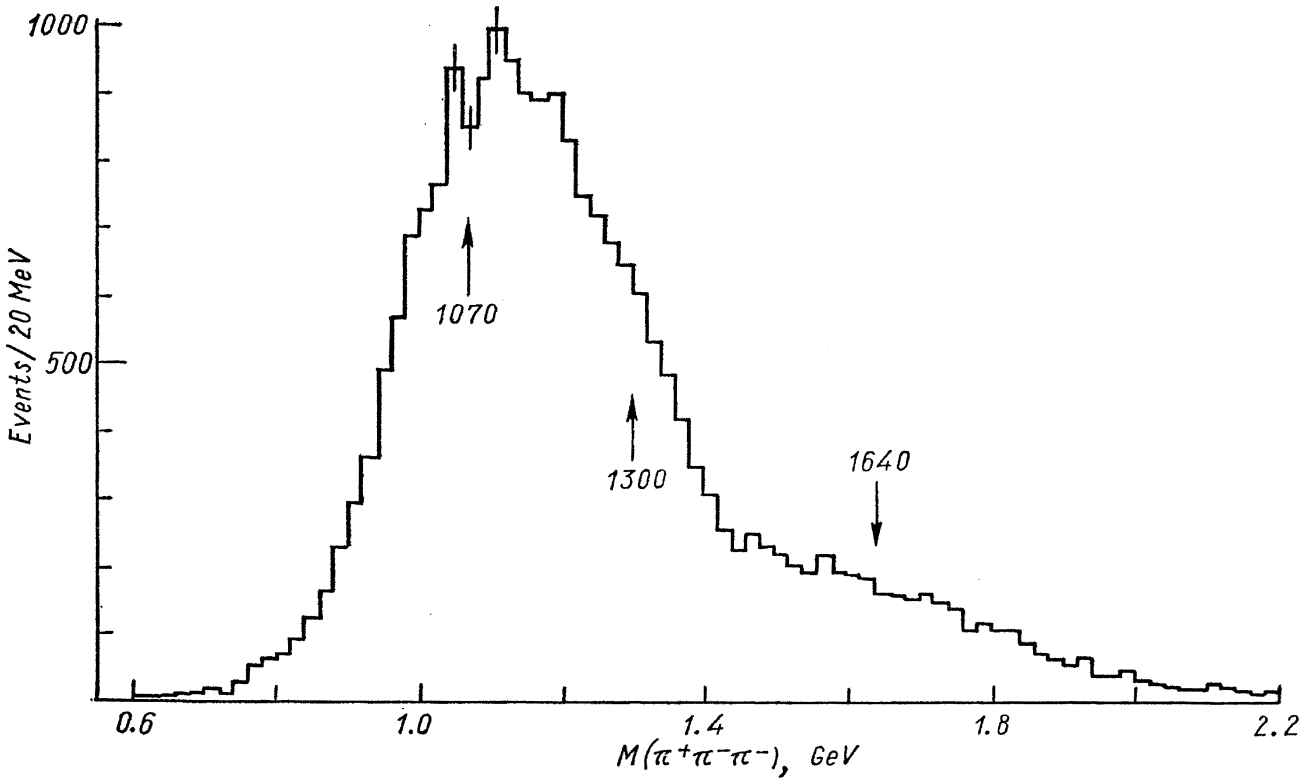

Fig. 76. Compilation of coherent production on Be, C, Al, Si, Ti, Ag, Ta, Pb at 15.1 *GeV/c* (22 679 events).

typical $d\sigma/dt$ distribution obtained in this experiment. Fig. 76 shows the combined 3π mass spectrum on all nuclei. The shape of the broad A enhancement was practically the same for all nuclei. Fig. 77 shows the result of calculation of the A-nucleon cross section. Dependence of the best fit of σ_{out} on the parameters α and c_0 of the optical model is shown in the table 2. The result $\sigma = 20 \div 25$ *mb* is similar to that obtained in the case of Q^-. Coherent production of pions in emulsion was studied in [41], using 60 *GeV/c* π^--beam from the Serpukhov accelerator. The Dubna group [41] concluded that coherent production takes place mainly on heavy nuclei (Ag, Br). This result, however, is preliminary.

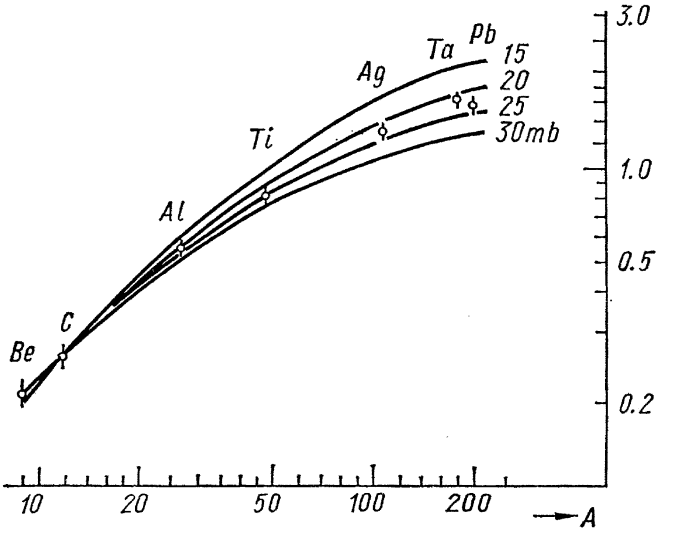

Fig. 77. A dependence of coherent production cross section (arbitrary units); $1 < M(\pi^+\pi^-\pi^-) < 1.2$ *GeV*. The curves are from an optical model density: $\rho(r) = \frac{\rho_0}{1 + \exp\left(\frac{r-c}{a}\right)}$; $c = c_0 A^{1/3}$, $c_0 = 1.14f$, $a = 0.545f$, $\sigma_{in} = 25.4$ *mb*, σ_{out} is the curve parameter. $\alpha = \frac{\mathrm{Re}\, f(0)}{\mathrm{Im}\, f(0)}$, $\alpha(\pi) = -0.1$, $\alpha(3\pi) = 0$.

Table 2

c_0	σ_{out}		
	$\alpha = -0.3$	$\alpha = 0$	$\alpha = 0.3$
$1.07f$	17	19	20
$1.14f$	20	23	24
$1.18f$	22	25	27

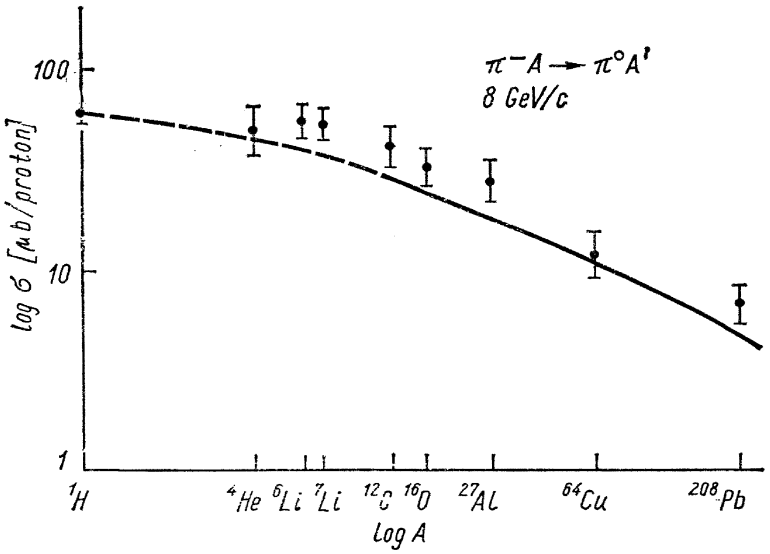
$\pi^- A \to \pi^0 A'$
8 GeV/c
log σ [mb/proton]
100
10
1
^1H
^4He ^6Li ^7Li ^{12}C ^{16}O ^{27}Al ^{64}Cu ^{208}Pb
log A

Fig. 78.

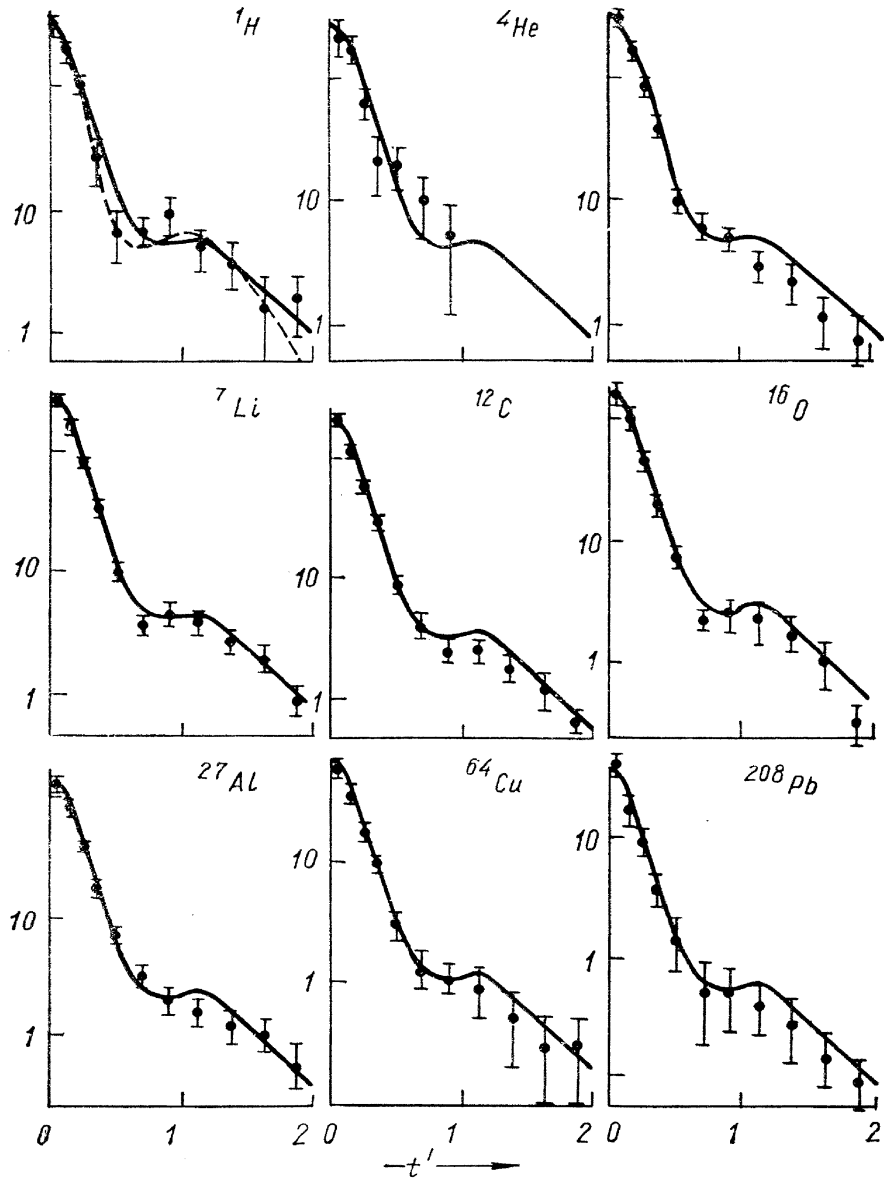
^1H
^4He
^7Li
^{12}C
^{16}O
^{27}Al
^{64}Cu
^{208}Pb
10
1
0
1
2
$-t'$

Fig. 79.

The Saclay — Desy group [114] studied the reaction $\pi^- A \to \pi^0 A'$ at 8 *GeV/c*, where A' is the residue of A after a charge exchange process. In this experiment both π^- and π^0 were detected but nothing concerning A or A' was measured. The results for total cross section are presented in Fig. 78. The curve was calculated assuming the «one step process». It is assumed that the reaction is due to the interaction of a π^- with a single proton in the nucleus. It must be then taken into account that both π^- and π^0 can be absorbed in the nuclear matter preceding and following the interaction point (shadow effect). Fig. 79 shows the results for $d\sigma/dt$ together with calculated curves. The reactions $\pi^- + C_6^{12} \to B_5^{12} + m\pi^0$ and $\pi^- + C_6^{12} \to N_7^{12} + \pi^- + \pi^+$ where studied in the Dubna propane chamber at 4 *GeV/c* [116]. The cross sections for these reactions were determined to be $\leqslant 0.12$ μb and $\leqslant 4 \pm 2.8$ μb, respectively.

8. Summary

There has been a remarkable progress in collecting data but do we analyse it in the best way? If one applies a particular model to a given reaction one is making cuts on masses and four-momentum transfer until finally one achieves reasonable agreement with the model. Furthermore, there is a large freedom of choosing free parameters to fit the data. Needless to say, different authors are using different methods, different cuts etc., so that the conclusions can not be easily compared. In my opinion more effort should be put into a unique analysis of data (search for correlations!). This is a very delicate problem since it involves the exchange of data summary tapes and I'm not going to offer you an easy solution of it. However, this, I think, is what should be done. Let me finish this talk by showing my last slide (Fig. 80). Thank you for your attention.

Fig. 80.

DISCUSSION

R o s e n t a l:

What can you say about collective correlations of the fireball type?

W r o b l e w s k i:

The only paper submitted to this session is that of Akimov et al., but there is no discussion of the effect which you are interested in.

K i t t e l:

1. In the paper by Hansen, Morrison and myself σ_A is called «asymptotic» only because it is defined to be identical to the experimental cross sections at asymptotic energies (say above 20 *GeV/c* for 3 body). We de **not** conclude, as you say, that the cross sections should continue to fall with an exponent $n_A \approx 2$ at higher energies. In fact, among the second order effects we make a strong statement that the reaction $\pi^- p \to \pi^- p \pi^+ \pi^-$ has a much flatter decrease with energy than others ($n_A \approx 1$). We ascribe that to diffraction dissociation dominating this reaction already at our energies. So our conclusion is in agreement, and **not**, as you say, in disagreement with your general observation of constant cross sections at very high energies.

2. For the investigation of double diffraction dissociation in the reaction $\pi^- p \to (p\pi^0)\ (\pi^+\pi^-\pi^-)$, (Ratti, Van Hove and myself) you suggest to look at $\pi^- p \to (n\pi^+)\ (\pi^+\pi^-\pi^-)$ before drawing any conclusion. This has, of course, been done, and the ratio is in reasonable agreement with the expected 1 : 2. We furthermore calculated the expected cross section from elastic scattering and single diffraction dissociation (assuming factorisation), in agreement with the experimentally observed cross section.

3. I slightly doubt the general usefulness of the $F\ (t)$ function. Since one averages all variables, except t_{pp}, over the whole phasespace, one forgets completely about the longitudinal momenta of the pions and their correlations with each other or the proton. The distributions are investigating in themselves, but one must be very careful in drawing conclusions about the matrix element.

W r o b l e w s k i:

1. I have argued against the word «asymptotic» for your exponent n_A since in your paper you conclude clearly that for the reactions of pion production is equal to about 2. If the Pomeron exchange processes dominate many-body reactions at higher energies then you will find out that your «asymptotic» exponent is a decreasing function of energy and eventually it decreases to zero.

2. There was nothing in your paper about the comparison of reactions $\pi^- p \to (p\pi^0)(\pi^+\pi^-\pi^-)$ and $\pi^- p \to (n\pi^+)\ (\pi^+\pi^-\pi^-)$ so I was not able to quote any figure in my talk.

M a g l i č:

1. I don't understand the reasons one is plotting and investigating angular correlations between 2 and 3 pions etc. We **know** these pions are the products of mesonic resonances decays. Goldhabers' correlations were done **before** the resonances were discovered. Two pions from the ρ-decay would indeed, on the average, have larger angle than those not coming from ρ (such as $\pi^+\pi^+$). Thus, I consider the angular correlations only as a very hard and insensitive indirect way of looking for resonances.

2. The resonances and their effects on angular correlations can be removed only if we were sure we **knew** all resonances. I think, however, with the resolution and statistics presently available, there are more resonances not discovered than discovered. Therefore, at present the interference effects and mass-spectra effects cannot be easily separated and are of limited usefulness.

B i a ł a s:

I would like to disagree with Professor Maglič. The people working on GGLP effect know that there are resonances and they take them into account in the analysis. It was shown in several papers that resonances cannot explain the effect. The most striking evidences for this seem to me

a) observation of the strong GGLP effect in 10-prong $\pi^+ p$ interactions of 8 *GeV/c* by the Krakow group. They see no deviations of mass distributions and single particle disributions from phase space, and still there is a dramatic difference between opening angles of like and unlike pion pairs.

b) in a recent paper, the CERN — Brussel collaboration observed no difference between the opening angles of $K^+\pi^+$ and $K^+\pi^-$ pairs produced in 6-prong K^+p interactions at 5 *GeV/c*. If resonances play an important role in GGLP effect then, contrary to this observation, we would expect rather strong difference because, as we all believe, there are no resonances in the $K^+\pi^+$ system whereas the $K^+\pi^-$ system is full of strong resonances.

c) in a recent analysis of 6-prong π^+p interactions at 8 *GeV/c* by the Warsaw group it was shown, very convincingly to my opinion, that the GGLP effect is caused by interference implied by symmetrization of identical pions.

Thus, it appears that, as suggested 10 years ago by Golhaber et al., the symmetrization of the pion wave function is mainly responsible for the effect.

C z y z e w s k i:

If Professor Maglič is right, then GGLP effect is in our case much more sensitive test for resonance presence than bumps in effective mass distributions. Every resonance or bump we see in our data is much less significant than angular correlations effects.

C o h e n — T a n n o u d j i:

I would like to mention that it is possible and easy to test the assumption of c. m. helicity conservation of Pomeron exchange. One has essentially to perform a Trennan — Yang test but in the helicity frame rather than in the Jackson frame. This test is easy to do; one can even re-analyse old data. It is important to know if this assumption is true not only for quasi-two body reactions but also in the case of the production of two uncorrelated packets of particles.

R o i n i s h v i l i:

My comment concerns many-body process models. It is rather well established that:

a) the inelasticity coefficient is constant over a wide energy range;

b) the multiplicity increases with the energy. It seems to me that these two facts are rather difficult to be explained in the frame of the limiting fragmentation model. Indeed, in this model the average energy per secondary in the centre of mass system increases as γ_c. As a result, the inelasticity coefficient has to increase proportionally to n_s. The opposite difficulty arises in the pure pionisation process. Therefore only the proper combination of these two processes can explain both of the mentioned experimental facts. This is just the situation with the multiperipheral models.

Y a n g:

a) The multiplicity can increase logarithmically in the hypothesis of limiting fragmentation.

b) The original form of the multiperipheral model is an example of models that satisfy the hypothesis of limiting fragmentation.

c) I agree with the speaker that extremely detailed models are probably not useful at this stage of our knowledge.

G a r e l i c k:

Have the $f(t)$ distributions, which are approximately independent of multiplicity, been compared to the t distribution given by $|G_M(t)^2|$ where $G_M(t)$ is the proton electromagnetic form factor?

W r o b l e w s k i: No.

P i g n o t t i:

I agree with Professor Yang's statement that the multiperipheral model (MPM) is consistent with the hypothesis of limiting fragmentation and Bali, Steele and I have presented a paper to this conference in which this was pointed out. I would also like to make a remark concerning pionization, because I believe that this is a physically interesting problem, and that there has been confusion about this term. I know of two precise definitions of pionization, and I am the author of neither one. The first one was used by Cheng and Wu in a Physical Review Letters article last year, and is the one that I have used in the past. According to this definition there is pionization if the **number** of pions, produced with center of mass energy less than an arbitrary fixed value W, tends to a constant as the incident energy goes to infinity, and there is no pionization if the **number** goes to zero. The model of Cheng and Wu and the MPM predict the existence of pionization in the sense of Cheng and Wu. The model of Professor Yang does not make predic-

tions about this definition of pionization *. The second definition of pionization is contained in a recent preprint entitled «Remarks about the Hypothesis of Limiting Fragmentation» by T. T. Chou and C. N. Yang. This definition is analogous to the first one, but instead of referring to the **number** of pions produced, it refers to the **fraction** of the total number of pions produced within a limited energy range in the centre of mass. In other words, the definition of Cheng and Wu is divided by the total number of pions produced. Because we agree that this total number increases without bound with increasing incident energy, the model of Cheng and Wu and the MPM predict a vanishing pionization in the sense of Chou and Yang. Limiting fragmentation is consistent with the presence or absence of pionization, but favors the absence. In summary: it is unfortunate that there are now two definitions of pionization, and I recommend to my colleagues to specify in the future what kind of pionization they refer to: whether Cheng and Wu's or Chou and Yang's. As far as physics is concerned, the models of Cheng and Wu and the MPM make stronger predictions than the model of limiting fragmentation. However, when the latter favors an alternative, it agrees with the other models.

REFERENCES

1. V. V. Akimov et al., paper 3a—40.
2. L. W. Jones et al., paper submitted to the Sixth Interamerican Seminar on Cosmic Rays, La Paz, Bolivia, July, 1970.
3. D. D. Reeder et al., paper 3a—60.
4. K. N. Erickson, Thesis, University of Michigan, April 1970.
5. G. B. Yodh, J. R. Wayland, Yash Pal, paper 3a—35.
6. V. V. Balashov and G. Ya. Korenman, Physics Letters **31B**, 310 (1970).
7. R. J. Phillips, Lectures on Regge Phenomenology (Schladmig Winter School, 1970).
8. Aachen — Berlin — CERN — Cracow — Warsaw Collaboration, Phys. Letters **22**, 230 (1966).
9. J. W. Waters et al., Nuclear Physics **B17**, 445 (1970).
10. F. Turkot — CERN Conference 1968. v. 1, 316.
11. E. Balea et al., paper 3a—25.
12. Yu. A. Budagov et al., paper 3a—3.
13. S. Ozaki et al., paper 3a—57.
14. G. Charriere et al., paper 3b—1.
15. Birmingham — Glasgow Collaboration, paper 3b—2.
16. S. L. Stone et al., this conference.
17. A. Wróblewski, Physics Letters, **32B**, 145 (1970).
18. J. Benecke, T. T. Chou, C. N. Yang and E. Yen, Phys. Rev. **188**, 2159 (1969).
19. H. Muirhead and A. Poppleton, Physics Letters **29B**, 448 (1969).
20. T. Hofmokl and A. Wróblewski, Physics Letters **31B**, 391 (1970).
21. J. Bartke and R. Sosnowski, Acta Physica Polonica **36**, 277 (1969).
22. S. Brandt, Physics Letters **32B**, 388 (1970).
23. A. Wróblewski, Review paper, Proceedings of the Colloquium on High Multiplicity Hadronic Interactions, Paris, May 13—15, 1970.
24. J. D. Hansen, W. Kittel and D. R. O. Morrison, paper 3a—58.
25. Yu. M. Antipov et al., paper 3a—50.
26. D. R. O. Morrison, Phys. Lett. **22**, 528 (1966).
27. F. Cerulus, Nuovo Cim. Suppl. **15**, 402 (1960).
28. J. Shapiro, Nuovo Cim. Suppl. **18**, 40 (1960)
29. J. Bartke, Nucl. Phys. **82**, 673 (1966).
30. J. Bartke and O. Czyzewski, Nucl. Phys. **B5**, 582 (1968).
31. J. W. Elbert et al., Nucl. Phys. **B19**, 85 (1970).
32. Bar Nir et al. Nucl. Phys. **B20**, 45 (1970).
33. Yu. A. Budagov et al., paper 3a—4.
34. S. Brandt, paper presented to the 14th International Conference on High Energy Physics (Vienna, 1968).
35. Aachen — Berlin — Bonn — CERN — Cracow — Heidelberg — Warsaw Collaboration, Nucl. Phys. **13B**, 571 (1969).

* Private communication from Professor C. N. Yang.

36. Scandinavian Bubblechamber Collaboration — Copenhagen, Helsinki, Oslo and Stockholm Universities, paper 3a—31.
37. C. P. Wang, Phys. Rev. **180,** 1463 (1969), Phys. Lett. **30B,** 115 (1969).
38. G. F. Chew and A. Pignotti, Phys. Rev. **176,** 2112 (1968).
39. O. Czyzewski and K. Rybicki, paper 3a—24.
40. Alma-Ata — Budapest — Cracow — Dubna — Sofia — Tashkent — Ulan-Bator Collaboration, Phys. Lett. **31B,** 237, 241 (1970).
41. N. Dalkhazhav, G. S. Shabratova, K. D. Tolstov, paper 3a—29.
42. J. Gierula, E. R. Gora, R. Holynski, S. Krzywdzinski, this conference.
43. N. A. Dobrotin et al., Canadian Journal of Physics, **45,** 675 (1968).
44. L. Caneschi, D. E. Lyon, Jr. and C. Risk, UCRL — 19814, June, 1970. Phys. Rev. Lett. **25,** 774 (1970).
45. L. Caneschi and A. Pignotti, Phys. Rev. Lett. **22,** 1219 (1969).
46. E. Balea et al., paper 3a—38.
47. M. M. Chernyavsky et al., paper 3a—55.
48. S. A. Azimov et al., paper 3a—34.
49. Z. Ming ma et al., paper 3a—33.
50. N. N. Biswas et al., paper 3a—22.
51. J. Le Guyader, M. Sene, paper 3a—20.
52. D. B. Smith, R. J. Sprafka and J. A. Anderson, Phys. Rev. Lett. **23,** 1064 (1969).
53. J. W. Elbert et al., Phys. Rev. Lett. **20,** 129 (1968).
54. R. P. Feynman, Phys. Rev. Lett. **23,** 1415 (1969).
55. S. D. Drell, Summary talk at the Int. Conf. on Expectation for Particle Reactions at New Accelerators, April 1970, Univ. of Wisconsin.
56. V. N. Akimov et al., paper 3a—42.
57. G. Bialkowski and R. Sosnowski, Phys. Lett. **25B,** 519 (1967).
58. Aachen — Berlin — CERN — Cracow — Heidelberg — Warsaw Collaboration, this conference.
59. A. Ziemiński, Nucl. Phys. **B14,** 75 (1969).
60. V. Picciarelli, D. Mettel and O. Goussu, paper 3a—9.
61. W. De Baere et al., CERN D. Ph II/PHYS 70—12, Nucl. Phys. (to be published).
62. G. Alexander et al., paper 3b—12.
63. J. Bartke et al., paper 3a—49.
64. H. Hulubei et al., paper 3a—26
65. C. Adcock et al., paper 3a—37.
66. A. Böhm et al., paper 3a—43.
67. Yu. M. Antipov et al., paper 3a—47.
68. V. V. Glagolev et al., paper 3a—2.
69. J. Debray et al., paper 3b—10.
70. V. Picciarelli, D. Mettel, O. Goussu, paper 3a—9.
71. Durham — Genova — Milano — Paris (EP and IPN), paper 3a—56.
72. G. Ascoli et al., paper 4a—20.
73. H. Braun et al., paper 3b—11.
74. C. Brankin et al., paper 3b—3.
75. I. Borocka et al. paper 3b—14.
76. M. Bardadin — Otwinowska, T. Hofmokl, L. Michejda, S. Otwinowski, R. Sosnowski, M. Szeptycka, A. Wróblewski, W. Wójcik, D. Zieminska (to be published).
77. G. Goldhaber, S. Goldhaber, W. Lee, A. Pais, Phys. Rev. **120,** 300 (1960).
78. O. L. Berdzenishvili et al., paper 3a—41.
79. Yu. A. Budagov et al., paper 3a—5.
80. E. O. Abdrachmanov et al., paper 3a—27.
81. M. Bardadin, L. Michejda, S. Otwinowski, R. Sosnowski, Proceedings of the 1963 Sienna Conference.
82. M. Bardadin, L. Michejda, S. Otwinowski, R. Sosnowski, Inst. of Nucl. Phys. Warsaw, Report (1964).
83. L. Van Hove, Phys. Lett. **28B,** 429 (1969), Nucl. Phys. **B9,** 429 (1969).
84. J. Ballam et al., paper 12—24.
85. O. Murro, V. Picciarelli, paper 3a—11.
86. Aachen — Berlin — CERN Collaboration and Aachen — Berlin — CERN — Cracow Collaboration, this conference.
87. Bonn — Durham — Nijmegen — Paris E. P.— Torino Collaboration, paper 3a—8.
88. J. Bartsch et al., Nucl. Phys. **B11,** 373 (1969).
89. H. Satz, Phys. Lett. **29B,** 38 (1969).

90. W. Kittel, S. Ratti and L. Van Hove, paper 3a—16.
91. Y. Cho et al., this conference.
92. P. Antich et al., paper 3b—4.
93. G. V. Beketov et al., paper 3a—7.
94. J. A. Chao and J. D. Prentice, paper 3a—12.
95. T. A. Mulera et al., paper 3a—19.
96. R. C. Badewitz et al., paper 3a—18.
97. P. Antich et al., paper 13b—28.
98. G. Charriere et al., paper 3b—1.
99. Birmingham — Glasgow Collaboration, paper 3b—2.
100. P. Schreiner, D. H. Stork, R. Ross and A. G. Clark, this conference.
101. J. Galletly et al., paper 13b—31.
102. B. Forman et al., this conference.
103. R. C. Badewitz et al., paper 3a—17, 18.
104. Durham — Geneva — Milano — Paris (EP and IPN) Collaboration, paper 3a—56.
105. S. Pokorski, M. Szeptycka, A. Zieminski, paper 13b—1.
106. J. Bartsch et al., Nucl. Phys. **B19**, 381 (1970).
107. M. W. Firebaugh et al., paper 3a—45.
108. P. Antich et al., paper 3b—13.
109. B. Eisenstein et al., paper 3b—5.
110. Durham — Geneva — Milano — Paris (EP, IPN) Collaboration, paper 3a—56.
111. M. Haguenauer et al., paper 3b—6.
112. A. M. Cnops et al., paper 4c—4.
113. C. Bemporad et al., paper 3a—59.
114. O. Guisan et al., paper 3a—54.
115. I. M. Dremin et al., paper 3a—28.
116. K. N. Abdullaeva et al., paper 3a—51.